Design of an Electrocardiographic Lead Reconstruction Algorithm Using Machine Learning in the context of Ambulatory Monitoring

Alejandro Grande Fidalgo

Supervisors: Javier Calpe Maravilla
Emilio Soria Olivas

Tutor: Javier Saiz Rodríguez

Department of Electronic Engineering
Universitat Politécnica de València

Programa de Doctorado en Tecnologías para la Salud y el Bienestar

Modelado, Señales e Instrumentación
Biomédica

December 2024

A mi hermano,
por haberse convertido en todo lo que quiero ser de mayor.

A Juanita,
ama de casa que sacó adelante prácticamente sola cuatro hijos y un hogar;
a Agustín,
quien dejó su vida en el pinar por la fábrica para mantener a su familia,
a Anita,
trabajadora desde niña que crio seis hijos y cuidó un hogar;
a Pepe,
albañil, minero y emigrante;
a mi padre,
quien cada madrugada descargaba camiones antes de ir a la universidad;
a mi madre,
que, embarazada de mí, seguía haciendo 120 km en autobús cada día para ir a trabajar;

Ésta es una muestra del fruto de todo el esfuerzo que habéis puesto en darles a vuestros hijos un futuro mejor.

Espero que, estéis aquí, o ya no, sintáis una milésima parte del orgullo que yo siento por vosotros.

Declaration

This work is part of a PhD Thesis with industrial mention due to work at Analog Devices Inc. in the Medical Products group in Paterna, Valencia. I hereby declare that except where specific reference is made to the work of others, the contents of this dissertation are original and have not been submitted in whole or in part for consideration for any other degree or qualification in this or any other university. While portions of this work are from publicly available sources such as articles or patents of the author, the contents of this Thesis are confidential. It should not be reproduced in any form without the express permission of the author.

Alejandro Grande Fidalgo
December 2024

Acknowledgements

Desde aquella entrevista de trabajo en la que se me preguntó por absolutamente todos los campos que un ingeniero biomédico debiera saber, supe que Javier Calpe, la persona que estaba enfrente de mí, era de esa clase gente que está hecha de otra pasta. Es complicado resumir todo el apoyo y el esfuerzo que has volcado en este chaval de Azuqueca desde el primer segundo en el que puse un pie dentro de Analog Devices, pero no lo es agradecerte todo lo que me has enseñado a nivel académico y, sobre todo, humano. Tu pasión por aprender y tu disposición a echar una mano son contagiosas, ojalá sigan inspirándome muchos años más. Gracias por ser tan brillante, cercano y amable. Y sobre todo, por tener un sentido del humor tan malo como el mío.

Esta Tesis trata sobre Machine Learning e Inteligencia Artificial, unos campos muy de moda pero, a la vez, muy maltratados. De esos en los que no dejan de aparecer "expertos" de debajo de las piedras que, lamentablemente, enturbian las aguas más que aportan. Por el contrario, yo tuve la inmensa suerte de contar con un verdadero experto y referente en estos temas, del que he aprendido mucho y me gustaría aprender todavía más. Gracias a Emilio Soria por haber aportado la sensatez en este trabajo y haber puesto tu conocimiento sobre estos campos a mi disposición para hacer de éste un trabajo del que sentirse orgulloso.

En resumen, gracias a los dos por haber aceptado dirigir esta Tesis, y a Javier Saiz por ser mi tutor dentro de la UPV. Quizás él no se acuerde, pero aquella llamada intempestiva para un estudiante universitario (las 10 de la mañana) aquel mayo de 2018 para comunicarme mi aceptación en el Máster de Ing. Biomédica en la UPV fue la primera ficha del dominó que corona este trabajo. Gracias por traerme a València, la ciudad más bonita del mundo.

En el momento de redacción de estos agradecimientos, llevo cinco años formando parte de Analog Devices, un lugar que definitivamente me ha cambiado la vida. La cantidad de gente buena que he conocido en esta empresa a lo largo de estos años solo es comparable a su calidad humana. Gracias a todos los que habéis o aun formáis parte de esta etapa de mi vida. No dejéis de enseñarme, prometo no dejar de aprender.

Dentro de Analog, formo parte del grupo Medical Products, donde puedo asegurar que todo lo mencionado anteriormente se eleva a la máxima potencia. Será difícil, cuando no imposible, conocer a gente tan brillante y tan maravillosa como con la que cuenta este equipo.

También tengo que agradecer de forma especial a Mónica Redón el haber apostado por mí, dedicándome su tiempo y su ayuda para sacar el máximo de todo el potencial disponible, eres increíble. Creo que quedará apropiado entonces, por el proyecto en el que estamos, y por esta Tesis, que a vosotros os dé las gracias de todo corazón.

Hay varios grupos de personas imprescindibles a la hora de haber mantenido el barco a flote durante estos cuatro años, los cuáles no siempre han sido fáciles. Los amigos son la familia que se elige, y encima tengo la mala costumbre de tener muchos pueblos (cosas del éxodo rural), así que tengo la inmensa fortuna de tener muchas familias de muchos lugares distintos. Primero gracias a Sandra, por todo. A mi familia de Valencia, por estar hoy otra vez en la carretera, a punto de escribir una nueva canción, aquella que no olvidaremos. A mi familia de Verín, no hay licorca en este mundo para compensar el oxígeno que sois para este azuqueco. A mi familia de Madrid, por enseñarme lo que había más allá del nido. Y a mi familia de Azuqueca de Henares, por haber creado un nido del que sentirse orgulloso de pertenecer.

Cuando tuve que decidir mi nombre de investigador, el nombre que aparecería en mis trabajos, publicaciones, etc., debía decidir qué apellido añadir. Al instante supe que no podría ser otro que Grande-Fidalgo. La suma de mis dos pilares fundamentales, mis familias elegidas, y esta vez también de sangre, tanto Grande como Fidalgo, gracias por darme fuerzas en todo este proceso.

Me he permitido la libertad de volver a incluir la dedicatoria de mi Trabajo de Fin de Máster, ya que pensaba que aquella sería mi última incursión en el mundo académico (ingenuo de mí...). Abuelas, papá, mamá, chache, poco que añadir. Sigo opinando lo mismo sobre vosotros, que todo esto es el resultado del esfuerzo que hemos puesto en nuestra familia por que los siguientes en venir lo tuvieran un poco más fácil en esta vida, por ayudarnos y querernos los unos a los otros ante todo, y que no puedo estar más orgulloso de todos vosotros.

Gracias.

Abstract

This PhD Thesis presents an algorithm for reconstructing the standard 12-lead system electrocardiographic (ECG) register using a reduced system of independent leads supported by machine learning models, with a focus on its integration into an ambulatory monitoring system. Traditional ECG lead reconstruction methods have relied on linear combination-based approaches, with limited exploration of evaluation methods and electrode positions. This thesis evaluates the effectiveness of new artificial neural networks and fuzzy c-means-based algorithms compared to classical linear regression methods, highlighting superior performance and emphasizing the importance of model explainability. Further enhancements, including expert committees and fuzzy models, are explored to improve accuracy and efficiency. Clinical validation at the Hospital Clínico Universitario de València and Hospital General Universitario de València demonstrates the algorithm's effectiveness in an accurate lead reconstruction, paving the way for ambulatory monitoring applications. The study also addresses challenges posed by implantable devices such as pacemakers and defibrillators; a subsequent study proposes a strategy to eliminate distorted pulses during reconstruction, improving signal quality under any condition. Overall, the thesis contributes to advancing ECG lead reconstruction methodologies for improved patient care.

Resumen

Esta tesis doctoral presenta un algoritmo para reconstruir el registro electrocardiográfico (ECG) estándar del sistema de 12 derivaciones utilizando un sistema reducido de derivaciones independientes mediante el uso de modelos de aprendizaje automático, centrándose en su integración en un sistema de monitorización ambulatoria. Los métodos tradicionales de reconstrucción de ECG se basan en enfoques basados en combinaciones lineales, con una exploración limitada de los métodos de evaluación y de las posiciones de los electrodos. Esta tesis evalúa la eficacia de nuevas redes neuronales artificiales y algoritmos basados en fuzzy c-means en comparación con los métodos clásicos de regresión lineal, destacando un rendimiento superior y subrayando la importancia de la explicabilidad del modelo. Se exploran otras mejoras, como comités de expertos y modelos difusos, para aumentar la precisión y la eficacia. La validación clínica realizada en el Hospital Clínico Universitario de València y en el Hospital General Universitario de València demuestran la eficacia del algoritmo en la reconstrucción precisa de derivaciones, facilitando el camino para aplicaciones de monitorización ambulatoria. El estudio también aborda los retos que plantean dispositivos implantables como marcapasos y desfibriladores; un estudio posterior propone una estrategia para eliminar pulsos distorsionados durante la reconstrucción, mejorando la calidad de la señal en cualquier condición. En conjunto, la tesis contribuye al avance de las metodologías de reconstrucción de derivaciones de ECG para mejorar la atención al paciente.

Resum

Aquesta tesi doctoral presenta un algoritme per a reconstruir el registre electrocardiogràfic (ECG) estàndard del sistema de 12 derivacions utilitzant un sistema reduït de derivacions independents mitjançant l'ús de models d'aprenentatge automàtic, centrant-se en la seua integració en un sistema de monitoratge ambulatori. Els mètodes tradicionals de reconstrucció de ECG es basen en enfocaments basats en combinacions lineals, amb una exploració limitada dels mètodes d'avaluació i de les posicions dels elèctrodes. Aquesta tesi avalua l'eficàcia de noves xarxes neuronals artificials i algoritmes basats en fuzzy c-means en comparació amb els mètodes clàssics de regressió lineal, destacant un rendiment superior i subratllant la importància de la explicabilitat del model. S'exploren altres millores, com a comités d'experts i models difusos, per a augmentar la precisió i l'eficàcia. La validació clínica realitzada a l'Hospital Clínic Universitari de València i a l'Hospital General Universitari de València demostren l'eficàcia de l'algoritme en la reconstrucció precisa de derivacions, facilitant el camí per a aplicacions de monitoratge ambulatori. L'estudi també aborda els reptes que plantegen dispositius implantables com a marcapassos i desfibril·ladors; un estudi posterior proposa una estratègia per a eliminar polsos distorsionats durant la reconstrucció, millorant la qualitat del senyal en qualsevol condició. En conjunt, la tesi contribueix a l'avanç de les metodologies de reconstrucció de derivacions de ECG per a millorar l'atenció al pacient.

Table of contents

List of figures

List of tables

Chapter 1

Introduction

1.1 The heart

The heart is one of the most important and interesting organs in our body. It is an organ from the circulatory system whose function is to pump the blood through the vessels in order to distribute the nutrients, gases, enzymes, metabolic waste, and cells that are dissolved in blood plasma. It is composed of two separate pumps that push blood through the peripheral organs (left part of the heart) and through the lungs (right part of the heart) [1].

The heart is divided into four chambers: right atrium (RA), right ventricle (RV), left atrium (LA), and left ventricle (LV). They are separated by cardiac valves: RA and RV are separated by the tricuspid valve, RV is separated from the pulmonary artery by the pulmonary valve, LA and LV are separated by the mitral valve, and LV is separated from the aorta by the aortic valve (Figure 1.1). The blood flows uninterruptedly to the atria through the cava and pulmonary veins and it is propelled outside the heart to the aortic and pulmonary arteries through the ventricles. That establishes a double circuit which is called the cardiovascular system.

1.1.1 Cardiac Cycle

The heart pumps the blood through the vessels by a continuous succession of contractions. Those contractions are related with a special mechanism which induces the constant functioning of the heart called cardiac rhythmicity. It spreads the action potentials all over the cardiac muscle to cause the heartbeat.

Originally, the heart is in a resting-state, with the atria filled with blood. Most of the cardiac cells are not auto-triggered, they need an external stimulus to trigger. There are some special cells in the sinoatrial node (S-A or sinus node) that are actually auto-triggered, and

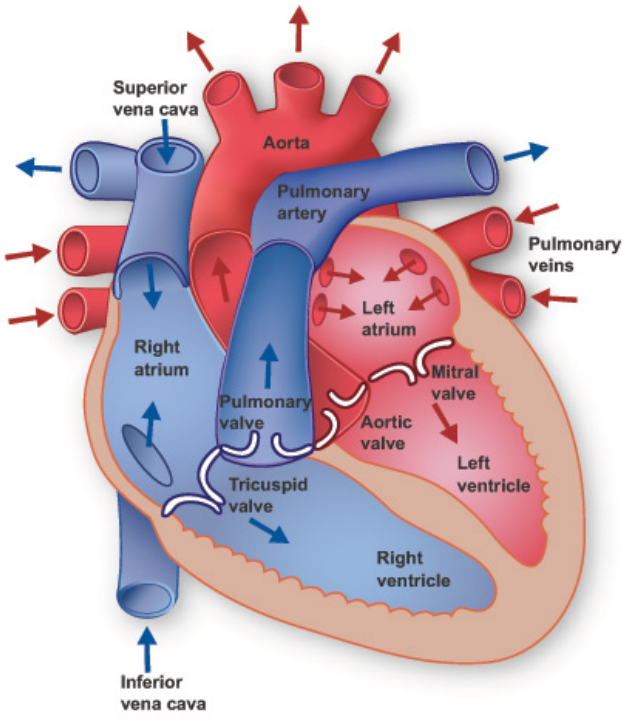

Fig. 1.1 Schematic illustration of the heart's anatomy. The arrows indicate the directions of the blood flow through the heart chambers and heart valves. Extracted from [2].

they are responsible for starting the cardiac cycle and its control. The action potential in the S-A node, which is allocated in the upper wall of the right atrium, will spread instantly to the atrial muscle wall due to its direct connection with the atrial muscle fibers, which empty the atria blood into the ventricles. The cardiac impulse is also propagated through the internodal pathways to the atrioventricular node (A-V node), located in the lower wall of the right atrium. The A-V node delays the impulse in order to allow enough time to complete the emptying of the atria. This process is called atrial systole.

The propagation continues crossing to the ventricles through the common bundle (His bundle or A-V bundle) in the continuous fibrous barrier. From this point, it divides through the bundle branches and later the Purkinje fibers, which innerves the entire ventricular chambers. Once the stimulus reaches the termination of the Purkinje fibers, the ventricular muscle mass depolarizes and contracts, provoking the ventricular contraction (or ventricular systole). In this part of the cycle, the blood is expelled from the heart by the ventricles through the arteries, irrigating the circulatory system with new blood and letting the heart at rest to re-fill the atria with new blood coming from the tissues and the lungs, and repeating the whole process [1].

1.1.2 Cardiovascular Diseases

Cardiovascular diseases (CVDs) are defined as every disease involving the heart or blood vessels [3], and they are among the most important health risks. They are the main death cause all over the world, so there are more people who die from cardiovascular disease than from any other cause. According to the World Health Organization, they provoke 17.9 million deaths per year, 31% of the total deaths in the world. CVDs are disorders of the heart and blood vessels, of which 85% of the deaths caused by them are due to heart attacks and strokes [4].

Personal, familiar, and social costs related to these pathologies are immeasurable. The total economic cost was $863B in 2010, approximately $151 per capita cost, which is detached from direct healthcare costs (55%) and productivity losses (45%). Furthermore, this value is predicted to rise to approximately $1,044B by 2030 [5].

Some of the most important CVDs are coronary artery diseases, which include angina and heart attack, or myocardial infarction; stroke; heart failure; hypertensive heart disease; rheumatic heart disease; heart arrhythmia; congenital heart disease, and valvular heart disease [3]. Most of these pathologies involve the heart and its functioning, which are called cardiopathies. Subsequently, some of these pathologies will be described to understand the affected mechanism, and far ahead, it will be related to some diagnosis techniques.

The American Heart Association (AHA) states that most cases are preventable by early detection. By being aware of the first signs of CVD, there will be a better chance of catching the illnesses at the beginning, with a probably most promising prognosis. Early detection of cardiovascular disease can be the difference between life and death. Some of the most important ways to assess the risk of getting CVD is to research the family history or to acquire and to analyze the electrocardiogram (ECG) signal of the patient's heart [6], which is the electrophysiological technique in which this work will focus for the rest of the study.

1.2 Electrocardiogram

The electrical activity of the heart can be characterized by measurements acquired at different locations, namely, intracavitary, at the epicardium, or on the body surface. The current study will focus on electrocardiographic measurements, while the study of the action potentials occurring in cardiac cells is also critical for understanding the mechanisms which underlie some cardiac disorders, for instance, arrhythmias [7].

An electrocardiogram is an electrophysiological tool to represent the electrical response of the heart which is recorded by electrodes placed on the body surface. The alterations of potentials measured by the electrodes are provoked by the action potentials of the cardiac

cells, which cause their contraction. Figure 1.2 illustrates that a typical ECG wave during each heartbeat is formed as the sum in time and space of many different waves coming from different parts of the heart. Furthermore, the ECG does not describe the direct measurement of the alterations in the membrane potential across the cell. It describes the electrical current generated in the extracellular matrix by these alterations in the membrane potential [8]. As [9] refers, the electrocardiogram is defined as a linear recording over time of the electrical activity of the heart, in other words, depolarization and repolarization of the cardiac muscle.

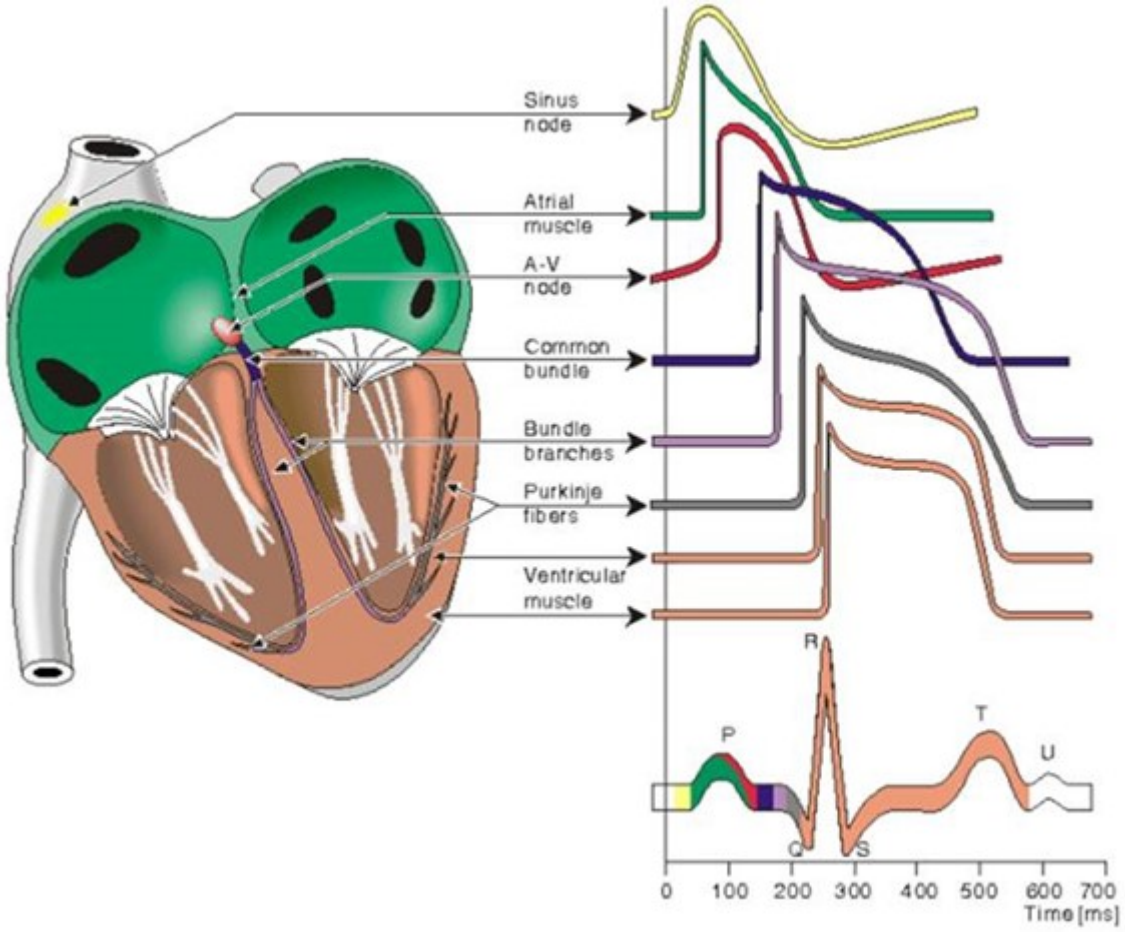

Fig. 1.2 Electrical activity of each part of the heart and the ECG wave representation according to the sum in time and space of them. Extracted from [10].

For each heartbeat, the ECG shows the P wave, which corresponds to the electrical potential of the atria depolarization. It also records the QRS complex, which is actually composed (but not always) of three separate waves (Q wave, R wave, and S wave), and it is related to the propagation wave of the ventricular depolarization. Finally, the T wave characterizes the ventricular recovery from the state of depolarization. Furthermore, the isoelectric line present among these waves has a physiological meaning and is also an

important parameter. These baselines are characterized by the peaks between which it is placed as, for instance, PR or ST segments.

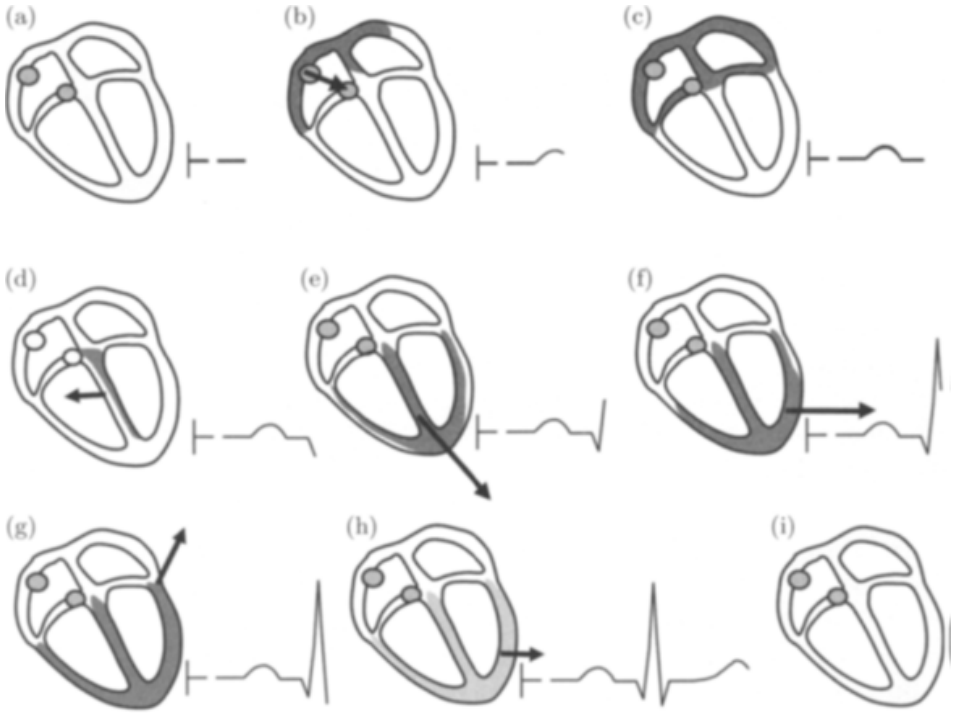

Fig. 1.3 Dominant vector along the heartbeat asides the resultant ECG recorded by an electrode allocated in the symbol. (a) shows the heart with all cardiac cells at rest, (b) shows the atrial depolarization, (c) the AV node being crossed by the electrical impulse, from (d) to (g) shows the ventricular depolarization, as (h) ventricular repolarization. Finally, (i) represents again all cardiac cells at rest. Extracted from [8].

For a better understanding of the ECG waves, it is common to use the dipole/vector representation. Each group of cardiac cells that depolarize together instantaneously can be represented as a dipole of current. This defines a certain dipole moment for a certain instant and in a defined volume, which integrated into the total surface of the heart gives rise to the finite dipole which facilitates the study of the electrical activity of the heart. As we can see in Figure 1.3, all vectors associated in a certain time-lapse can be summed into a unique vector, which is called dominant vector. The projection of this vector is the information which appears in the ECG signal.

The dipole can be associated to a vector that defines it, associating it with an orientation and a magnitude, as well as its variation over time. The orientation is defined as the direction in which the electrical potential is being generated, with the arrowhead in the positive direction.

Both monopoles are considered to be of opposite sign, but of equal magnitude, I_0, and are separated by a distance d. Considering a unit vector $\vec{u}$ that defines the direction of the link between the monopoles, the dipole can be defined as [11, 12, 13]:

$$\vec{p} = I_0 d\vec{u} = I_0 \vec{d} \tag{1.1}$$

Each unitary dipole $\vec{i}$, $\vec{j}$ and $\vec{k}$ has in its axis a different orthogonal decomposition called $p_x\vec{i}$, $p_y\vec{j}$ and $p_z\vec{k}$. By linearity, the dipole p can be decomposed into the sum of its three orthogonal components [11]:

$$\vec{p} = p_x\vec{i} + p_y\vec{j} + p_z\vec{k} \tag{1.2}$$

Each one of these dipoles will present a c value and will generate a potential called $\emptyset_P$ in point P. Like the vector $\vec{p}$, the coefficients $c_{i,j,k}$ can be simplified as the components of a vector $\vec{c}$, called an electrocardiographic vector, so that the potential at P is defined by the following equations [11, 13]:

$$\emptyset_P = c_x p_x + c_y p_y + c_z p_z = \vec{c} \cdot \vec{p} \tag{1.3}$$

The cardiac dipole $\vec{p}$ contains information that varies over time but is independent of the measurement point P, while the electrocardiographic vector $\vec{c}$ also contains geometrical information, so it depends on both time and position of P [11, 13].

In order to measure the electrical activity of the heart, a set of electrodes is placed on the skin. They are allocated in a certain way so they can reasonably record the spatiotemporal variations of the cardiac electrical field and may allow their use in clinical procedures. In the ECG context, a lead is defined as the potential difference between a pair of electrodes.

A lead is called monopolar when it reflects the variation of a unique electrode relative to a reference electrode or to a "central terminal", which is a defined reference, for instance, the Wilson central terminal. That reference point's voltage must not change too much during the cardiac cycle. Also, a lead is called bipolar when the voltage recorded is the difference between two electrodes allocated in, for instance, P_i and P_j. Therefore, these points have not been referenced to zero, but as it has been shown that a dipole $\vec{p}$ allocated at a specified point Q has a potential [11, 12]:

$$\emptyset = \vec{c} \cdot \vec{p} \tag{1.4}$$

Thus, the potential difference between $\emptyset_i$ and $\emptyset_j$, which are the potentials in points, P_i and P_j, can be described as follows, and decomposing its potentials, looks like:

$$V_{ij} = \emptyset_i - \emptyset_j = \vec{c}_i \cdot \vec{p} - \vec{c}_j \cdot \vec{p} = \vec{c}_{ij} \cdot \vec{p} \tag{1.5}$$

In this way, the potential difference V_{ij} can be defined as follows, where $\vec{c}_{ij}$ is the electrocardiographic vector of the V_{ij} lead [9, 11, 13]:

$$V_{ij} = \vec{c}_{ij} \cdot \vec{p} \tag{1.6}$$

It is a very common practice to record the ECG with a multiple combination of leads, which includes unipolar or bipolar leads, or both [8]. Later, a complete section will be dedicated to the study of ECG leads.

1.2.1 Ambulatory ECG

As mentioned before, the ECG is a non-invasive technique widely applied for cardiac disease diagnosis. To increase diagnostic sensitivity, ECG may be acquired during exercise, such as in stress tests or in an ambulatory system, as symptoms may occur while the doctor is not monitoring him/her. Ambulatory ECG (aECG), or long-term ECG, is a non-injurious test widely used to assess electrocardiographic abnormalities in a patient in a wide spectrum of cardiopathies. aECG is based in the capability to continuously monitor a patient over a huge period of time, which allows the patient to develop his/her normal activity and also to address the ECG study sideways different physical, psychological, and environmental states [14]. In addition, aECG principles may be also used in emergency conditions, such as transferring a patient with symptoms to the hospital, which allows for less intrusive follow-up that allows technicians to operate on the subject more efficiently, who may benefit from early interventional therapy [15, 16].

Traditionally, standard ECG provides a wide approach and a short time image from 12 standard leads, as it will be shown later, which records the electrical activity of the heart for a short period of time, about 10 to 30 seconds. On the other hand, the 24-hour (generally) aECG provides a narrower view of the data, using only 2 or 3 leads (The recorded leads are often V1 and V5, making a bipolar lead between them, and sometimes it is also added an additional modified lead aVF [17]), but with the ability to record dynamic changing electrical phenomena of the heart, which are often transient and short-lived. aECG provides a record of past events that allows an exhaustive and detailed analysis of dynamic and transient electrocardiographic changes, as well as allows online monitoring. Nowadays, recent innovative technology has attempted to introduce 12-lead technology, although this transition in the aECG has not been definitively established [18].

aECG has been shown to be the best electrocardiographic test, compared to others, in the detection of spontaneous cardiac arrhythmias, which are characterized by their great variability. In addition to the diagnosis of cardiac tachyarrhythmias and bradyarrhythmias, aECG has also become a very useful tool in the study of, for example, elevation of the ST segment in myocardial ischemia, and measurements of the QRS complex in abnormalities in ventricular repolarization [14].

State of the Art

Many physicians and scientists in general have worked on the development of aECG, which is why we now have a wide spectrum of options to use for this purpose, both in the form of conceptual designs or scientific approaches as in final commercial products already on sale.

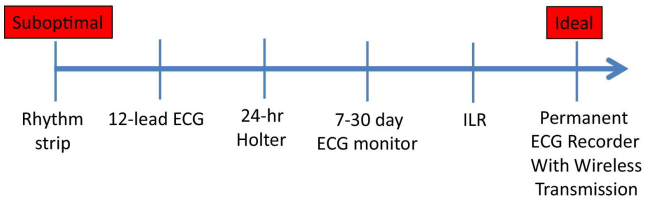

Fig. 1.4 Spectrum of aECG monitoring modalities. "As one moves from left to right, the duration of monitoring increases, which in turn increases the diagnostic yield. ILR = implantable loop recorder." Extracted from [19].

While the devices shown in Figure 1.5 are related to the atrial fibrillation identification, there is a significant representation of the different approaches most used for aECG systems. Most systems focus on the measurement of the RR interval [19, 20, 21], used to obtain the heart rate variability, despite it provides a rather poor diagnostic yield (Figure 1.4). There are several types of aECG monitoring devices which have been developed to face up different clinical situations. These types include Holter monitors as such, event monitors, patch monitors, and implantable monitors. Furthermore, consumer devices are now available that can perform some of the functions of aECG monitors.

A Holter monitor (Figure 1.5, A.A) is an aECG monitoring device which has several leads plugged into a portable battery-operated recording device. The device is worn for a short period of time (commonly between 24 and 48 hours), recording the heart electrical activity during that time. Once the recording is finished, the record is analyzed to look for possible pathologies or arrhythmias that occurred during that period. It is necessary to return the Holter recorder once the recording has finished, and it is not a real-time diagnostic device. On the contrary, once the specialist receives the Holter, he/she processes the record using specific software to analyze the variation of the heartbeat, reporting parameters such as the

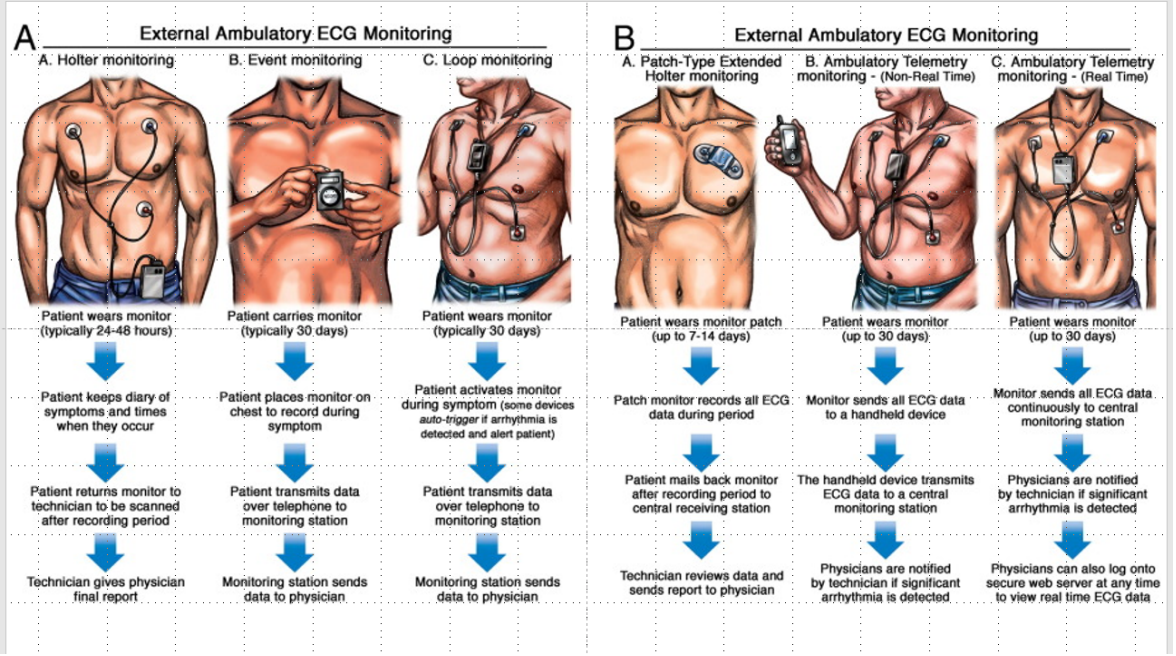

Fig. 1.5 *"Types of AECG Monitors Currently Available in Clinical Practice: (A) Holter, event, and loop monitoring; (B) patch-type extended Holter and ambulatory telemetry monitoring. AECG = ambulatory external electrocardiographic; ECG = electrocardiographic. Figure illustration by Craig Skaggs".* Extracted from [19].

maximum, minimum, and average heart rates, the total number of premature atrial complexes, and premature ventricular complexes and any episodes of possible ischemia [14, 19]. These monitors give the most detailed information of all the aECG monitors, but they can do so only for limited periods of time. So, it is commonly used for reporting frequent unexplained symptoms, which may occur during any given 24 - 48-hour period.

Event monitors (Figure 1.5, A.B-C and B.B-C) differ from the common Holter monitors in that they do not record the entire heart rate during the entire period of time it is worn, but only capture the specific episodes associated with arrhythmia. There are two types of event monitors, one is worn 24 hours a day and only records the events associated with arrhythmias, and the others are devices that the patient places on their body only when symptoms associated with their pathology are detected. Many of these devices are already designed to automatically send the record associated with the episode to the clinician. However, many of them still require further processing and are not designed to perform an emergency response to the arrhythmia. However, the time interval between the arrhythmia being detected and processed is greatly reduced.

Patch monitor (Figure 1.5, B.A) may be considered as a minimalist version of the devices mentioned above. Its function is the same, to record and store or transmit the heartbeat, but

all the electronics are embedded in a single device very compact and small that can be carried as a patch attached to the body. Currently, the most used device in this respect is the Zio® patch XT (iRhythm) [22].

Implantable monitors (not shown in Figure 1.5) differ from the other devices mentioned above. These, as their name suggests, are implanted in the body, under the patient's skin, and function for years. Their mechanism is similar to event monitors, also called loop recorders. However, these devices require a surgical implantation operation, making them unattractive devices for most cases in which an aECG is necessary.

Smartwatches and wristbands equipped with heart rate monitoring capabilities have revolutionized personal health tracking. These wearable devices utilize optical sensors or ECG technology to continuously monitor the user's heart rhythm throughout the day. The real-time data collected provides users with valuable insights into their cardiovascular health, allowing them to track changes, identify patterns, and make informed decisions about their sports training. In the clinical field, the ability to detect irregular heart rhythms or anomalies can serve as an early warning system for potential health issues [23]. As technology continues to advance, these devices are likely to play an increasingly significant role in preventive healthcare, as some of them are starting to certificate their products as medical products.

After nearly half a century of research, aECG or long-term ECG has been shown to be one of the most cost-effective non-invasive clinical tools in the diagnosis and evaluation of cardiac symptoms, determination of prognosis or risk stratification in diverse populations, and in the evaluation of many cardiac therapies. For this reason, we consider the aECG as the objective of our study, seeking to approximate the imminent union between the conventional recording of the 12-lead system and the long-term monitoring by working on cardiac leads and their physiological understanding. Therefore, the reconstruction of the 12-lead system from a reduced electrode system that can be implemented in an aECG device is an interesting approach, which will be developed in this Thesis. Following, we will explain how this 12-lead system and other lead systems are used in clinical practice.

1.2.2 ECG Leads

As mentioned before and represented by Equation 1.5, an ECG lead is defined as the potential difference between a pair of electrodes:

$$V_{ij} = \emptyset_i - \emptyset_j \tag{1.7}$$

The information that provides one certain lead is very useful, as there may be information in that lead that is not noticeable or hardly noticeable in the rest of leads. Therefore, a great

variety of electrocardiographic leads have been created to try to answer all the questions that cardiac pathologies pose.

Standard 12-Lead System

Frontal Leads (bipolar): In 1912, Einthoven addressed the Chelsea Clinical Society in London and described an equilateral triangle formed by his standard leads I, II, and III, later called 'Einthoven's triangle' [24]. The bipolar leads correspond to the standard leads of the extremities, which are V_I, V_{II}, and V_{III}; or I, II, and III. By convention, V_I has the positive electrode on the left arm and the negative electrode on the right arm, and therefore measures the potential difference between the two arms. On the other hand, in V_{II}, the positive electrode is on the left leg, and the negative electrode is on the right arm. Lead V_{III} has the positive electrode on the leg and the negative electrode on the left arm. Therefore, these leads present the following equations [11, 12, 24]:

$$V_I = \emptyset_L - \emptyset_R \tag{1.8}$$

$$V_{II} = \emptyset_F - \emptyset_R \tag{1.9}$$

$$V_{III} = \emptyset_F - \emptyset_L \tag{1.10}$$

Where $\emptyset_R$ is the potential in the right arm, $\emptyset_L$ is the potential in the left arm, and $\emptyset_F$ is the potential in the left leg.

Augmented Frontal Leads (bipolar): In 1934, Frank Wilson joined the wires from the right arm, left arm, and left foot with 5000 Ohm resistors, defining an 'indifferent electrode' later called the 'Wilson Central Terminal' (WCT). As mentioned before, the reference used for this purpose must not change too much during the cardiac cycle. It can be shown that the WCT has a potential very close to zero and can be expressed as:

$$\emptyset_{WCT} = \frac{\emptyset_R + \emptyset_L + \emptyset_F}{3} \approx 0 \tag{1.11}$$

The combined lead acts as ground and is attached to the negative terminal of the ECG. An electrode attached to the positive terminal then becomes 'unipolar' and can be placed anywhere on the body. Wilson defined the unipolar limb leads VR, VL, and VF, where 'V' stands for voltage [26]. Later, in 1942, Emanuel Goldberger increased the voltage of Wilson's unipolar leads by 50% and created the augmented limb leads aVR, aVL and aVF, turning the WCT into the average of the potentials of the other two extremities which can be expressed as follows [11, 12, 24, 25]:

$$V_{aVR} = \emptyset_R - \frac{1}{2}(\emptyset_L - \emptyset_F) \tag{1.12}$$

$$V_{aVL} = \emptyset_L - \frac{1}{2}(\emptyset_R - \emptyset_F) \tag{1.13}$$

$$V_{aVF} = \emptyset_F - \frac{1}{2}(\emptyset_R - \emptyset_L) \tag{1.14}$$

Precordial Leads (unipolar): The precordial leads are unipolar electrodes positioned in succession on the front and left side of the chest to make available a more detailed view of the heart activity, added to the limb leads information. The six precordial leads, labeled from V1 to V6 by convention, are related to the WCT. Leads V1 and V2 primarily reflect the activity of the right ventricle. Leads V3 and V4 primarily view the front of the left ventricle (anterior wall), while its side (lateral wall) is viewed by V5 and V6 [8]. In general, the ECG waveforms of the six limb leads have relatively low amplitude and tend to be noisier, lower signal-to-noise ratio than the precordial leads since the electrodes are positioned on the extremities at larger distances from the heart.

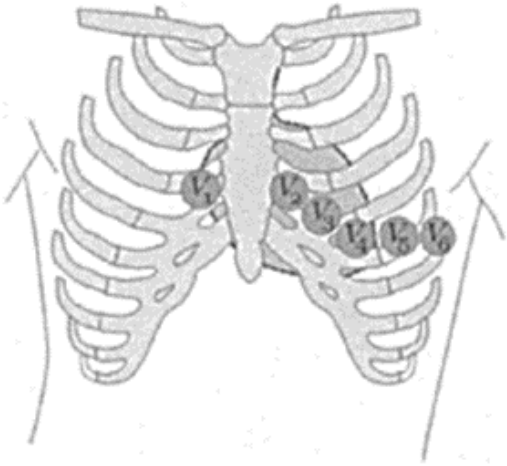

Fig. 1.6 Representation of the Precordial leads (V1-V6), which are also referred to the WCT. Part of the standard 12-lead system, combined with Figure 1.7. Extracted from [8].

When added to Einthoven's three limb leads and the six chest (precordial) leads, we arrive at the 12-lead electrocardiogram that is used today.

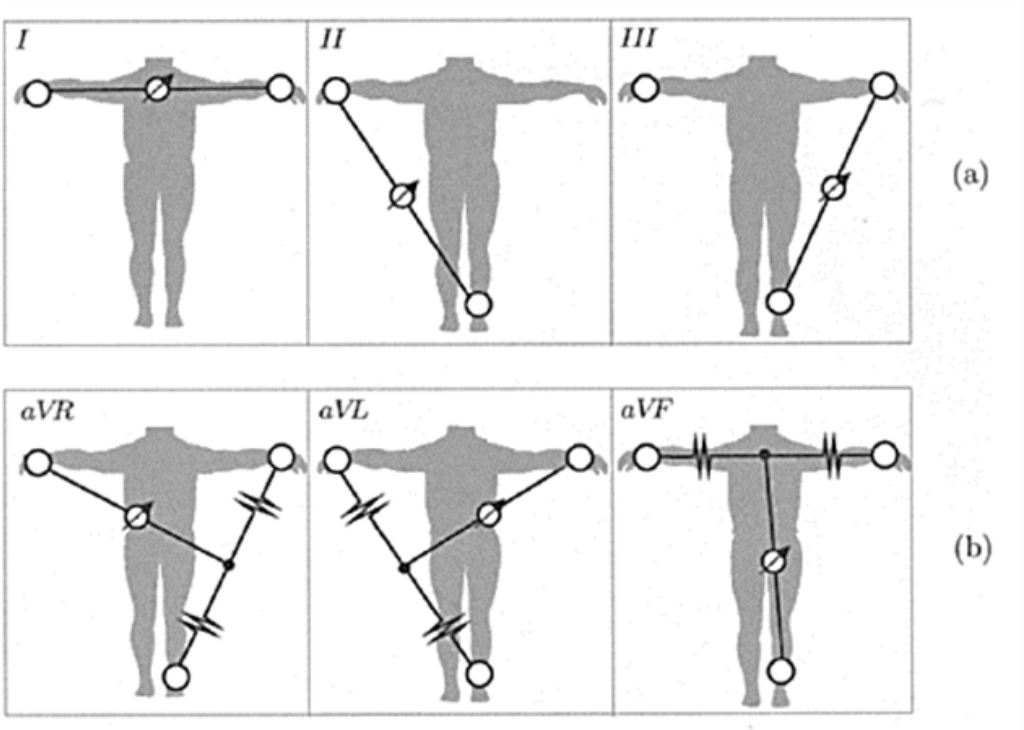

Fig. 1.7 The position of the recording electrodes in (a) corresponds to the bipolar limb leads I, II, and III (together these three leads define Einthoven's triangle), (b) corresponds to the augmented unipolar limb leads aVR, aVL, and aVF (the output signal is measured between the two resistors or by using the WCT). These are the so-called "Frontal leads". Part of the standard 12-lead system, combined with Figure 1.6. Extracted from [8].

Right-sided and Posterior Precordial Leads

Under certain pathological conditions, it is necessary to extend this system by using additional electrodes on the right side of the patient's torso or on the patient's back. These electrodes form what are known as right precordial leads and posterior precordial leads, respectively. They are very useful in the diagnosis of certain pathologies of difficult detection using only the standard.

For example, right precordial leads are useful in pathologies such as acute anterior myocardial infarction [26] or acute inferior wall myocardial infarction [27]. These leads are located symmetrically to the common precordial leads and are denoted by the name of their counterpart plus a capital R, e.g., V3R.

On the other hand, posterior precordial leads are useful in the study of pathologies related to posterior myocardial infarction [28]. They are placed after the V6 lead and are denoted with the numbers 7 to 9, e.g., V7-V9.

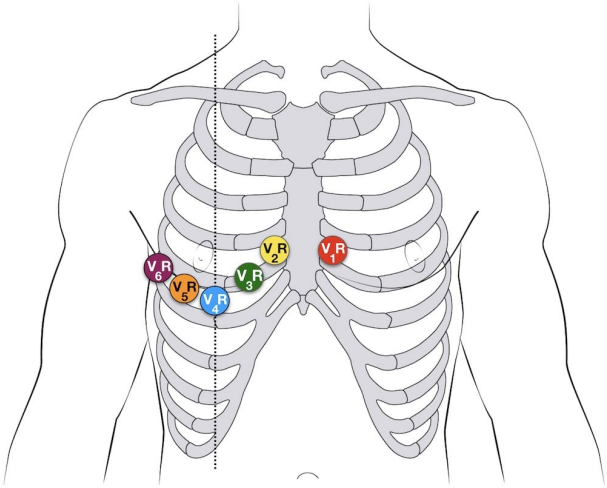

Fig. 1.8 Right precordial leads placement. These leads are located symmetrically to the common precordial leads and are denoted by the name of their counterpart plus a capital R, e.g., V3R.

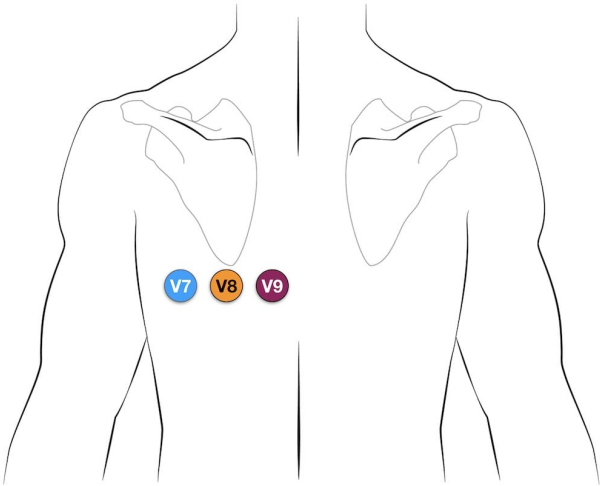

Fig. 1.9 Posterior precordial leads placement. V7 is placed in the left posterior axillary line, in the same horizontal plane as V6, V8 is allocated on the tip of the left scapula, in the same horizontal plane as V6, and finally V9 is over the left paraspinal region, in the same horizontal plane as V6 [28].

Mason-Likar's Leads

In some situations, the standard 12-lead system is presented as an impractical and inconvenient system to use. Placement of electrodes in areas such as extremities causes noise due to muscle contraction, or myoelectric noise, to worsen the signal-to-noise ratio and make it difficult to extract information from it [29]. For instance, in medical tests where the ECG

reading is required during physical exercise, the Mason-Likar 12-lead system is shown to be an efficient alternative for this purpose.

In this system, the electrodes corresponding to the joints are positioned on the torso, thus reducing myoelectric noise and motion artifacts. The precordial leads are not altered and remain in their original place. The electrodes corresponding to the upper extremities are allocated in the intraclavicular fossae slightly below the lower edge of the clavicle, in the medial area of the deltoid muscle. The electrodes corresponding to the lower extremities are placed in the anterior axillary line. The right lower electrode serves as the ground as in the standard 12-lead system (Figure 1.10).

Despite the fact that the system is very similar to the previous one, there are deformations in the representations of the extremities leads, such as, for example, the masking of the Q wave. The main difference between standard 12-lead and Mason-Likar is the extremity front leads electrodes placement [30].

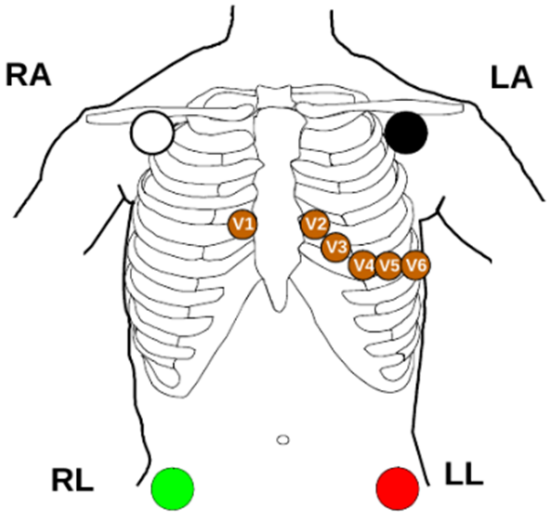

Fig. 1.10 Mason-Likar 12-lead system. The precordial leads are in the same position as in standard 12-lead system. The difference lies in the extremities electrodes position, which are now placed in the torso.

Fontaine Leads

Fontaine leads were designed by Guy Fontaine in 1977 to assess specifically the potentials developed in the right ventricle [31]. Epsilon waves are small positive deflections hidden in the end of the QRS complex. They appear in arrhythmogenic right ventricular dysplasia (ARVD). ARVD is an inherited myocardial disease associated with paroxysmal ventricular arrhythmias and sudden cardiac death. ARVD is characterized by fibro-fatty replacement

of the right ventricular myocardium [30, 32]. The three Fontaine bipolar precordial leads (Figure 1.11) are FI (manubrium sternum negative, xiphoid positive), FII (manubrium sternum negative, V4 location positive) and FIII (xiphoid negative, V4 positive). The vertical bipolar lead FI, (like aVF lead), seems to be the most appropriate to record epsilon waves; and it also magnifies the atrial potential.

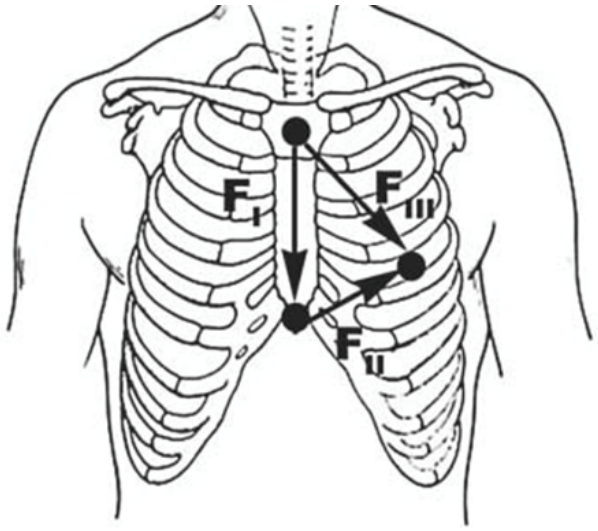

Fig. 1.11 The Fontaine bipolar precordial leads. Extracted from [30].

Frank Lead System

As shown above, the cardiac vector is not static, but varies over time both in orientation and magnitude, depending on the direction and intensity of the activity of the cardiac cycle. To represent these changes over time, and not just show their projection value in a lead, a technique called Vectorcardiography (VCG) is used. VCG is an electrophysiological method to record the heart activity by using a continuous series of vectors which form curves around a central point called zero reference point, which will be the origin of the representation of all the following cardiac vectors throughout the cardiac cycle [1].

Orthogonal Leads, XYZ or Frank Lead system, were developed in the mid ‘50s by E. Frank [33] to apply the VCG. As the cardiographic vector is found in a three-dimensional space, the idea is to seek the reconstruction of it from three leads as orthogonal as possible to each other capturing all the electrical information, represented by the transversal (X), longitudinal (Y) and anteroposterior (Z) axes, as seen in Figure 1.12. With this orthogonality, the maximum possible projection of the cardiac vector is found, which yields the best quality for the signal obtained, that is, the greatest amount of information from this vector [34].

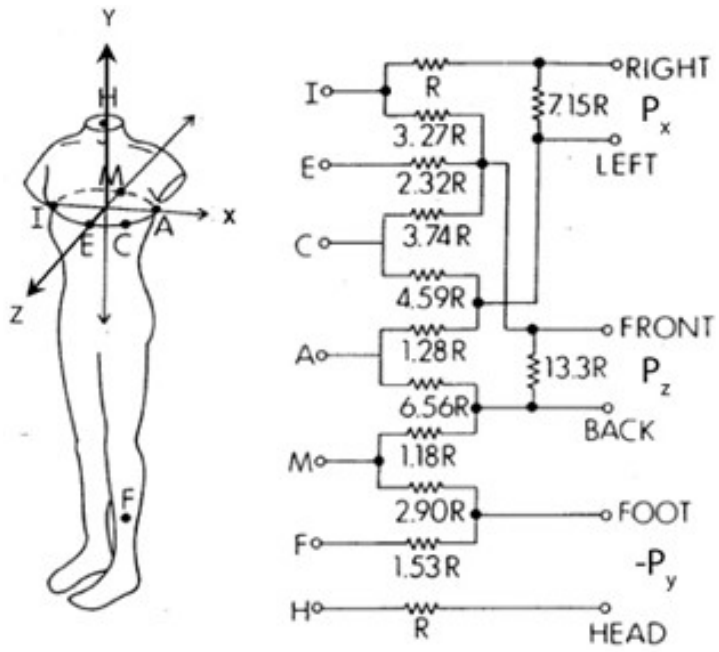

Fig. 1.12 Frank Lead system to record the three-dimensional projection of the heart dipole. The circuit shown was originally used to obtain the three virtual leads through relationships between the electrodes placed in positions I, E, C, A, M, F, and H. It can be seen how for vertical projection, Py, the electrodes M, F, and H are used. For horizontal projection, Px, the electrodes A, C, and I are used. And finally, for transverse projection, Pz, the electrodes I, E, C, M, and A are used this time to recreate the virtual lead. Extracted from [33].

EASI Lead System

As mentioned above, the Frank Lead system provides the best representation of the cardiac vector by obtaining the greatest orthogonality among its leads, which translates into the maximum projection of the cardiac vector in each lead. Based on these principles, the EASI Lead system was developed in 1988 by Dower [35]. Moreover, electrodes E, A, and I are also used by this system (seen in Figure 1.13), plus an additional electrode S, located on the manubrium sterni [30, 36].

The EASI system is composed of the bipolar leads ES, AS, and AI, which form a quasi-orthogonal signal, x'y'z', that can be approximately transformed into orthogonal XYZ signals by means of a matrix derived from the EASI lead vectors. The result forms a good basis for deriving the 12-lead ECG, using previously published coefficients for the Frank lead system [35].

Although the topic of reconstruction of ECG leads will be developed below, it is noteworthy that EASI possesses great strength in the reconstruction of the standard 12-lead

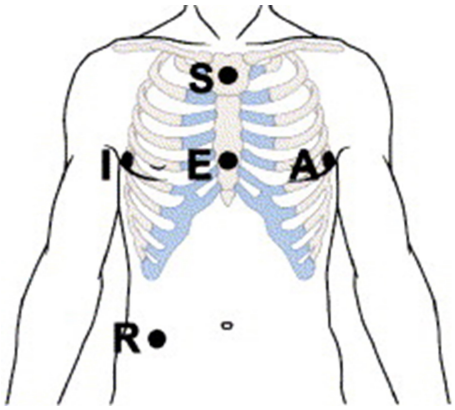

Fig. 1.13 EASI Lead system, where only five electrodes are necessary. Electrodes E, A, and I are the same as XYZ Lead. S is allocated on the manubrium sterni and ground R is placed at any convenient location. Extracted from [36].

system. This allows for a high degree of diagnostic precision with a much smaller number of electrodes and wires, with the advantages that this entails [37].

EASI leads are easier to apply in aECG than the other leads. Due to the smaller number of electrodes and wires, it provides a better adaptability and satisfaction to the patient. Despite Mason-Likar has less troubles during his application during exercise recording than standard 12-lead, EASI is less susceptible to myoelectrical noise than Mason-Likar, which is less susceptible to myoelectrical noise than standard 12-lead. However, both EASI and Mason-Likar leads are affected by baseline wander in a similar way [29].

1.3 ECG Reconstruction

The continuous recording of the 12 leads commonly used in electrocardiography comes with some complications. Placement and monitoring of this placement are crucial for obtaining a quality and interpretable ECG signal, as well as reducing the risk of misdiagnosis.

The greater the number of electrodes, the greater the risk of problems related to the adhesion of an electrode or the deterioration of a wire and its connection to the recording device. This also applies to moving artifacts, which will be greater if there are more cables that may be involved in the appearance of this noise [29]. In addition, a larger number of electrodes increases the risk that the placement of electrodes may vary along the different registers taken, which in turn increases the risk of ECG signal deviations due to this [38]. Many times, it is not possible to have all the electrodes available for recording. For example, during and after cardiac surgery, V1 and V2 electrodes cannot be placed.

To avoid all these complications, the reconstruction of ECG leads is a useful tool of increasing importance. Most reconstruction techniques are used to reconstruct any unavailable leads from the redundant information inherent in the 12-lead system. Based on the initial assumption that the electrical activity of the heart can be represented by a dipole model, or a cardiac vector, only three orthogonal leads will be necessary for the complete reconstruction of the heart [39]. Computerized algorithms have been developed to reconstruct the ECG of missing leads [40]. In the beginning, a set of reduced leads of the 12-lead system was used, such as the II, V2, and V6 leads [41]. Dower later used a sub-system of Frank's leads, the EASI system, from which to extract the 12-lead standard system [35]. These methods have in common the use of a unique matrix from which to extract the general coefficients, preventing the specific reconstruction for each patient, with the problems that this entails.

Reconstruction can be done by using either general or patient specific models [30]. The dilemma between general reconstruction versus specific reconstruction was studied by [39], which concludes that a higher level of accuracy in the reconstruction is possible using specific models in comparison to general models, decreasing the deviation in the results for each patient.

To support the reason for using these methods, it has been shown that limited lead systems have faithfully reproduced the information contained in the standard 12-lead system. This has been demonstrated through accurate reconstruction of the original 12-lead ECG waveforms and through accurate diagnosis of abnormalities using derived ECG leads. In conclusion, limited lead systems will play an important role in ECG recording in the future, both to recover temporarily missing or degraded lead or allowing the use of less channels to increase the wearability of aECG monitoring [42].

To carry out this reconstruction of the ECG signal, many studies have been published over time that use a wide range of methods. The most relevant ones will be described below.

Linear regression

Linear regression reconstruction models are based on the cardiac vector reconstruction by using its projections in the obtained leads. This is carried out using linear regression adjustment, the oldest and most widely used method. The goal is to minimize the sum of the errors squared to fit a straight line in the data set.

Thus, the potential measured at an arbitrary point of the body can be defined in Equation 1.15 as the projection of the cardiac vector, $\vec{H}$, with the corresponding vector generated from pointing to that point from the midpoint of the cardiac vector, $\vec{L}$ [43]:

$$V = \vec{H} \cdot \vec{L} = aX + bY + cZ, \tag{1.15}$$

where $\vec{H} = X\vec{i} + Y\vec{j} + Z\vec{k}$ and $\vec{L} = a\vec{i} + b\vec{j} + c\vec{k}$. Furthermore, X, Y, and Z coefficients can be replaced by any set of leads due to the linear condition of the cardiac model. In addition, a, b, and c are the transformation coefficients that can be modeled by the Least-Squares Linear Regression model, providing the following solution for, as instance, three independent leads, $L_{1,2,3}$:

$$\begin{bmatrix} a_i \\ b_i \\ c_i \end{bmatrix} = \begin{bmatrix} \sum L_1^2 & \sum L_1 \cdot L_2 & \sum L_1 \cdot L_3 \\ \sum L_1 \cdot L_2 & \sum L_2^2 & \sum L_2 \cdot L_3 \\ \sum L_1 \cdot L_3 & \sum L_2 \cdot L_3 & \sum L_3^2 \end{bmatrix}^{-1} \cdot \begin{bmatrix} \sum V \cdot L_1 \\ \sum V \cdot L_2 \\ \sum V \cdot L_3 \end{bmatrix}, \tag{1.16}$$

which can be written as:

$$NewLead = Coef1 \cdot \vec{Lead}1 + Coef2 \cdot \vec{Lead}2 + Coef3 \cdot \vec{Lead}3. \tag{1.17}$$

These coefficients can be applied globally, although different ECG wave morphologies can also be taken into account to select different coefficients for some waves. As suggested in past studies, we may use two different set of coefficients, one for the reconstruction of the general ECG and the other for the reconstruction of the much lower energy P wave [39, 44]. This will be taken into account later.

The EASI Lead system plays an important role in this method. Several works are proposed to obtain the 12-lead standard from this reduced number of leads for its reconstruction by means of general coefficients that can be reviewed to the application of specific coefficients for each patient [45]. In this aspect, it has been demonstrated that EASI, and as mentioned before, can properly reconstruct the standard 12-lead, providing similar results in pathologies diagnosis [36, 37, 42, 45, 46, 47].

Statistical methods

Subordinate to the linear regression model, statistical methods have been proposed to determine the best placement of electrodes for ECG recording or reconstruction.

To accomplish this, an exhaustive mapping of the patient's torso is carried out with electrodes, although they can also be placed on the back to obtain a better resolution. Then, all leads are analyzed to find the best values of the quality parameters as, for instance, the lowest Root Mean Squared error (RMS) and the highest correlation coefficient (CC), between the reconstructed leads, by using the studied lead, and the desired standard 12-lead.

Thus, some of the best matches were used to accomplish the reconstruction. These methods are currently used not only to obtain the best reconstruction of the standard 12-lead system [48] but also to obtain maximum information on certain morphologies such as, for example, atrial fibrillation [49, 50] or monitoring devices [51, 52].

Independent Component Analysis

Independent Component Analysis, or ICA, is a method of separating blind sources that extracts statistically independent sources, also known as independent components, or ICs. It is a method widely used in fields as diverse as filtering noisy images, audio tools or interpretation of electroencephalographic signals. In fact, this analysis has previously been used in the field of electrocardiography to extract and separate maternal and fetal ECG [53].

For this method, the rows of sources, s, are related to rows of observations, x, by the mixing matrix, A, which is commonly square:

$$x = As \tag{1.18}$$

Then, the ICs are obtained from the three-lead set, defined as the matrix of the observations x_{RLS}, from which each row contained samples of a sole lead taken during the training beat:

$$x_{RLS} = \begin{bmatrix} x_x \\ x_y \\ x_z \end{bmatrix} = As = \begin{bmatrix} a_x & b_x & c_x \\ a_y & b_y & c_y \\ a_z & b_z & c_z \end{bmatrix} \cdot \begin{bmatrix} IC_1 \\ IC_2 \\ IC_3 \end{bmatrix} \tag{1.19}$$

Hence, the patient specific 12-by-3 reconstruction transform matrix, A_r, is obtained using the pseudoinverse matrix, where x_{obs} is a matrix of the observed 12-lead during the single detected beat:

$$A_r = x_{obs} s^T (ss^T)^{-1} \tag{1.20}$$

In the studied publications, the results of this method have certain advantages and certain disadvantages. It needs a very short calibration time, using a single heartbeat to perform it. Two three-lead systems can be used: I, II, V2 leads, and Frank Leads. The percentual correlation obtained is above 96%, which is higher than other methods studied. The method balances signal propagation changes that occurred due to breathing, which provokes a reduced precision variation in the reconstruction between heartbeats, showing that this method might be robust to changes occurring after calibration [54, 55].

Artificial Neural Networks

Around the 1950s, new data processing systems based on a simplistic version of brain functioning emerged. These systems are called Artificial Neural Networks (ANN) and are one of the most widely used systems in the field of machine learning algorithms to date.

ANNs are widely used in applications as diverse as image recognition, system identification and control, 3D reconstruction, data mining or even medical diagnosis.

The functioning of a conventional ANN is based on a set of nodes called "neurons" that roughly mimic the functioning of a neuron in a real brain. These collect information through synapses, process it, and then emit another signal through synapses toward other neurons, thus allowing the transfer and processing of information. Thus, in an ANN, these signals are actually real numbers, which enter each neuron adjusted by a weight, which is what learning regulates. Inside the neuron, signals pass through a non-linear function and, after a threshold that determines if the signal is propagated or not, it continues towards the rest of the neurons connected to it [56].

As the machine learning algorithms that comprise the different types of ANNs, learning is carried out using examples, as these networks are not pre-designed for any specific purpose. Only through training and learning these networks accomplish their purpose. Neurons that form the network are usually aggregated in layers, which perform different tasks. The signal feeds the first layer, the input layer, and is processed by crossing several intermediate layers, or hidden layers, until it reaches the last layer, the output layer. There are circumstances in which ECG reconstruction is not optimally performed with linear approximations. In these cases, non-linear methods such as ANNs come into play, improving those aspects of the approach in which linear methods fail [57].

In the field of ECG lead reconstruction, the most common procedure is to use some lead signals as input parameters and then use them to reconstruct other leads at the output of the ANN, as shown in Figure 1.14. They may improve the ECG leads reconstruction obtained with linear regression [59, 58, 60, 61]. There are several ways to increase the performance of these systems, for example, by incorporating them into ANN committees to improve the output result and obtain higher accuracy [58] or by applying genetic algorithms for the extraction of learning data [60, 62]. Furthermore, this method is so robust that the differences between original ECG and the reconstructed ECG are due to electrodes movements or to the ECG differences along the day of recording, and not provoked by the method itself [59].

With the rise of the Deep Learning field, several teams are addressing this challenge using this approach, which has gained popularity in recent years. To do so, they use much more complex models with a high number of parameters to carry out this task. Some teams take advantage of the capability of memory recursive neural networks such as Long-Short Term Memory (LSTM) cells to perform this reconstruction [63]. Other studies have employed Convolutional Neural Networks (CNN), which also have some level of "memory" as the convolutional part takes several samples from previous and following stages [64]. Finally, regression trees are also analyzed as a possible choice to perform the reconstruction [65]. All

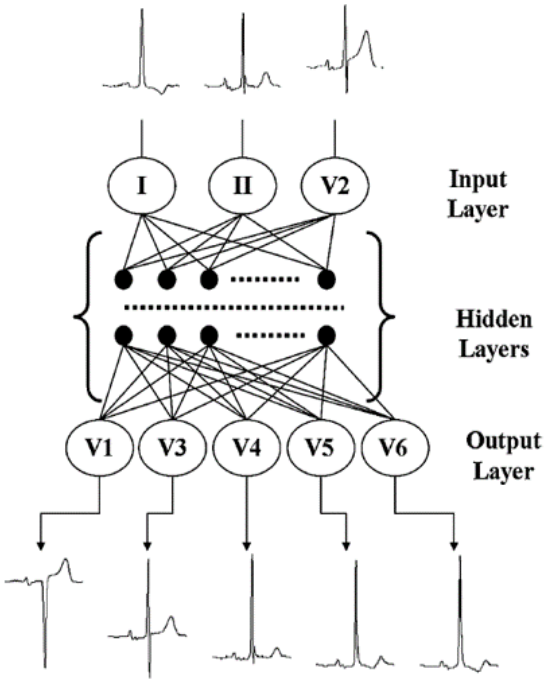

Fig. 1.14 ANN model for the reconstruction of five of the precordial ECG leads, in the output layer, from two frontal leads and one precordial lead in the input layer. As can be seen, the architecture of the model, such as the number of hidden layers or their size, is variable and must be adjusted to the type of problem we want to solve, as well as to the nature of the data available to train the network. Extracted from [58].

these models are computationally demanding, and the use of some memory involves some disadvantages when reconstructing abnormal events that have not appeared in the training stage. The drawbacks of this kind of methods will be studied in further chapters of this Thesis, showing that a different approach by using simpler models can perform the same task with the same, or even higher, level of accuracy.

1.4 Objectives

aECG is a powerful tool in the diagnosis and monitoring of possible heart diseases. The evolution of these technologies has increased the comfort of use, allowing longer records for improved diagnosis. Moreover, the possibility of obtaining the same information as with the older and redundant methods by the use of minimalist and much less cumbersome systems is a great advantage, both for long-term monitoring and for other possible applications such as emergency monitoring [15, 16].

At this point, ECG lead reconstruction methods come into play, allowing the reconstruction of reliable but very cumbersome systems, the standard 12-lead system, from a reduced number of electrodes. This means an increase in patient comfort and, if necessary, of the specialists working on the patient at the same time. It also means a decrease in many of the artifacts or complications that such a complex system, with so many components, may cause. This method allows all this while avoiding or minimizing the loss of information that may happen in older systems [29, 38, 39].

As previous studies suggest, this reconstruction is possible by means of the representation of the cardiac vector and its projections through the standard leads. This process is greatly improved by the use of orthogonal leads that obtain the best resolution of cardiac vector projections from which to reconstruct the rest [35].

When proposed as part of an aECG system, this reconstruction should take into account changes in the patient's position, which could modify the conditions of the reconstruction. However, it has been determined that a 12-lead electrocardiogram derived from a vector reconstruction can be used in different body positions without altering ECG parameters, so this aspect is not relevant to the study [66]. We will use this knowledge to develop a machine learning model. Which will be the final model is yet to be determined according to the results obtained by the thorough experiments carried out.

This model will be validated with data collected from several clinical trials developed in hospitals from Valencia, Spain. The first one will be dedicated to validate the model against several pathologies and conditions, as a proof of concept. The second one will be used to validate the algorithm and the system itself during the ambulatory operation where the final device is intended.

With a view to implement this system in a real situation, a patient-specific reconstruction system will be considered, which will allow for a more reliable reconstruction than general methods do [40]. For this reason, the study will include two parts, first studying which method of reconstruction provides the best results and then studying the best possible electrode placement to obtain the best reconstruction quality aligned with the needed requirements. All these processes must be deployed according to the clinical and regulatory entities' specifications. Why this is needed and how it does apply to this development will be fully explained in the following chapters, and good practices while developing fully operational software will be described.

1.5 Thesis Structure

The main objective of this Thesis is to develop an ECG lead reconstruction algorithm using machine learning in the context of ambulatory monitoring diagnosis. This Thesis will explore the process of how such a system with this kind of algorithm is developed and implemented in the context of an aECG recording device.

The content of the Thesis is organized as follows:

- **Chapter 1**, focuses on the motivation behind this Thesis and summarizes the main points from the fields of cardiology, electrocardiography, and the state-of-the-art of existing ECG lead reconstruction algorithms, which are addressed and needed in this work for a better understanding. Additionally, this introductory chapter establishes the specific objectives addressed in the Thesis and the resulting contributions to the field.

- **Chapter 2**, proposes using an aECG recording device with a low number of leads and then estimating the views that would have been obtained with a standard ECG location, reconstructing the complete standard 12-lead system, the most widely used system for diagnosis by cardiologists. Four approaches have been explored, including Linear Regression with ECG segmentation and Artificial Neural Networks (ANN). This chapter supports the hypothesis that it is possible to reconstruct the standard 12-lead system using an aECG recording device with less leads. The research described in this chapter generated the following publications:

  - Grande-Fidalgo, A., Calpe, J., Redón, M., Millán-Navarro, C., & Soria-Olivas, E. (2021). Lead reconstruction using artificial neural networks for ambulatory ECG acquisition. Sensors, 21(16), 5542 [67].

- **Chapter 3**, refines the previous algorithms trying to solve some problems encountered in the previous results. So, a brand new ECG lead reconstruction algorithm is proposed. A Fuzzy c-means clustering with a Linear Regression algorithm is proposed as the best option for the implementation of a reconstruction algorithm in the final device. It will be studied along with new features to ensure the robustness of the reconstruction in the "on air" mode and to ensure this model accomplishes the clinical specifications needed from the doctor's point of view. Also, we compare this algorithm with some recent algorithms employing Deep Learning to study the advantages and limitations of this kind of algorithms. The research described in this chapter generated the following patent:

  - Alejandro Grande, Javier Calpe Maravilla, Monica Redon Segrera, Venugopal Gopinathan, Tony Akl (2021). Electrocardiogram lead reconstruction using machine learning. (WO2022043196A1) WIPO (PCT) [68].

- **Chapter 4**, shows the results obtained for the previously proposed algorithm when assessed in the first clinical trial, which took place in the *Hospital Universitario Clínico de Valencia*, in association with the *Instituto de Investigación Sanitaria INCLIVA*. This chapter includes the outlines of the clinical trial report generated with some further clarifications and some new considerations of the final system. The clinical trial was carried out with 100 patients: 30 patients undergoing an ECG assessment as part of a preoperative test, and the remaining 70 patients visiting the cardiologist due to suspicion of cardiopathies and/or prescribed to undergo 24-hour Holter monitoring. The results from this research generated the following conference presentation:

  - Grande-Fidalgo, A., Calpe, J., & Soria-Olivas, E. (2023, September). Challenges in ECG Lead Reconstruction in Patients with Pacemakers and Implantable Defibrillators. In Proceedings of the 2023 10th International Conference on Bioinformatics Research and Applications (pp. 101-106) [69].

- **Chapter 5**, shows the results obtained for the proposed algorithm in the second clinical trial, which took place in the *Hospital General de Valencia* and approved by the *Agencia Española del Medicamento (AEMPS)*. This study includes the ambulatory assessment of the reconstruction algorithm in a real environment of device operation. New considerations must be addressed regarding the form factor and the specifications of a potential device. The clinical trial was carried out with 30 patients prescribed to undergo 24-hour Holter monitoring.

- **Chapter 6**, finally presents the conclusions of this Thesis along with considerations for future prospects.

Chapter 2

ECG Lead Reconstruction using ANN for aECG Acquisition

2.1 Introduction

As mentioned, aECG is a powerful tool in the diagnosis and monitoring of possible heart diseases. The evolution of these technologies allows longer records for improved diagnosis, as they are minimally intrusive, enabling normal activity and detection of infrequent arrhythmias. Moreover, the possibility of obtaining the same information as the older and more consolidated methods by the use of minimalist and much less cumbersome systems is a great advantage, both for long-term monitoring and for other possible applications such as emergency monitoring [15, 16], due to its simpler form factor.

At this point, ECG lead reconstruction methods come into play, allowing the reconstruction of reliable but cumbersome systems, such as the standard 12-lead system, from a reduced number of electrodes. This means an increase in patient comfort and, if necessary, of the specialists working on the patient at the same time; it also means a decrease in many of the artifacts or complications that such a complex system, with so many leads, may cause. This method allows all this, avoiding or minimizing the loss of information that the classical systems provided in real-world use cases [29, 38, 39].

As previous studies suggest, this reconstruction is possible by representing the cardiac vector and its projections through the standard leads. This process is greatly improved by the use of orthogonal leads that obtain the best resolution of cardiac vector projections from which to reconstruct the rest [35].

When proposed as part of an aECG system, this reconstruction should take into account changes in the patient's position, which could modify the conditions of the reconstruction.

However, it has been determined that a 12-lead electrocardiogram derived from a vector reconstruction can be used in different body positions without altering ECG parameters [66].

A patient-specific reconstruction system will be considered, which might allow a more reliable reconstruction than general methods do [40]. For this reason, the study will be performed in two stages, first studying which method of reconstruction provides the best results and then studying the best possible electrode placement to obtain the best quality in the reconstruction.

The hypothesis of this study is that it is possible to obtain a faithful reconstruction of the standard 12-lead system by means of a reduced system of electrodes located in the trunk of the patient, which will allow the design of a minimally intrusive system of aECG recorder. This section contains an adaptation of the published paper [67].

2.2 Objectives

The aim of this study is to refine an ECG reconstruction system that can be implemented on an aECG form factor. For this goal to be reached, two specific objectives have been defined:

- Proposing and developing the best ECG reconstruction methodology to be implemented in the aECG monitoring device. Different methods will be tested to carry out the reconstruction, from methods of normalization of the ECG signal through the use of linear regression with two sets of coefficients for different segments of the ECG waveform to the use of artificial neural networks. A fixed placement will be determined to evaluate these methods based on the best results obtained in the simplest and widely used reconstruction method, the linear regression. In addition, this placement must be located on the patient's torso to simulate the behavior of the final device as faithfully as possible.

- Optimization of the electrode placement for the best possible reconstruction quality. Thereafter, the chosen reconstruction method will be applied for the study of the final disposition of the electrodes, and an analysis of certain previously chosen evaluation parameters will be carried out. Due to the multiple locations for the leads, an initial study was carried out to reduce the number based on clinical and usability considerations. We impose certain lead allocation and combination restrictions to ensure a good ECG signal reconstruction and some technical boundaries. For instance, studies have demonstrated that SNR is admissible for each lead measured from electrodes placed 3 centimeters or further away from each other [52, 70]. Also, we may consider allocating the electrodes in the patient's back to obtain the lead's highest orthogonality [33].

2.3 Materials and Methods

2.3.1 ECG Recordings

Electrocardiogram records lasting between 60 seconds and 120 seconds were collected, accomplishing GDPR regulation by ensuring full patient anonymization. They were taken in a supine position with the patient completely relaxed to mitigate movement artifacts. The number of records differs from the number of patients since more than one record was taken for each patient. A total of 25 records from 11 patients were used in this work. This is an initial study to validate the viability of the idea before running a complete clinical study.

However, in order to evaluate the quality of the recorded signals, an evaluation algorithm was designed based on [71], in which the records are evaluated for motion artifacts, electrode movements, baseline wandering, and high-frequency noises, among others. The records that did not pass this test were discarded so that they did not worsen the results by affecting the reconstruction, which would distort the conclusions of this initial study. This reduced the number of available records to 20 from 7 different patients, five men and two women, aged 23 to 54 years, with different morphologies. One of them presented a right bundle branch block, and another one had premature ventricular contractions. Despite the presence of abnormal events or conditions, it is noteworthy that this does not allow us to affirm its validation for reconstructing cardiac pathologies, and this should be explored further.

The robustness of the reconstruction algorithm was validated by acquiring records from the same individual at different times and days, and the reconstruction was carried out without retraining. The chosen algorithm will only be trained with the first 16 seconds of the first record, and the model will perform the reconstruction of the rest of the records without any feedback.

2.3.2 Signal Pre-Filtering

In order to properly analyze and work with the ECG, an exhaustive pre-filtering is necessary. The noise sources that corrupt the raw ECG signals include baseline wandering, power line interference (50 Hz or 60 Hz), electromyographic (EMG) or muscle noise, and artifacts due to electrode motion or electrode contact noise.

Baseline wandering is one of the most common artifacts appearing in ECG records, which are mainly caused by the impedance alterations in the skin-electrode connection due to electrochemical (Nernst) potentials generated by the interface of the electrolytic gel with the skin and with the metal electrode. It may cause variations around 300 mV and highly perturb

the signal representation. That is why a robust baseline wandering removal is necessary. Also, respiration typically shows as a low-frequency baseline wandering.

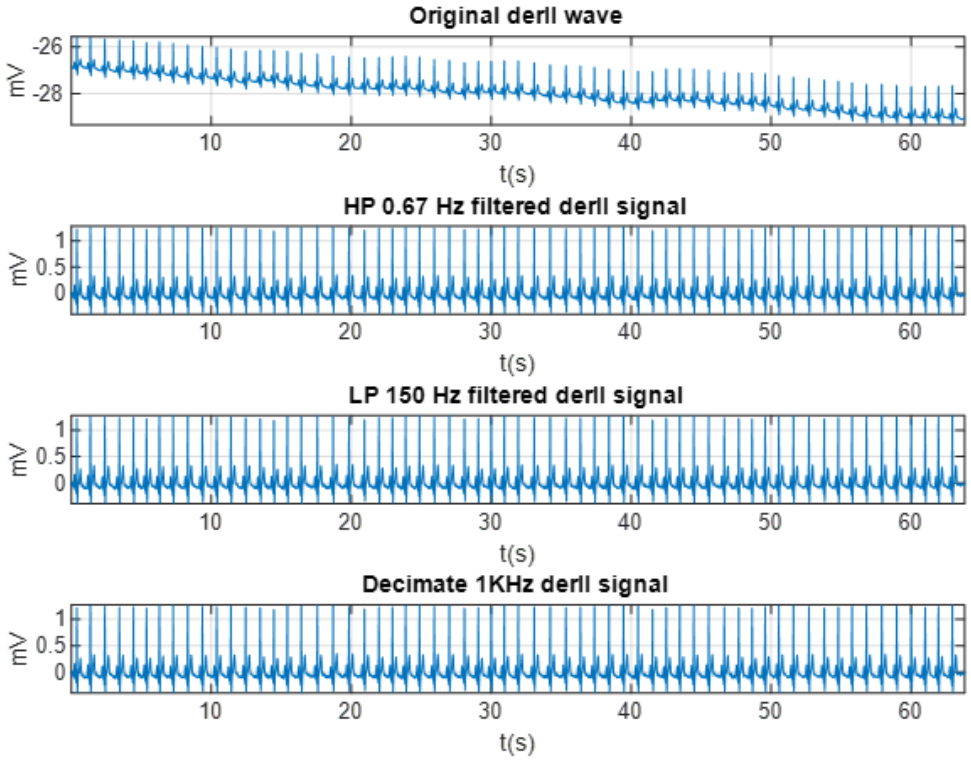

Fig. 2.1 Pre-filtering representation for lead II in an arbitrary record. The figure shows the effect of the successive application of the different filters, as well as the decimation of the signal. It is appreciated how the most noticeable artifacts are eliminated. It is remarkable that the baseline wandering is completely removed by the high-pass 0.67 Hz IIR filter and that the signal has no DC offset.

To remove these artifacts, an exhaustive study [72] was conducted to evaluate most of the baseline drift elimination methods and determine the best approach. It concluded that the best way to remove the baseline wandering should be a method based on a Finite Impulse Response (FIR) high-pass filter with a cut-off frequency of 0.67 Hz, which also eliminates the DC component of the signal, followed by an Infinite Impulse Response (IIR) high-pass filter with the same cut-off frequency. IIR can achieve a more accentuated transition region with fewer coefficients than an FIR filter. Nevertheless, IIR filters have a non-linear phase response that distorts the ECG signal. So, a 4th-order Butterworth bi-directional IIR filter was used to avoid this distortion and to simplify the computation of the filter for each channel [8] although it precludes its use in real-time processing.

There are many artifacts or noises that can alter the signal, which are characterized by a spectral composition centered in the high frequencies, at least high in relation to the

ECG, whose main components lie in the band between 10 and 30 Hz. These noises will be categorized as high-frequency noises, and a low-pass filter will be used to eliminate them. A low-pass filter (LPF) must be used for many reasons in this pre-filtering step. For instance, a 150 Hz LPF eliminates most of the EMG noise component whose spectrum is below 1 kHz. In addition, an LPF could be useful to decimate the ECG signal and to decrease the sample rate from 2 kHz to 1 kHz, which allows a more efficient computation, filtering, and processing of the ECG signal. Its cut-off frequency is high enough to allow high-frequency QRS analysis. An example of the effect of this filtering in the ECG signal can be seen in Figure 2.1.

2.3.3 ECG Reconstruction Methods

As previously mentioned, three ECG leads are the theoretical minimum number required to obtain the standard 12-lead system ECG [41]. This minimum use case of three leads is used in this work, formed by four independent electrodes. Reconstruction was carried out as described in Figure 2.2. The reconstruction algorithm model was trained for an empirically fixed time, and the rest of the record was processed with the obtained model. The reconstruction's goodness was evaluated by comparing the estimated signal with the actual one recorded at the standard leads position using the five Figures of Merit (FoM) that will be defined in Section 2.3.4.

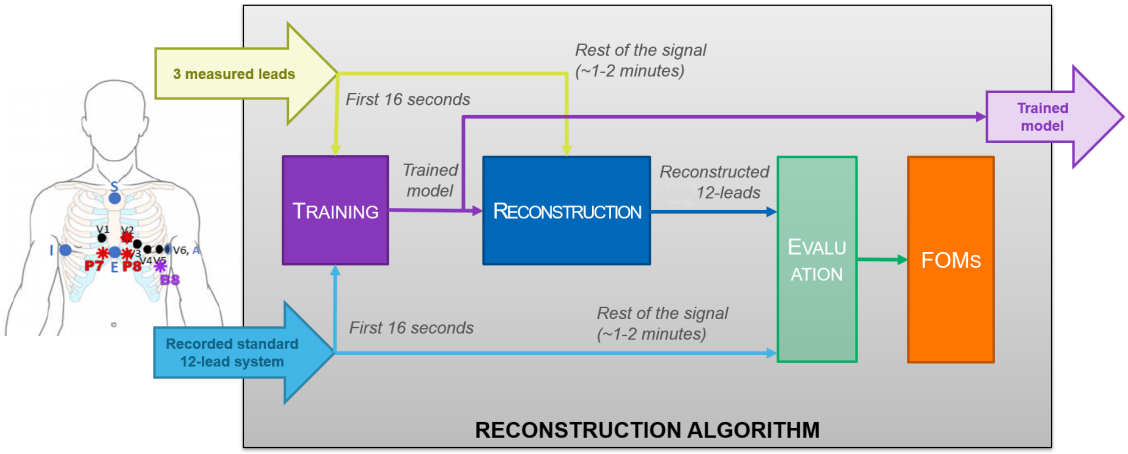

Fig. 2.2 Reconstruction methodology diagram.

Linear Regression

In order to carry out the first part of the study, we will model the cardiac vector representation on each lead from the standard 12-lead system by the Least Squares Linear Regression, as described in Equations 1.16 and 1.17. This approach is very common, presents easily comparable results, and facilitates a preliminary approach to the problem, as it is a very deterministic part of it. As a reminder, linear regression by minimum square reconstruction models is based on cardiac vector reconstruction using projections in the obtained leads. The goal is to minimize the sum of the errors squared to fit a straight line in the data set. This is a well-known approach, and it will be the control case to compare the rest of the algorithms and assess their efficacy.

The least squares method tends to focus on the areas with higher energies, which is the QRS complex in the case of the ECG, and may ignore other waves with lower energies in the ECG signal, such as the P-wave, which decreases its reconstruction performance.

ECG Segmentation

To avoid this underestimation of the P-wave, we explored the strategy of dividing the ECG signal into two segments, separating the P wave from the rest and assigning different coefficients to each segment, applying the linear regression separately to the P wave and to the rest of the ECG signal, thus using two sets of reconstruction coefficients.

An ECG pattern identification method must be implemented to generate the ECG segmentation. In this case, since only the identification of the P wave was necessary, the delimitation of the P wave was carried out from a parameter much easier to identify and implement, such as the R peaks, measuring RR intervals, and then defining time lapses around the R peak.

The detection of R peaks is a widely discussed topic in the field of electrocardiography, where the most famous method is the Pan-Tomkins algorithm. This algorithm is very robust as it uses adaptive thresholds that minimize the chance of false positives and false negatives, so that the detected beats are actually the real ones. The development of this algorithm is widely explained in [73].

Once the location of the R peaks in the signal is extracted, the succession of RR intervals, defined as the distance in terms of time between R peaks, is created. From this, the P wave beginning and end are defined in terms of the relative percentage of the duration of the RR interval. These values were obtained by looking for the P wave to always be defined within the two extremes, P1 and P2, with the smallest possible isoelectric segment and for any type of heart rhythm, from bradycardia to tachycardia, in the available records. The values

obtained were 57.5% of the RR interval for P1 and 92% of the duration of the RR interval for P2, as shown in Figure 2.3.

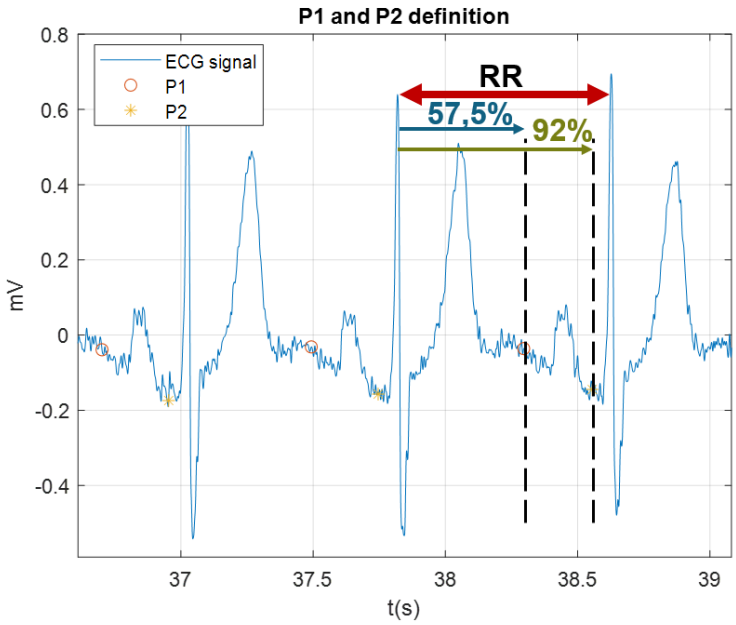

Fig. 2.3 P1 and P2 labeling to isolate the P-wave from the rest of the ECG signal. P1 is allocated at the 57.5% of the RR interval, and P2 is at the 92% of the RR interval.

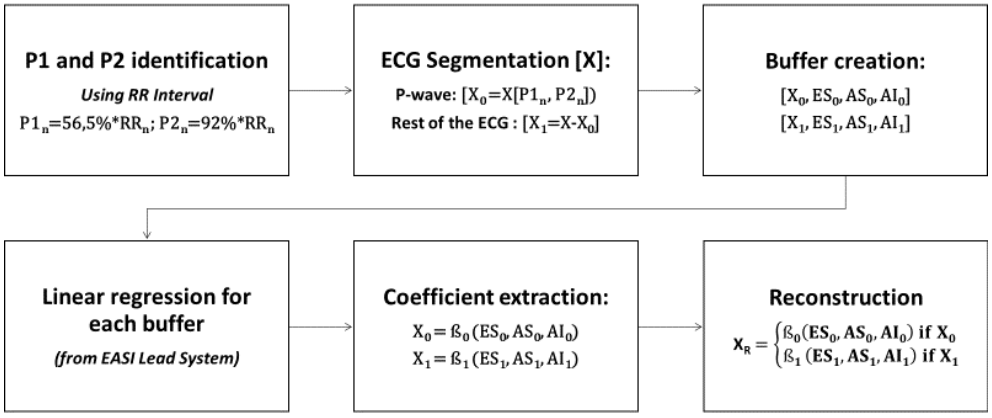

Fig. 2.4 Block diagram of the P wave segmentation algorithm to reconstruct the ECG signal.

In Figure 2.4, the reconstruction algorithm used by this method is explained by means of a block diagram. For each RR interval, a set of P1 and P2 values is created at which the P wave is expected to be found. The complete ECG signal is divided for each lead to be reconstructed, X, into the P wave segment, X_0, and the segment of the rest of the signal, X_1.

The buffers are created, and the algorithm is trained with the training segments corresponding with each buffer's first moments of the record. The set of coefficients extracted for each specific buffer, β_0 and β_1, respectively, are applied to the signal received from the input leads buffers, and the reconstructed final signal, X_R, is recomposed.

Artificial Neural Network

The possibilities offered by the use of artificial neural networks are much broader than those from linear methods. The enormity of variations in their characterization (topology, size, transfer functions, learning algorithms, etc.) make this field the subject of unique studies focused exclusively on the variation of a set of these parameters. However, and only in order to obtain a general view of the method itself, only two methods will be described here. One of them uses 12 ANNs (ANN/Lead), one per reconstructed lead (Figure 2.5a); therefore, each ANN has a single neuron in the output layer. On the other one, a single ANN has 12 output neurons (All-Lead ANN), one per lead (Figure 2.5b).

These approaches are based on ANN using a Multilayer Perceptron (MLP). To synthesize each of the 12 leads from the three acquired leads, a one-hidden layer feed-forward ANN system is trained with the Levenberg–Marquardt algorithm [74]. The non-linear transfer function applied in the hidden layer is the hyperbolic tangent sigmoid function. As the objective of this work is the reconstruction of a patient's ECG from previously obtained records and this reconstruction study is specific to each patient, each ANN has been trained individually for each patient.

The decision on the final architecture of the ANN was made based on previous experience in working with ANN on biomedical signals, as well as a bibliographic review [58, 59], where the architecture is determined experimentally in a similar way to our approach. The same number of neurons in the single hidden layer was used for both architectures, and it was decided empirically based on a sweep of different layer sizes, considering a trade-off between the optimal result and a convenient computational expense. This was based on the results of the stability and accuracy for the most demanding of the two models, which is the reconstruction of the ANN with twelve outputs. In this way, we may fairly compare both architectures, as the single output ANNs are simpler and might require fewer neurons in the hidden layer.

2.3.4 Reconstruction Assessment

The choice of the FoMs to evaluate the accuracy of the reconstruction is not trivial. Choosing certain FoMs and not others will lead to evaluating some characteristics and not others.

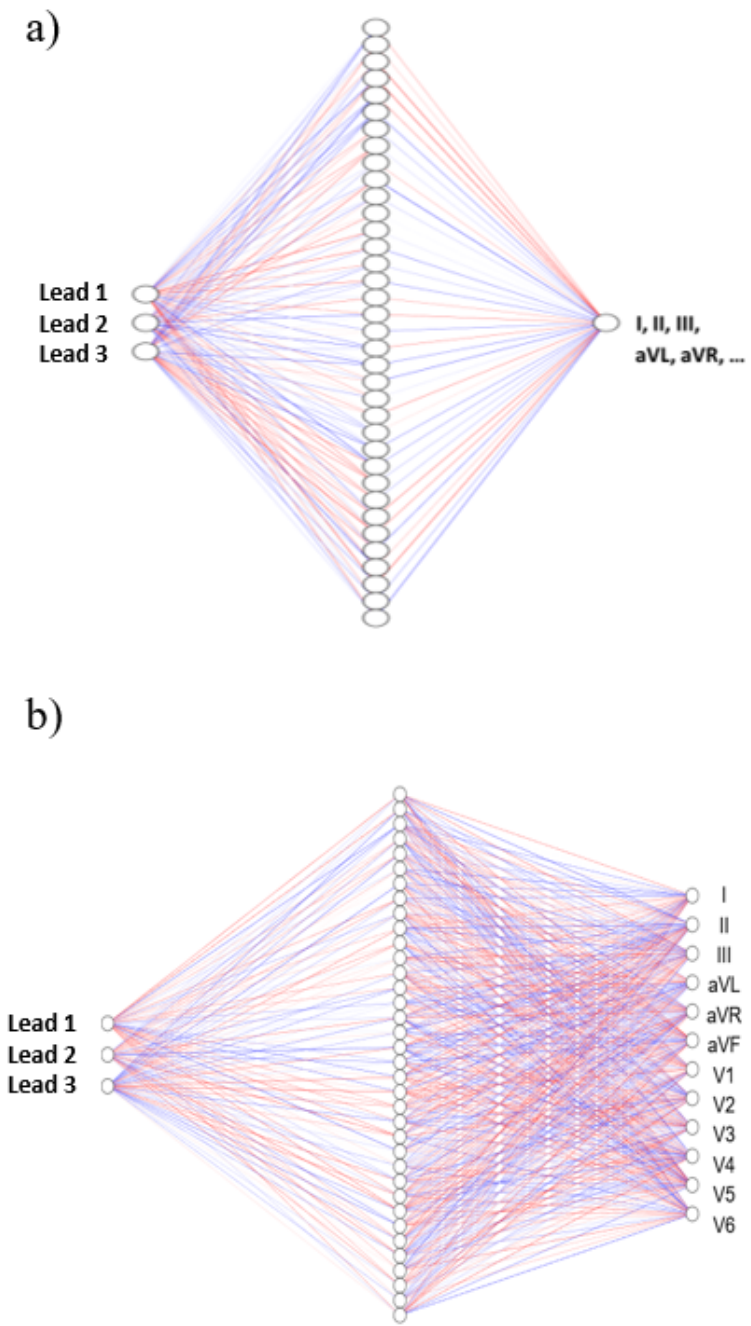

Fig. 2.5 ANN architecture to reconstruct: (a) a single lead of the standard 12-lead system and (b) all leads of the standard 12-lead system simultaneously.

In [75], a study on which should be a robust set of parameters was conducted to evaluate the fidelity of the ECG signals reconstruction. Although this work was done for ECG compression, its principles are applicable to our field, as we also elaborate on a kind of ECG

decompression. According to the results and conclusions from [75] and our own pre-analysis, five FoMs were selected to assess the reconstruction quality of the ECG signal.

- **Root Mean Square Error, RMS or** V_{RMS}, is mathematically described by Equation (2.1), where x_n is the original signal, $\tilde{x}_n$ is the reconstructed signal, and n is the index of each sample of the signal of length N. V_{RMS} has the advantage that it keeps the original units of measure, millivolts (mV), although here it has been converted to microvolts (μV) to facilitate its representation in future graphic representations [76].

$$V_{RMS}(\mu V) = \sqrt{\frac{1}{N}\sum_{n=1}^{N}|\tilde{x}_n - x_n|^2} \tag{2.1}$$

- **Cross-Correlation, CC**, expressed as a percentage is defined by Equation (2.2), where μ_{x_n} and $\mu_{\tilde{x}_n}$ are the global averages of the original and reconstructed signals, respectively, and σ_{x_n} and $\sigma_{\tilde{x}_n}$ are the standard deviations of the original and reconstructed signals, respectively, in addition to the variables defined above. As mentioned before, many authors use this method, so our results can be easily compared with theirs [76, 77]. Nevertheless, the CC is not an accurate estimator of the reconstruction goodness because most of its value relies on the fitting of the isoelectric line and, in any case, on the high-energy QRS complex. So, the rest of the ECG wave morphologies, which may be critical to the diagnosis of certain pathologies, do not substantially affect this parameter.

$$CC(\%) = 100 \cdot \frac{1}{N-1}\sum_{n=1}^{N}\left(\frac{\tilde{x}_n - \mu_{\tilde{x}_n}}{\sigma_{\tilde{x}_n}}\right)\left(\frac{x_n - \mu_{x_n}}{\sigma_{x_n}}\right) \tag{2.2}$$

- **Maximum Amplitude Distance, or Maximum Amplitude Error, MAD or MAX**, is mathematically described by Equation (2.3). It brings information about local distortions of the signal and is usually calculated separately for each cycle, while here, it was measured for the complete recording. MAD also maintains the original units of measure, millivolts (mV), although here, as with RMS, it has been converted to microvolts (μV) to facilitate graphic representations. It is one of the most used similarity metrics [75, 77].

$$MAD(\mu V) = \max_{n}|\tilde{x}_n - x_n|, 1 \leqslant n \leqslant N \tag{2.3}$$

- **Sum of the Square of the Distances, SSD**, is defined by Equation (2.4). It allows us to measure the accumulated error and gives an approximation of how the signals differ

in their full length [77]. As it is the square of the differences, its measurement units are, in this case, square millivolts (mV^2) to simplify its interpretation with the rest of the parameters.

$$SSD(mV^2) = \sum_{n=1}^{N} (\tilde{x}_n - x_n)^2 \tag{2.4}$$

- **Signal to Noise Ratio, SNR**, assumes the noise as the difference between the original signal and the reconstructed signal, as described in Equation (2.5), where $\tilde{x}$ is the reconstructed signal and $\bar{x}$ the mean of the original signal. As SNR expresses signal levels, its measurement units are decibels (dB).

$$SNR(dB) = 10 \cdot \log_{10} \left(\frac{\sum_{n=1}^{N} [x_n - \tilde{x}_n]^2}{\sum_{n=1}^{N} [x_n - \bar{x}_n]^2} \right) \tag{2.5}$$

The five FoMs are obtained for each reconstruction method and electrode location. The significance between the control method and the rest of the reconstruction methods will be evaluated using the Wilcoxon rank sum test [78] for each FoM.

2.3.5 Leads Location

A crucial part of the creation process of this system is its physical design, including its shape, size, and location, which greatly condition the course of this study. This design is not arbitrary, and several aspects must be taken into account. The orthogonality of the selected electrocardiographic leads plays a crucial role in this task, as it presumably allows a better reconstruction of the vectorcardiogram from which to reconstruct the standard 12-lead system heart [35, 39, 41]. In addition, the inter-electrode distance (IED) directly determines the amount of ECG information, defined as the signal-to-noise ratio that can be collected from electrodes. In certain studies, it is determined that the minimum IED that provides additional information would be around 5 cm [48, 51].

After an iterative validation process evaluating different options, an initial design was proposed. This design has four electrodes that obtain the three electrocardiographic leads that will reconstruct the standard 12-lead system. One of these electrodes is located farther away from the rest to allow positions that enhance this orthogonality and can be placed, for example, on the back of the patient.

For studying the best leads location to reconstruct the standard 12-lead system, a Body Surface Potential Map (BSPM) was performed. Electrodes were distributed non-uniformly

across the subject's chest and back, seeking to cover the area that our system could theoretically reach, following the layout shown in Figure 2.6.

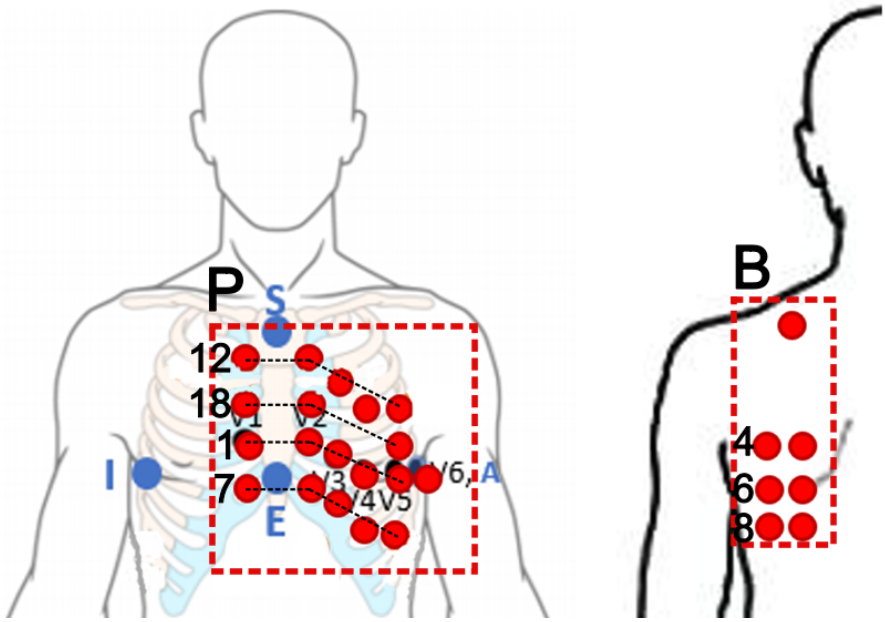

Fig. 2.6 BSPM electrodes configuration. Each red dot represents the location of an electrode, and the numbers, along with the letter, uniquely identify each electrode. For example, the precordial leads V1-V6 here are P1-P6. Note that six electrodes correspond to the precordial electrodes of the standard 12-lead system. Plus, the electrodes belonging to the EASI system have been added, in blue, although they have not been taken into account in the possible combinations. Left panel: chest. Right panel: back.

The location of the chest electrodes was decided in relation to the location of the precordial leads. Once these were placed on the chest, the first five positions were moved vertically up and down, creating two parallel rows above and one below. However, in order to take into account the morphology of the female torso, of which access is not always possible due to the breast, the two electrodes above V3 and V4 were removed. We observed that all publications are based on male subjects; therefore, they make no restrictions on location based on female anatomy.

The electrodes on the back were placed uniformly, following the distribution along the vertical axis, as was done in the frontal area of the first two posterior precordial leads, V7 and V8. In addition, two more rows of electrodes were placed up and down with respect to those already defined. Finally, an electrode was added at the back that would correspond to the left arm electrode of the Mason-Likar lead system, called ML/LAP. Thus, giving a total of seven electrodes possible locations on the back.

Proposed Location

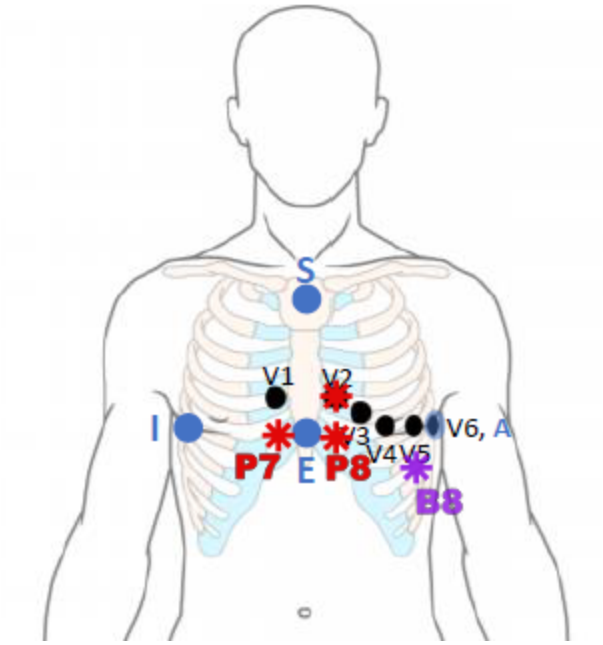

Fig. 2.7 Additional electrodes location. In blue dots is the Dower location, and in red and purple is our proposed location. Red dots (V2, P7, and P8) are located in the patient's chest, and the purple one (B8) is placed in the back. In black, the standard precordial leads are shown for reference.

Then, once we have defined the preliminary potential electrode configurations that we want to implement and the mapping to be done, we will define the possible configurations that it can adopt in the subject, being placed in the positions that form the grid. We decided to reduce the number of possibilities to consider the usability, restrictions that may apply, and our preliminary studies. In addition, different leads formed by different combinations of electrodes within the same electrode configuration were tested.

Finally, we propose a location that might result in electrode positions that adapt better to physiological and anatomical constraints, such as a voluminous breast, a scar in standard positions, etc. It involves four electrodes, three of them located on the chest. V2 is the same as in the standard 12-lead system, P7 is located in the fifth intercostal space just to the right of the sternum, P8 is located in the fifth intercostal space just to the left of the sternum, and B8, horizontally following the line that V5 and V6 form, opposite to V5. Thus, forming three leads: P8-P7, V2-B8 and P8-B8. See the layout in Figure 2.7. These leads were selected for several reasons. They are closer together than those forming the EASI,

which makes placement and wearability more comfortable. The formed leads form a set of quasi-orthogonal leads in the same direction as the EASI does.

2.4 Results

Our analysis involves comparing the performance of four methods. The first method is a simple linear regression, which we use as the control case. The second method involves a linear regression model with wave segmentation. The third and fourth methods involve two different artificial neural network (ANN) architectures - one model for each lead and one model for all leads. These methods are trained for every patient in order to achieve the best results. The size of the training set was empirically established and is set to 16 s (16,000 samples). The remaining of the record, 104 s (104,000 samples), is used for the test. All results shown have been obtained from the test part of the records.

The results have been expressed in terms of median and interquartile ranges represented in the form of boxplots in Figure 2.8. The results for both linear regression methods are represented in blue and red for the simple and P-wave segmentation methods. The ANN strategies are represented in green and purple for the ANN/lead and the unique ANN methods. Figure 2.8 shows the FoMs for each method to reconstruct the standard 12-lead system from the three leads of the Dower location.

The independence of each group of results has been studied for each FoM between the control method (simple Linear Regression) and the other three proposed reconstruction methods, as shown in Table 2.1. The improvements of all the FoMs in both methods involving ANN with respect to the control are highly significant. On the contrary, the P wave segmentation method does not show significant differences for any of the five FoMs. No significant difference was found between the two ANN-based algorithms by means of the Wilcoxon test.

Therefore, the results for both ANN strategies are significantly better than the Linear Regression methods for the five FoM analyzed. No meaningful differences exist between the original and reconstructed signals by both strategies based on ANNs. As for the execution time, a single network with 12 outputs is slower to compute than the 12 single-output networks. For that reason, this is the preferred implementation, although it is very likely that these networks would require fewer neurons in the hidden layer, although this requires a more thorough validation to confirm.

An example of the reconstruction of an ECG fragment of lead II from a random patient is shown in Figure 2.9. This choice was randomly determined to ensure no bias in the quality of the reconstruction, either by a healthy or pathological patient or by other biases

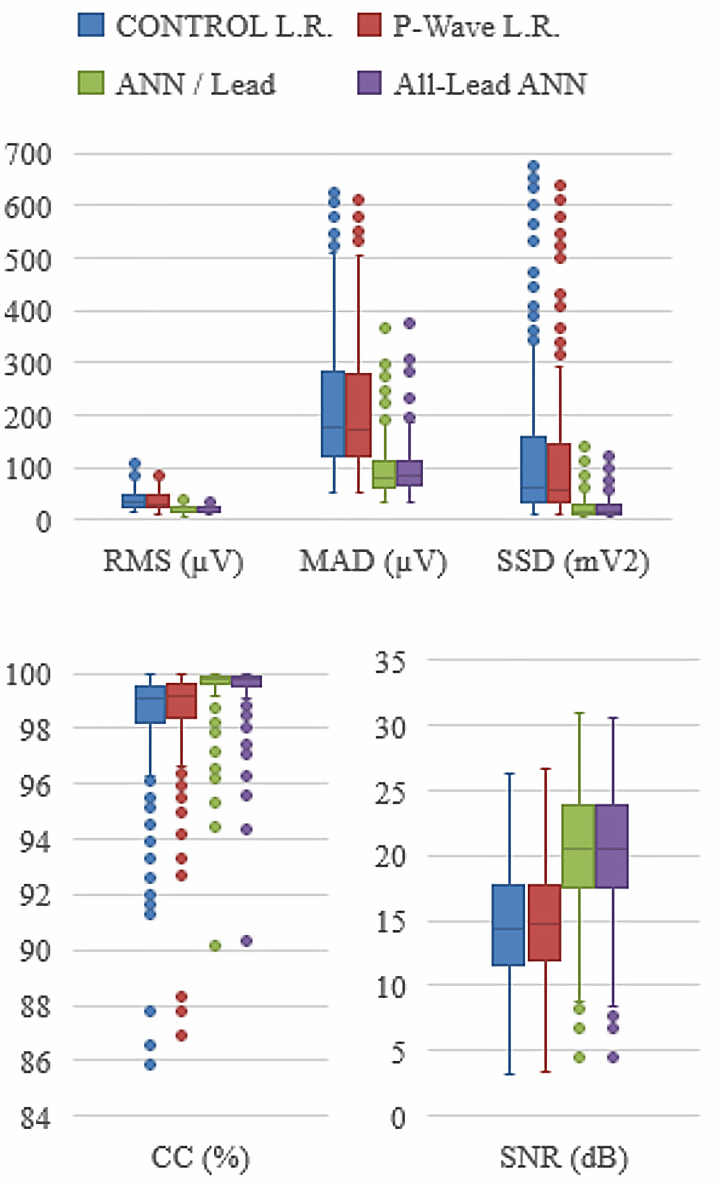

Fig. 2.8 Boxplot graphical representation of the five FoMs for each of the four ECG reconstruction methods studied. The results for both linear regression methods are represented in blue and red for the simple and P-wave segmentation methods. The ANN-based strategies are represented in green and purple for the ANN/lead and the single ANN methods. The parameters have been divided into three graphs to facilitate their visualization and interpretation.

such as signal quality due to skin type or quality of skin-electrode contact. It can be seen that the reconstruction is acceptable in all cases, being, as the general results in Figure 2.8 show, better in the case of reconstruction by ANN than by both linear approaches. A slight

	P-Wave Segm.	ANN/Lead	All-Lead ANN
RMS	0.21	**<0.001**	**<0.001**
CC	0.26	**<0.001**	**<0.001**
MAD	0.79	**<0.001**	**<0.001**
SSD	0.22	**<0.001**	**<0.001**
SNR	0.28	**<0.001**	**<0.001**

Table 2.1 p-values of the independence test between the control reconstruction algorithm, the single Linear Regression, and the rest of the ECG reconstruction algorithms.

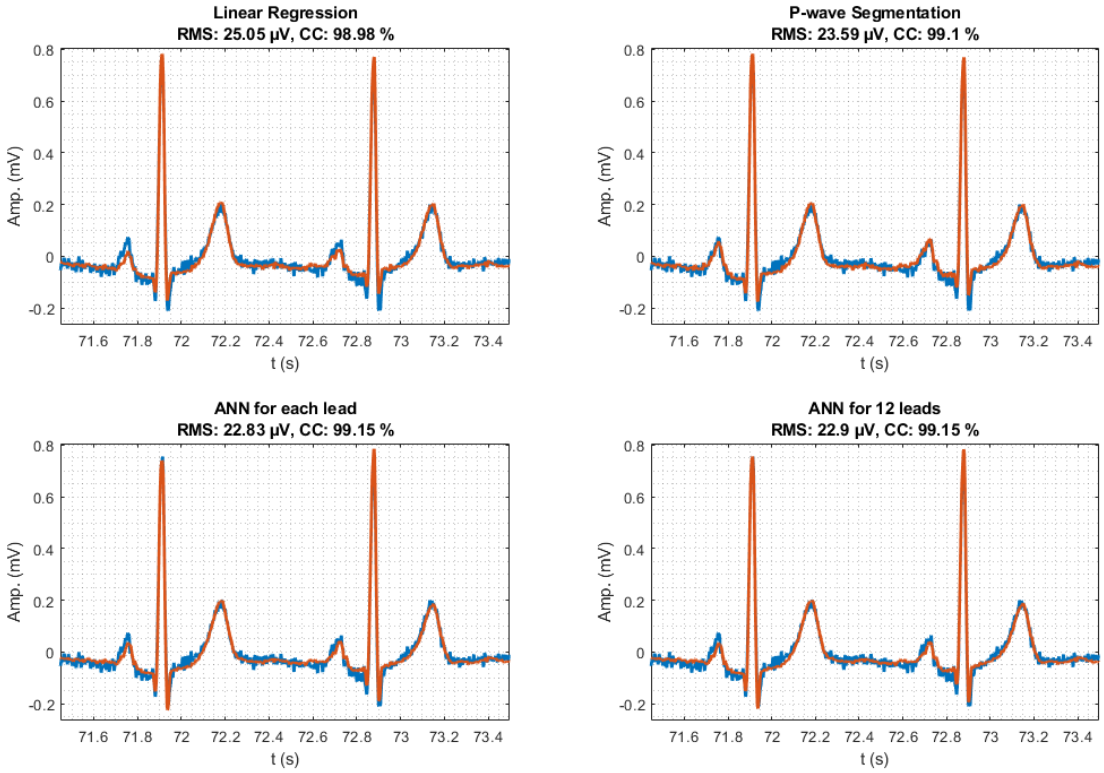

Fig. 2.9 Reconstruction by the described methods of an ECG fragment of lead II for one of the patients. Proposed leads were chosen to perform the reconstruction. Two of the five FoMs, RMS error and CC, are indicated. In blue is the original signal, and superimposed in orange is the reconstructed signal.

underestimation of the amplitude can be appreciated in Figure 2.9, where these second types of regressors are less accurate in the reconstruction of the P wave, as well as the peaks of the QRS complex, especially in the Q and S waves.

2.5 Discussion

The reconstructions carried out by the algorithms based on both ANN approaches are visually perfect. There are no differences between the original and reconstructed signals, as shown in Figure 2.9. Table 2.1 shows the comparison in terms of the significance between the sets of results obtained in reconstruction using the methods cited. We did not obtain significant values of independence between the FoMs obtained from the simple Linear Regression and the Linear Regression with two sets of coefficients, one of them for the P-wave, although the reconstruction of the P-wave is better than in the control case. In contrast, both groups corresponding to the ANN reconstruction showed a very high significance in their independence from the control group, the Linear Regression. For these sets, the evaluation values of the RMS, MAD, and SSD reconstruction adjustment fell sharply, and the CC and SNR increased. Our results are supported by the results of other publications on the topic [59, 58, 61], which confirm that the best algorithm for reconstructing the electrocardiographic leads of the standard 12-lead system are based on artificial neural networks.

Compared with other works, our proposed location improves the reconstruction of the standard 12-lead system compared to others that use electrodes arranged in a pseudo-arbitrary way on the patient's chest, as seen in Table 2.2.

Method	**RMS Error** (μV)	**CC** (%)
ANN [61]	27.4	97.9
LSTM [65]	20.41	98.7
ANN/Lead (ours)	**12.99**	**99.73**

Table 2.2 Comparison between the best location from [61], [65] and our proposal. According to the results, our proposed location outperforms all other methods in both metrics.

One of the problems with the choice of any FoMs is that if the original signal with which to compare the reconstruction presents noisy artifacts, the FoMs will worsen. As the reconstruction algorithm tends to filter that noise, FOMs values decrease as the reconstruction does not accurately match the original. But this is a positive effect, as seen in Figure 2.9. In this example, the reconstructed signal, in orange, is smoother than the original, the blue one. This smoothing is due to the absence of noise in the reconstructed signal, which is caused by, among other reasons, the use of several leads to reconstruct, which reduces the noise of the resulting signal. This may be misleading as the actual ECG signal does not contain those disturbances, as it is noise added to the signal, so FoM should always be critically analyzed. Furthermore, when we reconstructed a certain lead under moderate exercise, we might observe that the actual signal had poorer quality than the reconstructed one, which

was affected by electromyographic noise. In other words, the captured signal may not always be a trustworthy ground truth.

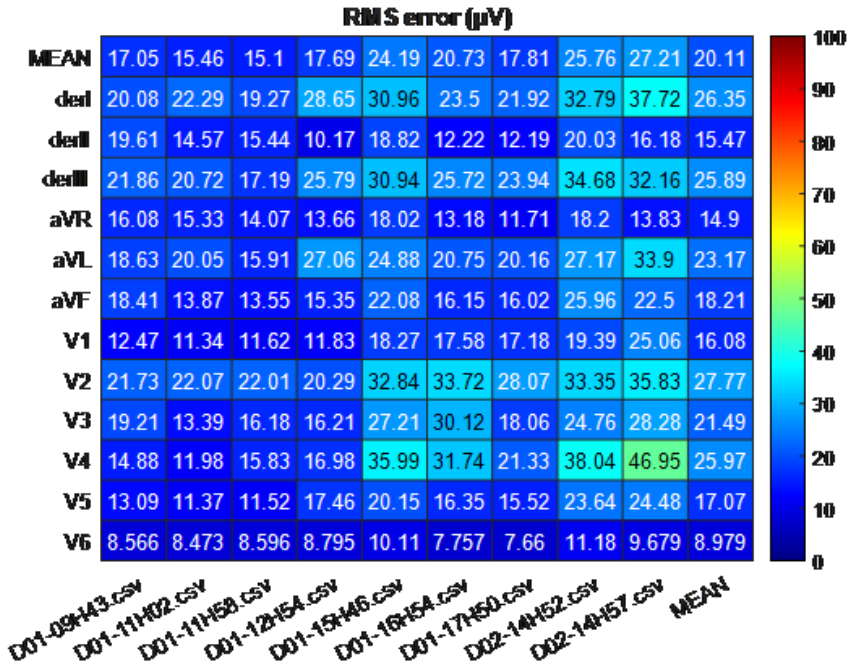

Fig. 2.10 Results for one of the FoMs, the RMS error, where the reconstruction is evaluated for the same patient over several days at different time instants. The x-axis shows the records, identified with the day Dxx and the time xxHxx at which they were taken, and the y-axis shows the standard leads, as well as their mean RMS Error value for each record.

As the robustness of the reconstruction algorithm is an important aspect in our use case, the ambulatory environment, where the patient can be recorded for an entire day, the effectiveness of this reconstruction algorithm over time has been studied. It was validated by acquiring records from the same individual over different hours and days. To carry out this reconstruction, the algorithm, an ANN for each lead, was only trained within the first 16 seconds of the first record, and the model performed the reconstruction of the rest of the records without any retraining or feedback. Despite some worsening in the FOMs due to the eventual dryness of some electrodes and the noise that they carry, as discussed before, no significant degradation in performance was noticed, as shown in Figure 2.10.

2.6 Conclusions

In this chapter, we have demonstrated the possibility of creating and refining a reduced system that can reconstruct the ECG extracted from the standard 12-lead system, the most used method in cardiology medical diagnosis.

We evaluated different reconstruction methods and proposed variations to them, which clearly improved the reconstruction accuracy. We determined that the best reconstruction method consists of using artificial neural networks that carry out this task after specific training for each patient. Moreover, this patient-specific training is also carried out to determine the best location for the electrodes of the final device, which maximizes the accuracy of the reconstruction.

We have also provided added value by paying special attention to the issue of the figure of merit with which to validate the results. This has offered a better evaluation of each part of the process and an advantage over the current literature, as it is more exhaustive than previous studies. This will allow, on the one hand, to increase the number of publications on the subject that can be used as a comparison with this work and, on the other hand, to provide greater confidence in the assumptions and validations made as they are supported by a greater number of parameters that are independent of each other.

In addition, from the conception to the validation of the algorithm, both genders and their different physiognomies were taken into account. This allows the work to be tested and validated for the entire population, as opposed to most works or projects that show some gender bias, limiting the public that can benefit from this work. This work has also raised the possibility that this system could not be placed exclusively on the patient's torso but also on the back, which opens the path to a very wide range of new possibilities that, as has been demonstrated, are equally valid. However, this system must still be validated through clinical studies that endorse its robustness in monitoring and diagnosing cardiac pathologies, the ultimate aim of this work.

In view of these results, we can state that the reconstruction of the ECG recorded by the standard 12-lead system using a reduced monitoring device is not only possible but a good approach to advance in the field of remote monitoring of the heart health of the population.

2.6.1 Next Steps

The next steps that will be taken in this work consist of the following steps.

Evaluate the possibility of modifying the neuronal network, adding new inputs that are not only the electrocardiographic leads used to reconstruct but also new external parameters such as respiration, which can be extracted from the ECG itself, as some studies suggest. Another

option is to add the cardiac vector, whose information provides additional characterization to the neural network, to use this information to improve ECG reconstruction. Furthermore, the possibility of evaluating additional algorithms that increase the performance of ANN reconstruction will be considered, such as the use of committees.

We will also explore new algorithms besides ANN, leading to more complex approaches, such as convolutional or recurrent networks, or simpler methods that may overcome this performance by exploring the nature of this task, the ECG reconstruction.

All of these approaches will be evaluated on new records with diagnosed pathologies, such as the case of premature ventricular contractions or alterations in the cardiac vector.

In addition, the robustness against the exact location of the positions that the algorithm identifies as optimal for a large number of individuals will be evaluated to find out if there is any type of pattern that could allow a generalization of the method and reduce processing, patient preparation, and work times.

Chapter 3

Refining ECG Lead Reconstruction

3.1 Introduction: The Premature Ventricular Contraction Case

In the previous chapter, we described the good results we achieved by means of the proposed reconstruction algorithm. We developed a robust reconstruction model, and this research allowed us to obtain a deeper knowledge of the topic, so it became clear that these results could be improved using a simpler and more efficient model. This chapter aims to refine the final application by exploring new techniques, contributing to the deployment of a more mature device. The current models were not particularly heavy or slow, but any improvements were welcome due to the need for these algorithms to run as light as possible to reduce waiting times due to processing.

While refining the reconstruction algorithm, we considered the inclusion of pathological or uncommon ECG registers, even when they were not seen in the training stage, to assess the reconstruction's robustness. One particular type of pathological event emerged as particularly relevant due to its spurious nature: premature ventricular contraction (PVC). This kind of event might be present even in the healthy population, and its frequency may be related to some kind of pathologies. Analyzing the performance of our algorithm in the presence of PVC, with or without its presence in the training set, allowed us to characterize our algorithm better and propose and analyze new approaches that might better respond to this class of events.

Premature Ventricular Contractions

Normally, the heart's electrical system coordinates contractions to pump blood efficiently throughout the body. The blood first enters the atria, and then the electrical impulse originated

in the S-A node contracts the atria, pushing the blood inside the ventricles. After a pause, the electrical impulse will propagate downwards and provoke the ventricle contraction to push the blood outside the heart towards the rest of the body through the arteries [1]. A PVC is a type of arrhythmia that originates from the ventricles, where an abnormal heartbeat occurs prematurely before the next regular heartbeat. While occasional PVCs are common and often harmless, frequent or sustained PVCs may be indicative of an underlying heart condition or other medical issues. PVCs are typically represented on an ECG by distinctive waveforms. In an ECG register, PVCs appear as abnormal, wide, and bizarre QRS complexes that occur earlier than expected, often disrupting the regular rhythm. The QRS complex during a PVC is typically wider than normal because the impulse originates from an abnormal site within the ventricles. Additionally, following the PVC, there is usually a compensatory pause before the next normal heartbeat, indicating a brief interruption in the heart's rhythm. This pause is often longer than the normal cardiac cycle interval, as the heart resets itself after the premature contraction, as shown in Figure 3.1

A relevant question in our problem is whether any of these events happened during the training. It was clear that if the event appeared during the training time, the reconstruction of the event should be positive and almost perfect, as was the rest of the ECG. But what would happen when the model did not see this event during its training phase? Our algorithm's response when reconstructing these PVCs was quite good, even when it was not exposed to PVC during the training phase. The clinicians always identified the event in the reconstructed ECG as a PVC when the ECG was reconstructed by means of a basic ANN, as shown in Figure 3.2. Although a slight amplitude reconstruction failure can be seen in both the positive and negative components, both signs of the biphasic wave are maintained. The width of the peak is also correctly reconstructed, much wider than that of a healthy QRS. Both features allow clinicians to correctly identify this spurious event, although this reconstruction has room for improvement.

3.2 New Proposed Models

As mentioned, the interest in improving the quality of the reconstructed ECG led us to explore new reconstruction methods. For example, although our current algorithm does not use historical information of any kind, it has been suggested that access to a certain temporal component, such as past events or a certain time window, could improve the reconstruction results. Another option is to add new information to the model or modify its architecture.

Several approaches explored these goals. Either by improving the existing algorithm, adding new training techniques, such as using new training metrics or expert committees,

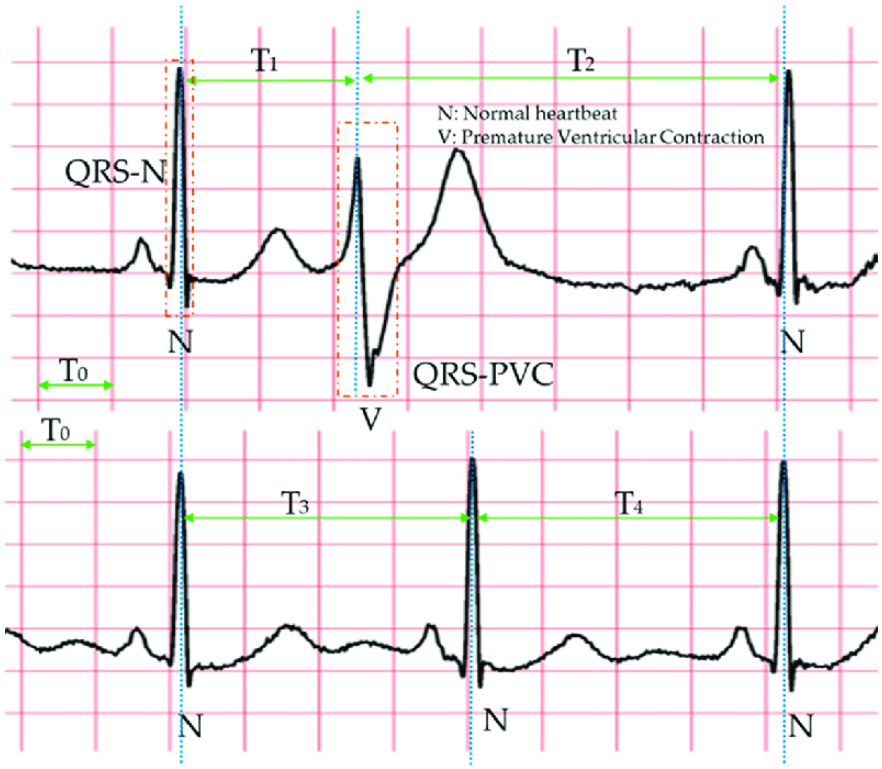

Fig. 3.1 The waveforms of PVC and normal heartbeat. The two ECGs in this picture are from the same person. Each symbol is defined as follows. N (normal heartbeat); V (premature ventricular contraction); T_0 (0.20 s); T_1 (R-R interval); T_2 (R-R interval); T_3 (R-R interval); T_4(R-R interval); QRS-N (QRS complex of normal heartbeat); QRS-V (QRS complex of PVC). The important thing is that T_3 and T_4 are usually equal, and the sum of them is generally similar to the sum of T_1 and T_2. The blue dotted line indicates the location of the R wave peak in each heartbeat. Extracted from [79].

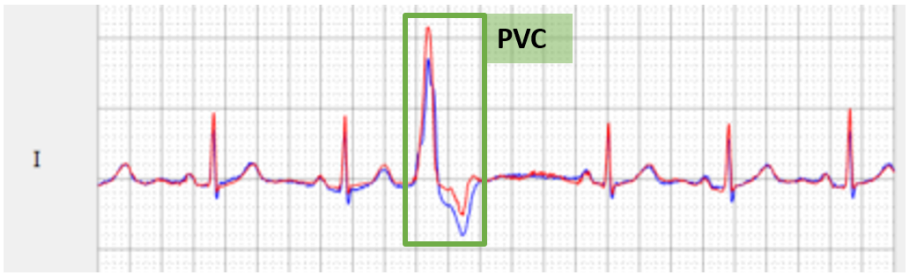

Fig. 3.2 Reconstruction of ECG lead I of a patient with a PVC, framed in green. The original signal is in blue, and the reconstruction is superimposed in red.

or modifying its architecture by adding new input components, such as cardiac vector information. Or by trying completely different algorithms, from simpler algorithms based on

linear techniques with aggregate fuzzy clustering algorithms to more complex algorithms based on deep learning, such as convolutional networks or long short-term memory cells.

All these new proposals will be studied to a greater or lesser extent depending on their feasibility, both from a performance point of view and from a practical and ease of implementation point of view. As a proof of concept, the reconstruction of the healthy ECG and spurious PVC, which has not appeared during training, will be sought, thus forcing the model to reconstruct events for which it has not been specifically trained.

Frontal Lead Regularization

This section and its contents are described and protected by patent with international extension WO2022043196A1 [68]. The frontal leads from the standard 12-lead system are six leads formed by different mathematical operations between the potentials recorded by three electrodes on the patient's limbs and leg. The first three frontal leads are the bipolar frontal leads, described in the previous section 1.2.2 as:

$$V_I = \vec{\emptyset}_L - \vec{\emptyset}_R \tag{3.1}$$

$$V_{II} = \vec{\emptyset}_F - \vec{\emptyset}_R \tag{3.2}$$

$$V_{III} = \vec{\emptyset}_F - \vec{\emptyset}_L \tag{3.3}$$

where $\vec{\emptyset}_R$ is the potential in the right arm, $\vec{\emptyset}_L$ is the potential in the left arm, and $\vec{\emptyset}_F$ is the potential in the left leg. The other three leads, the augmented limb leads aVR, aVL, and aVF, can be expressed as follows:

$$V_{aVR} = \vec{\emptyset}_R - \frac{1}{2}(\vec{\emptyset}_L - \vec{\emptyset}_F) \tag{3.4}$$

$$V_{aVL} = \vec{\emptyset}_L - \frac{1}{2}(\vec{\emptyset}_R - \vec{\emptyset}_F) \tag{3.5}$$

$$V_{aVF} = \vec{\emptyset}_F - \frac{1}{2}(\vec{\emptyset}_R - \vec{\emptyset}_L) \tag{3.6}$$

With these equations, these formulas can be related to each other, creating equations between the different leads. For simplicity, we will define the lead signals at each time instant by their name: I, II, III, aVR, aVL, and aVF. Four equations have been defined from these relationships, as follows:

$$f_1 : II - I = III \leftrightarrow II - I - III = 0 \tag{3.7}$$

$$f_2 : aVR = -\frac{1}{2}(I + II) \leftrightarrow aVR + \frac{1}{2}(I + II) = 0 \tag{3.8}$$

$$f_3 : aVL = I - \frac{1}{2}II \leftrightarrow aVL - I + \frac{1}{2}II = 0 \tag{3.9}$$

$$f_4 : aVF = II - \frac{1}{2}I \leftrightarrow aVF - II + \frac{1}{2}I = 0 \tag{3.10}$$

As these relations must always be accomplished in the real case, where the same three electrodes form these leads, these equations must result in zero-sum:

$$\sum f_n = 0 \tag{3.11}$$

But, when reconstructing the six frontal leads these relations may not be fulfilled, obtaining some error. We then define the robustness function, $f_{RobustnessValue}$, as a function of time that gives a metric of the goodness of the reconstruction at each point. The smaller the value of this function at a given time instant, the better the reconstruction might be:

$$f_{RobustnessValue} : \sum f_n = \varepsilon_n \tag{3.12}$$

Being ε_n, the error value obtained from each f_n substituting the terms for the reconstructed leads at each time instant. This value is very useful since it gives us an estimate of the reconstruction quality even when ground truth is unavailable, for example, during the ambulatory recording of the patient, where FOM metrics are unavailable. This can be used in multiple ways, from visualizing the goodness of reconstruction by means of a color gradient that indicates how the reconstruction is performing at each moment, as shown in Figure 3.3. Also, this parameter can be used as a component of the cost function that the ANN must take into account for its training, which we call the Frontal Lead Regularization (FLR) term.

In our previous work, the cost function, J, of our ANN was the classic MSE:

$$J = \frac{1}{N}\sum_{i=1}^{N}(y_i - \hat{y}_i)^2, \tag{3.13}$$

where N is the number of data points, y are the observed values and $\hat{y}$ are the predicted ones. We thus define the new cost function, J', as the addition of this first one with this new term, creating the training cost function with FLR:

$$J' = \frac{1}{N}\sum_{i=1}^{N}(y_i - \hat{y}_i)^2 + \alpha \cdot f_{RobustnessValue} \tag{3.14}$$

The alpha term, α, is the regularization term that controls the strength of the FLR. A higher α value will force the ANN to accomplish these frontal leads relations.

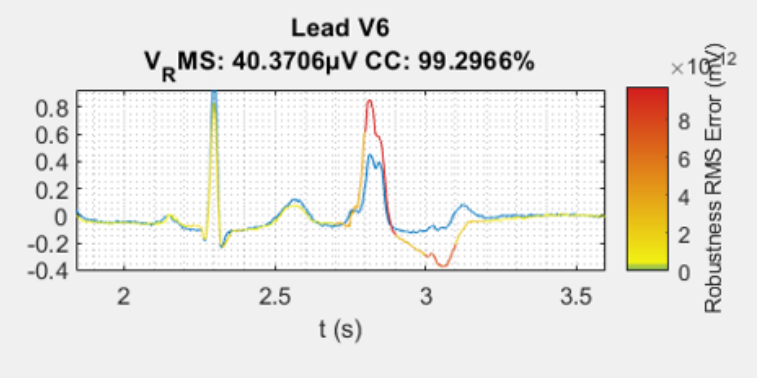

Fig. 3.3 ECG reconstruction of a normal beat and a PVC. The original signal is in blue, and the reconstructed one is in a gradient from green to red, following the robustness function value at each point. A higher robustness function value represents a worse reconstruction accuracy, shown in colors closer to red. A lower value is represented in green, indicating a good reconstruction quality.

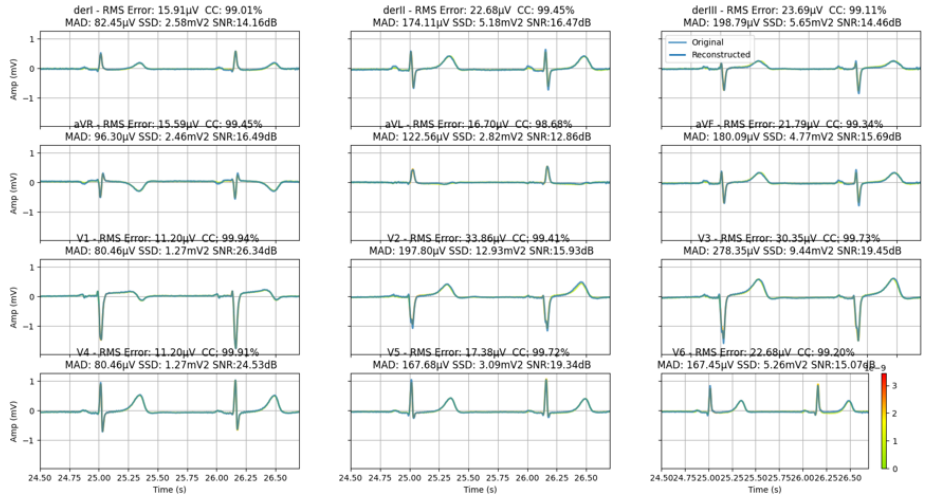

Fig. 3.4 ECG reconstructed by using FLR with $\alpha = 0$. The original signal is in blue, and the reconstructed one is in a gradient from green to red, following the robustness function value at each point.

Results are shown in Figures 3.4, 3.5, and 3.6 for the same ECG record. The value of the regularization term, α, has been tested to study the effect of this FLR in the output of the model for three values: 0, 0.01, and 0.1. There is hardly any difference. For a small alpha value of $\alpha = 0.01$, shown in Figure 3.5, there is hardly any difference with respect to the reconstruction without the FLR shown in Figure 3.4. The variation in the FOMs is minuscule

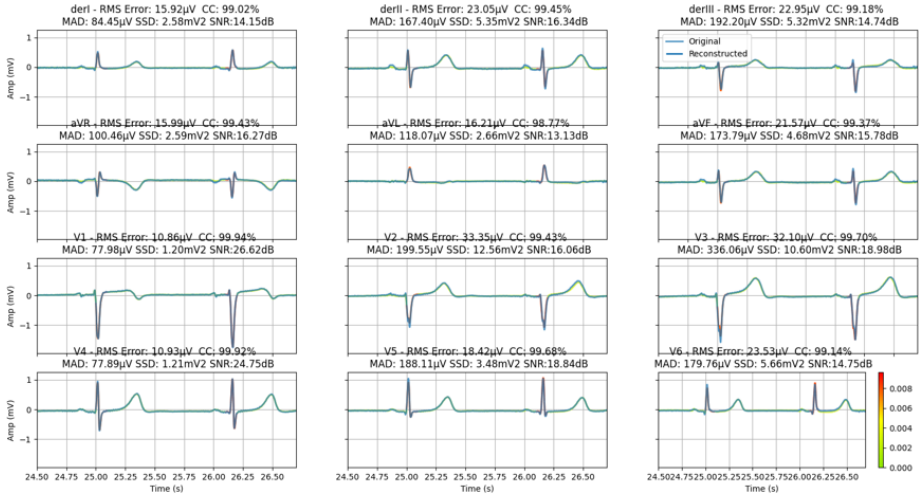

Fig. 3.5 ECG reconstructed by using FLR with $\alpha = 0.01$. The original signal is in blue, and the reconstructed one is in a gradient from green to red, following the robustness function value at each point.

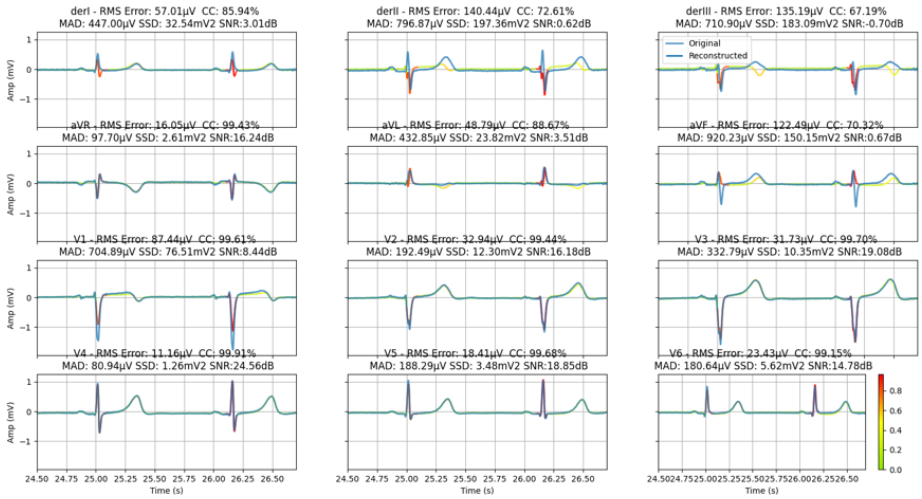

Fig. 3.6 ECG reconstructed by using FLR with $\alpha = 0.1$. The original signal is in blue, and the reconstructed one is in a gradient from green to red, following the robustness function value at each point.

and can either get better or worse; there are no significant differences, so it follows that the regularization term must be larger to have any effect.

When we increase the alpha value ten times, $\alpha = 0.1$, we begin to see its effects as in Figure 3.6. The reconstruction tends to minimize the amplitude of these channels so that,

regardless of the accuracy of the reconstruction, the error term, ε_n, is as small as possible, which does not necessarily mean a better reconstruction. This leads to the conclusion that, although this idea seems promising, its calibration and tuning must be very fine, and in the current study, this trade-off has not been achieved for the use of this term to be efficient and robust in real-world conditions.

In conclusion, the incorporation of the robustness value proves to be a valuable asset in evaluating reconstruction methods. However, the inclusion of this parameter within the training of the system still poses difficulties that we have not been able to solve. Its application to precordial leads is still under study, so integrating this parameter into a final system training remains challenging, presenting unresolved issues. It may be studied using this parameter in real-time training scenarios, requiring further calibration and refinement. Consequently, further research is essential to overcome these limitations and fully harness the potential of the robustness value.

ANN committee

This section and its contents are described and protected by patent with international extension WO2022043196A1 [68]. An Expert Committee, or ANN Committee in particular, is a specialized form of artificial neural network that merges the responses of multiple neural networks into a unified output. This methodology aims to enhance the performance of machine learning models by leveraging individual networks' unique strengths.

Within a committee machine framework, each neural network, often called an "expert," undergoes training on distinct subsets of the dataset. These subsets may be defined based on various criteria, such as data characteristics or domain-specific knowledge. After training, the predictions generated by these expert models are combined to produce a final prediction. This fusion process can be achieved through various methods, including ensemble averaging, where the outputs of different predictors are linearly combined, or boosting, which iteratively improves the performance of weak algorithms until achieving high accuracy [80].

This may be proven as follows, let Ω be a set of training data $\{(x_n, y_n), n = 1, \ldots, N\}$ and $\phi(x, \Omega)$ a single predictor for y. The expert committee, Ω_k, is a sequence of K learning sets of N independent observations drawn from the same underlying distribution as Ω. The goal is to obtain a better prediction using this sequence $\{\phi(x, \Omega_k) : 1 \leq k \leq K\}$ than a single predictor $\phi(x, \Omega)$. For y, we replace the single $\phi(x, \Omega)$ by the average of $\phi(x, \Omega_k)$, i.e. $\phi_A(x) = E_\Omega[\phi(x, \Omega_k)]$. So, given a pair (x, y), the Mean Squared Error (MSE) is:

$$E_\Omega[(y - \phi(x, \Omega_k))^2] = y^2 - 2yE_\Omega[\phi(x, \Omega_k)] + E_\Omega[\phi^2(x, \Omega_k)]. \tag{3.15}$$

As $\phi_A(x) = E_\Omega[\phi(x,\Omega_k)]$, and applying $E[Z^2] \geq (E[Z])^2$ to the last term:

$$E_\Omega[(y-\phi(x,\Omega_k))^2] \geq y^2 - 2y\phi_A(x) + \phi_A^2(x) = (y-\phi_A(x))^2. \tag{3.16}$$

Integrating both sides over the joint (x,y) distribution yields that $\phi_A(x)$ has less MSE than $\phi(x,\Omega)$. How much lower depends on how unequal these are:

$$(E_\Omega[\phi(x,\Omega)])^2 \geq E_\Omega[\phi^2(x,\Omega)] \tag{3.17}$$

which depends on how different is $\phi(x,\Omega)$ given different replicas Ω. The higher the variance of $\phi(x,\Omega)$, the more improvement aggregation may produce.

Utilizing a committee machine offers several advantages, including improved accuracy and robustness to overfitting, as it avoids the local minimum problem and makes the result more stable. By leveraging multiple models trained on different subsets of data, committee machines can effectively mitigate noise and biases present in the dataset, resulting in more reliable predictions. Additionally, the diversity of expert models within the committee can enhance the model's generalization capabilities, allowing it to perform well on unseen data. However, it's worth noting that there are also challenges associated with using committee machines, such as the computational expense involved in training and maintaining a large number of expert models. Training each model requires computational resources and time.

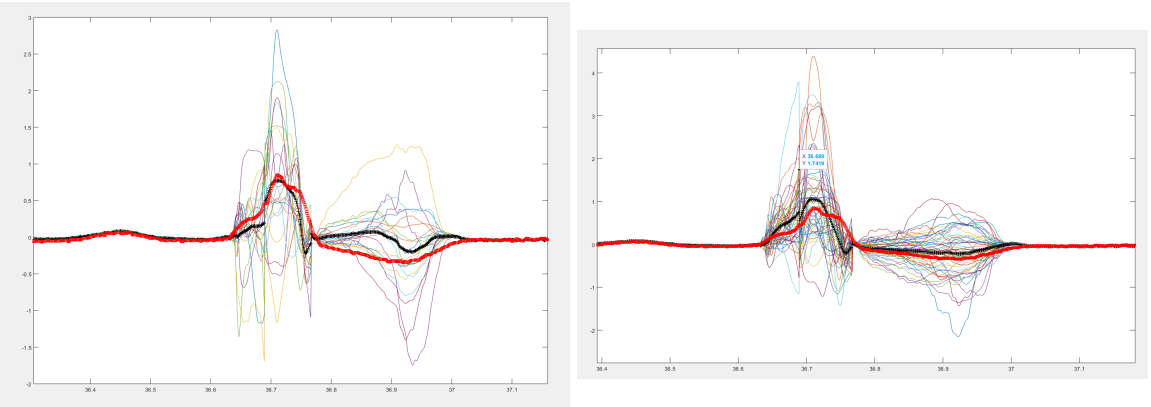

Fig. 3.7 Reconstruction of a PVC by an expert committee of 20 ANNs (left) and 50 ANNs (right), respectively. The original signal is in black, and the committee's output is in red. The remaining thin colored lines represent the individual outputs of all the nets.

As shown in Figures 3.7 and 3.8, results will improve when this Expert Committee is applied to the reconstruction. The model's output was designed to be the mean of the whole set of the individual ANNs included, or preferably as the median of the whole system output. Additionally, as the number of networks increases, the results eventually improve, reaching

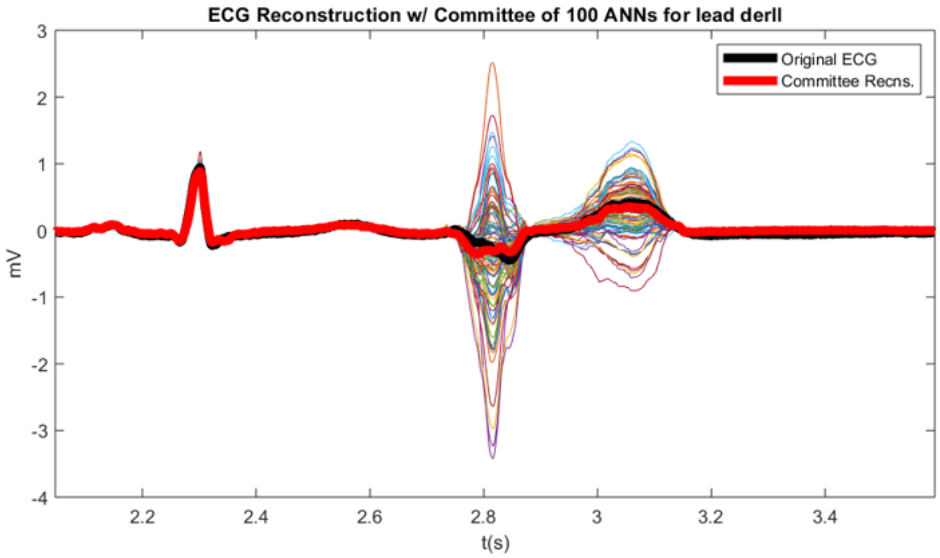

Fig. 3.8 Reconstruction of a PVC from a different ECG record by an expert committee of 100 ANNs. The original signal is black, and the committee's output is red. The remaining thin colored lines represent the individual outputs of all nets.

the highest performance when using 100 ANNs simultaneously, as in Figure 3.8. Although this strategy increases the performance of our proposed model, it requires a lot of time and computational cost, as we have to train one hundred times the same model. Even if the training was parallelized to reduce its cost, it significantly increases execution times.

Finally, this had a bad effect on the explainability of the model. When these outputs were shown, the visualization of this model's response led the clinicians and regulatory entities to wrongly think that this model is not properly trained and that this reconstruction goodness is just a matter of luck. So, due to its drawbacks, this approach was discarded.

Using the Cardiac Vector as an Input

There are some cases when trying to classify a sample by means of an ANN given some input parameters the classification does not give satisfactory results. But when adding a transformation of them, such as the sinus of the input data, the set of inputs the model uses without modifying anything else, the problem is solved perfectly. This modification has nothing to do with adding new information but with transforming existing data to be more useful to the model; some works have been published in this regard [81] and, more specifically, applying trigonometric transformations [82]. We developed our proposal based on this input data transformation assumption.

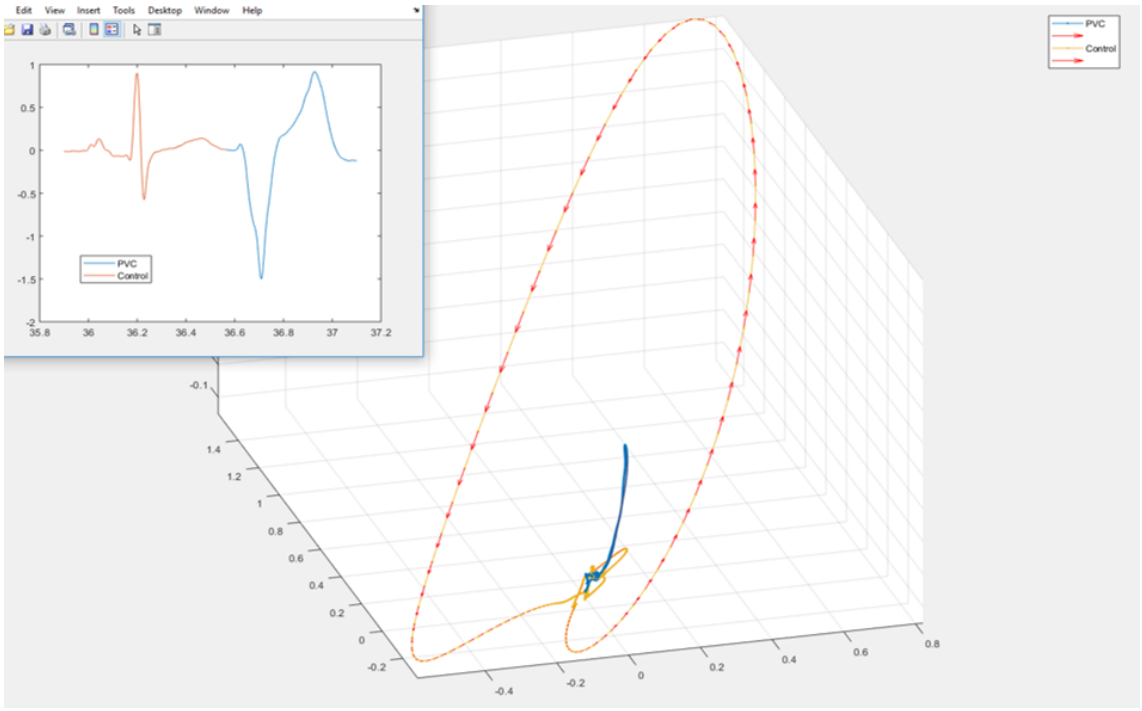

Fig. 3.9 Representation of a normal beat in orange and a PVC in orange. In the large left part, the ECG signal of these two beats can be seen in a normal ECG lead. The big picture shows the quasi-orthogonal projection recorded by the three quasi-orthogonal leads, thus forming the cardiac vector.

The cardiac vector usually has a similar path in each beat, represented by the projection of the same in the three orthogonal derivations that record it, the Dower leads in this case. This representation can be affected in critical events such as premature ventricular contraction. Figure 3.8 represents the quasi-orthogonal vectorcardiogram of a control heartbeat, in orange, and the subsequent premature contraction, in blue. The projection of both is not the same, so it is possible to assume that this information may be useful as parameters for future reconstruction. Although reconstruction through the use of ANNs is almost perfect in most cases, there are critical situations in which this may fail. The main changes we have found that cause a failure in reconstruction are pathological events such as premature ventricular contractions and displacements of the cardiac vector several degrees with respect to the main axis collected during training.

Figure 3.9 shows that a normal heartbeat's cardiac vector is quite different from the PVC projection. This is due to the different origins of the impulse and the different paths that this impulse follows across the heart. This is the reason that leads us to modify our network inputs to add this useful information, forcing the network to reproduce these changes that are more obvious in the spherical domain.

A modified version of the previously proposed reconstruction has been proposed in which we add the information of the cardiac vector by means of its projections in spherical coordinates. The reason for using spherical coordinates is that the projection of the cardiac vector into cartesian coordinates is already represented by the potentials of the three leads collected, of which the initial reconstruction is carried out. Therefore, we need a new way of representing them, which also involves a non-linear transformation of the data, as follows:

$$r = |CardiacVector| = \sqrt{Lead_1^2 + Lead_2^2 + Lead_3^2} \tag{3.18}$$

$$Azimuth, \phi = \arctan \frac{Lead_1}{Lead_2} \tag{3.19}$$

$$Elevation, \omega = \alpha_{CardiacVector} = \arccos \frac{Lead_3}{r} \tag{3.20}$$

Due to the nature of this projection, the azimuthal value, ϕ, can pass from π to $-\pi$ instantaneously, generating abrupt changes that the network cannot overcome. To solve this, the azimuthal projection defined in Equation 3.18 is divided into two parts, generating two vectors with the semi-circumferences of the orthogonal route and allowing smooth vector displacement over time.

$$\beta_{CardiacVector} = \arctan \frac{|Lead_1|}{Lead_2} \tag{3.21}$$

$$\gamma_{CardiacVector} = \arctan \frac{Lead_1}{|Lead_2|} \tag{3.22}$$

The ANN architecture with the new proposed inputs is shown in Figure 3.10, where the hyper-parameters employed for this study are defined. Note that this architecture is based on a single ANN for each lead, thus providing a higher speed of execution, as mentioned in the previous chapter. The rest of the architecture is quite similar despite the four new inputs that feed the ANN. These are the four transformations specified by Equations 3.18, 3.19, 3.21 and 3.22.

A positive aspect of this type of architecture, including the cardiac vector, is the use of "simple" networks based on MLP that allow us a very useful visualization of the behavior of the system. With the right tools, we can visualize the responses of such models and better understand their behavior. This means that we can better characterize their performance both when defining the capabilities and limitations of our models and improving the explainability when exposing them to a more general public, who will inevitably have to come into contact

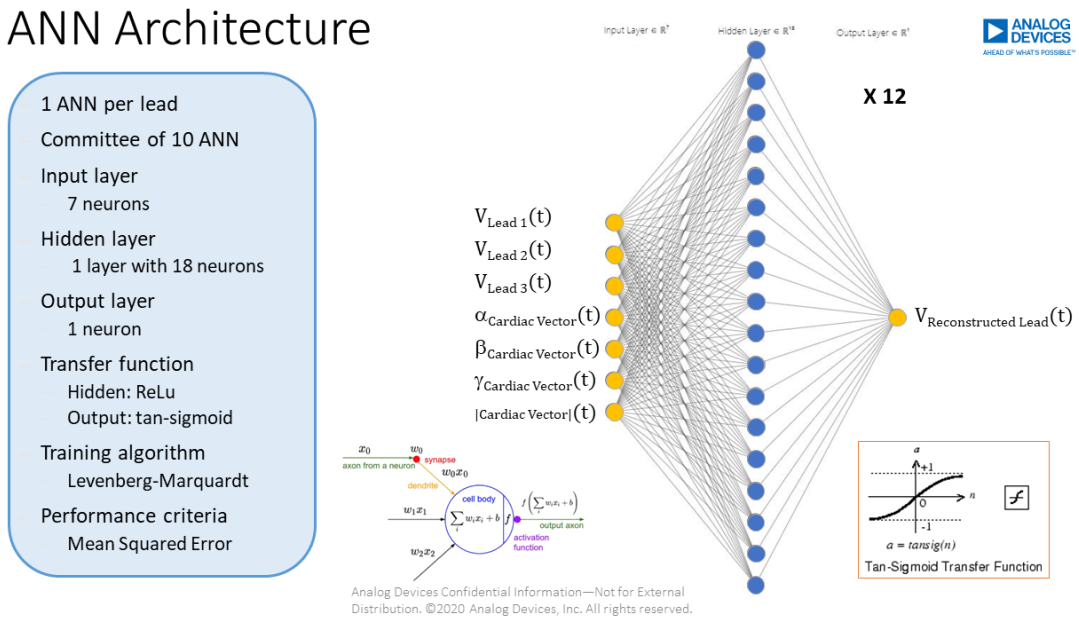

Fig. 3.10 ANN architecture with the new proposed inputs, along with the hyperparameters specifications employed for this study.

with this type of systems, whether they are regulatory agencies or the clinicians in charge of using this system.

For example, in Figures 3.11 and 3.12, two different instances of the reconstruction of an ECG signal presenting a normal beat and a PVC have been represented. The proposed architecture was used in both cases, using an expert committee based on ten networks, but one has been trained with an ectopic event, the PVC, and the other one has not. The networks are represented in such a way that the core of each neuron corresponds to its output, the input in the case of the input layer (being a bypass). The black dots represent the neuron outputs of positive values, and the red ones are negative. The color of the lines that join the different neurons represents the weight that it has in the transfer function of the following neuron: blue if it adds (its weight is positive) and red if it subtracts (its weight is negative). If the weight of that neuron barely affects the next neuron, weight $w < 0.01$, the line is omitted. In addition, the transparency of the line specifies the relevance of each weight on the final output.

It can be seen how both reconstructions during a normal beat remain similar in Figure 3.11. But, during PVC reconstruction shown in Figure 3.12, the reconstruction diverges considerably for both models. This example shows a poor reconstruction of the PVC when the system has not been trained with it, although it has been shown that this situation is not always related to the accuracy of the model but to the position of the electrodes from which

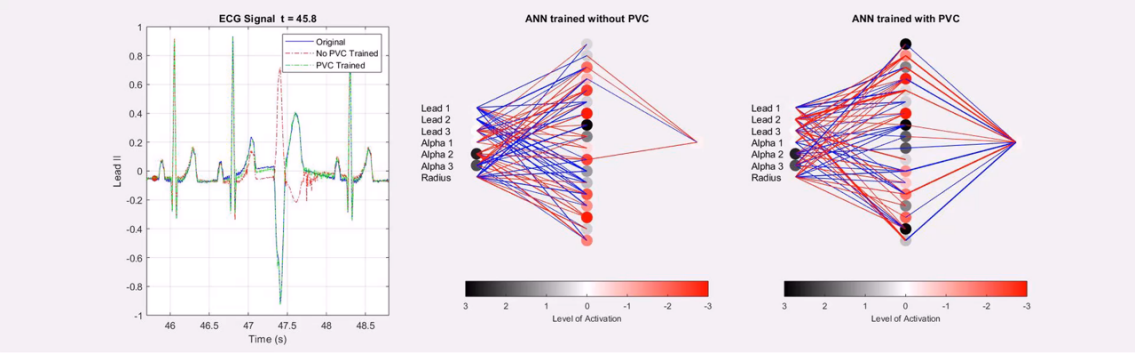

Fig. 3.11 Reconstruction of a normal heartbeat in lead II. On the left is the ECG reconstruction, the blue line being the original signal, the red dashed signal is the reconstruction of the model trained without the PVC as part of the training set, and the green solid signal is the reconstruction of the model trained with the PVC as part of the training set. The colored dots indicate the instant being reconstructed at the time of activation of the networks. In the center and on the right, the two ANNs used to carry out the reconstruction, the 7 input neurons being the same, the potential of each lead plus its representation in spherical coordinates, with the azimuthal projection doubled to avoid jumps and a single output neuron, since a single network has been used for a single lead.

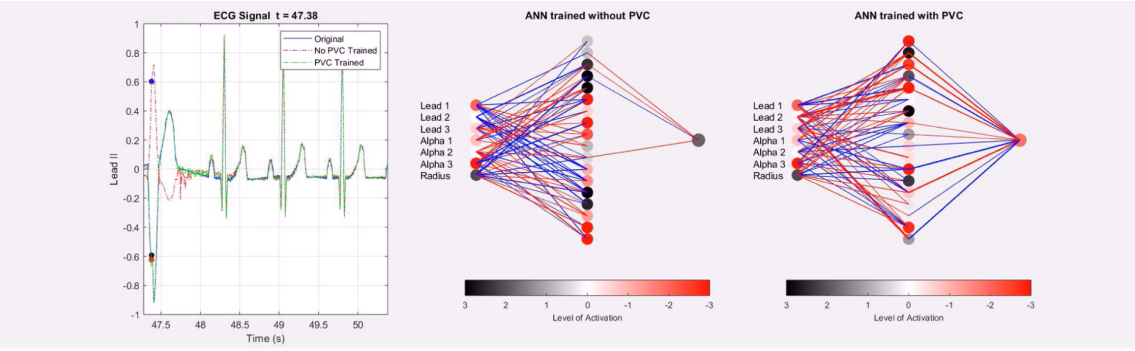

Fig. 3.12 Reconstruction of a PVC heartbeat in lead II. On the left is the ECG reconstruction, the blue line being the original signal, the red dashed signal is the reconstruction of the model trained without the PVC as part of the training set, and the green solid signal is the reconstruction of the model trained with the PVC as part of the training set. The colored dots indicate the instant being reconstructed at the time of activation of the networks. In the center and on the right, the two ANNs used to carry out the reconstruction, the 7 input neurons being the same, the potential of each lead plus its representation in spherical coordinates, with the azimuthal projection doubled to avoid jumps and a single output neuron, since a single network has been used for a single lead.

the reconstruction has been carried out. However, at the same position, optimal or not, we see that training the model with these ectopic events improves the reconstruction, as would be expected. This leads us to ask whether adding a "memory" element or an element capable of

capturing the system's dynamics, rather than a single time instant, could be an improvement, which will be studied in Section 3.4 that deals with deep learning approaches. However, if the placement of the electrodes is optimal for the reconstruction, as shown in the following figures, there is an improvement both visually and in the FOMs when we apply this model, compared to using the network with only the input of the first leads even when the algorithm is not trained with ectopic beats. This can also be seen in the level of activation of the output neuron, which is affected by a greater number of neurons of the hidden layer, which means a better characterization of its response.

Fig. 3.13 Reconstruction of a recording showing a PVC using a model without cardiac vector information in the form of spherical coordinates. In blue is the original signal, and in orange is the reconstruction. In addition, the FOMs of the reconstruction performance are shown in the title.

In a record from another patient, we show the reconstruction of a pathological event, the PVC, whose recording did not present any anomalous beats in the training phase, so the model has not seen any of these events. The model that does not use the information of the cardiac vector in spherical coordinates does not perform a reliable reconstruction of the PVC, as shown in Figure 3.13, presenting an overestimation of the amplitude of the positive phase of the wave and a series of artifacts in the negative phase of the wave, which does not happen in the second reconstruction, in Figure 3.14, in which the model has been fed with this information. In addition to the visual analysis, the FOMs of both reconstructions, although very similar and could be both classified as adequate, are slightly better in the case of considering the cardiac vector information, going from 34.39 μV to 28.19 μV for the RMS Error and from 95.52% to 97.03% for the CC.

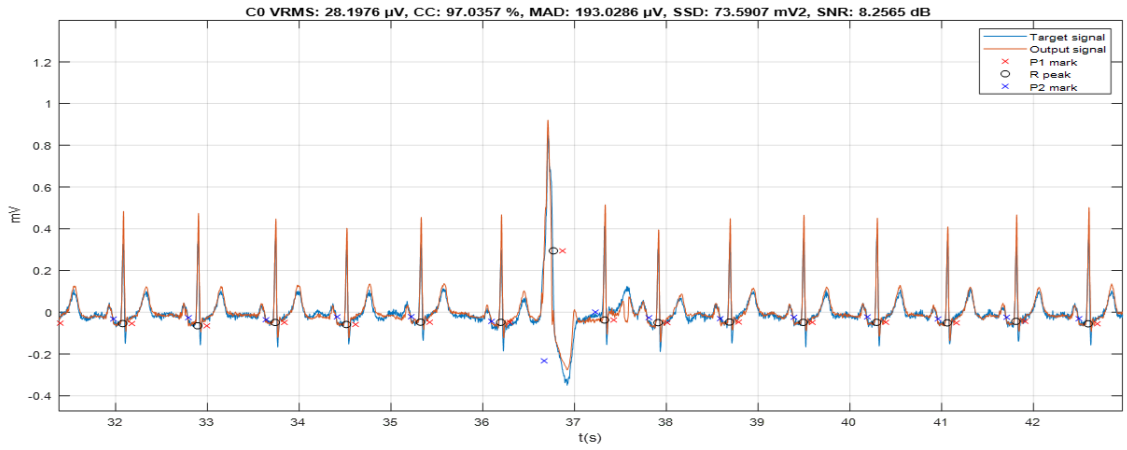

Fig. 3.14 Reconstruction of a recording showing a PVC using a model with the cardiac vector information in the form of spherical coordinates. In blue is the original signal, and in orange is the reconstruction. In addition, the FOMs of the reconstruction performance are shown in the title.

Although the implementation of ANNs committees represents a significant improvement in the quality of reconstruction over time and in very adverse situations, incorporating new transformations of the input data to feed the reconstruction model seems to further improve the quality of reconstruction. Despite this approach being a step closer to obtaining a more accurate and more explainable model, this architecture has several disadvantages. The results, still quite good, are not a notable improvement for the contraindications they present due to the increased complexity of the model and the consequences this entails. So, we explored simpler and more efficient models that may overcome all of these limitations.

3.3 Fuzzy c-means

This section and its contents are described and protected by patent with international extension WO2022043196A1 [68]. First, we should mention the intrinsic difficulty of using these machine learning models in the medical environment, where a professional's decisions can literally mean a patient's life or death. This is why regulatory entities such as the FDA and clinicians emphasize the need for the explainability of the models, especially those that differ from the more classical ones, and delve into more abstract fields such as Machine Learning or AI [83]. Previously proposed models collided entirely with this issue since, although the reconstruction was more than correct, the lack of explainability of the model dynamited its implementation and adoption by third parties.

In the search for new, simpler, and more explainable reconstruction algorithms, but at the same time more efficient, we revisited one of the first implemented algorithms, linear regression coupled with waveform segmentation, as proposed in [39, 44]. In the previous section 2.3.3, we developed and tested the division of the ECG into two parts, the P wave and the rest of the signal, and we applied two sets of linear regressors trained independently of each other. This posed several problems. First, we needed a previous stage in which the P-waves of the whole signal were detected. If the system could not find these waves for whatever reason, the system would not work nicely. In addition, using different regressors between the two parts of the signal generated jumps between the P-wave and the rest of the signal. The problem with this is that this segmentation is based on our prior knowledge of the problem, but it may or may not correspond to the best solution for every register. It is correct that the different parts of the heart and the different events that occur in them can, and perhaps should, be reproduced with different models. However, it is also true that this segmentation can be done more automatically.

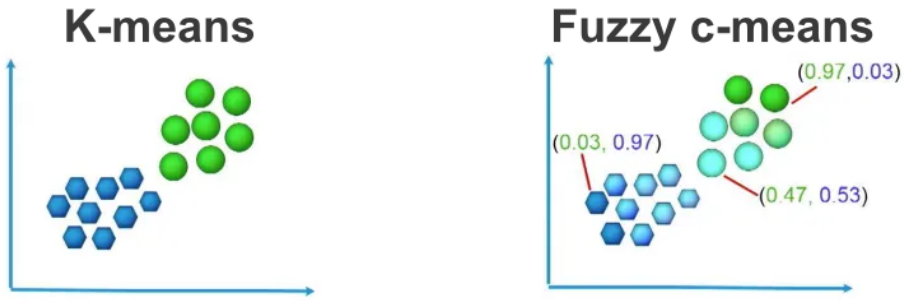

Fig. 3.15 Difference between discrete k-means-based clustering and FCM-based clustering. In k-means, each point belongs exclusively to one category; in the other, each point has a degree or probability of belonging to all categories. Extracted from [84] and modified by the author.

Our new proposal is to let the system itself decide which groups are optimal. To achieve this, automatic, label-free classification algorithms will be implemented to perform automatic signal segmentation without any prior information about the problem. Subsequently, different regressors will be trained for each of these subgroups, and both systems will form the new reconstruction algorithm. To avoid the discrepancies or discontinuities that segmentation or boundaries cause, it has been decided to use fuzzy classification systems, such as the fuzzy c-means clustering algorithm, to carry out this task.

The fuzzy c-means (FCM) clustering algorithm is very similar to the k-means algorithm, but each data point can belong to more than one cluster [85]. The FCM algorithm attempts to partition a finite collection of n elements $X = \{x_1, .., x_n\}$ into a collection of c fuzzy clusters

according to some criteria, which tends to minimize some objective function. Given a finite set of data, the algorithm returns a list of c cluster centers $C = \{c_1, \ldots, c_c\}$ and a partition matrix $W = (w_{i,j})$, where each element, $w_{ij} \in [0,1]$, tells the degree to which element, x_i, belongs in cluster c_j, for $i = 1, ..., n$; and $j = 1, ..., c$. Given a fixed sensitivity threshold, ε, the algorithm is described in Algorithm 1.

Algorithm 1 Fuzzy c-means clustering algorithm

Require: $c \geq 2, \varepsilon > 0$
  Randomly initialize the c cluster's centroids, c_j
  Compute the coefficients to each point for each cluster, w_{ij}.
  while $||\Delta W|| > \varepsilon$ **do**
    Compute c_j
    For each data point, compute w_{ij}
  end while

Where the centroid of a cluster is the mean of all its points, weighted by their degree of belonging to the cluster, or, mathematically:

$$c_j = \frac{\sum_i w_{ij}^m x_i}{\sum_i w_{ij}^m}, \tag{3.23}$$

where m is the hyper-parameter that controls how fuzzy the cluster will be. The higher it is, the fuzzier the cluster will be in the end. In the limit, $m \to 1$, the memberships, w_{ij}, converge to 0 or 1, and the FCM objective coincides with that of k-means.

The FCM aims to minimize the objective function:

$$f(W, C) = \sum_{i=1}^{n} \sum_{j=1}^{c} w_{ij}^m ||x_i - c_j||^2, \tag{3.24}$$

where:

$$w_{ij} = \frac{1}{\sum_{k=1}^{c} \left(\frac{||x_i - c_j||}{||x_i - c_k||} \right)^{\frac{2}{m-1}}}. \tag{3.25}$$

These membership grades indicate the degree to which data points belong in each cluster. Thus, points on the edge of a cluster, with lower membership grades, might belong in the cluster to a lesser degree than points in the cluster's center.

Model Architecture

As mentioned, our method is based on a prior clustering of the input data using fuzzy c-means. Then, a specific linear regressor is trained for each subset of points. Once both models are

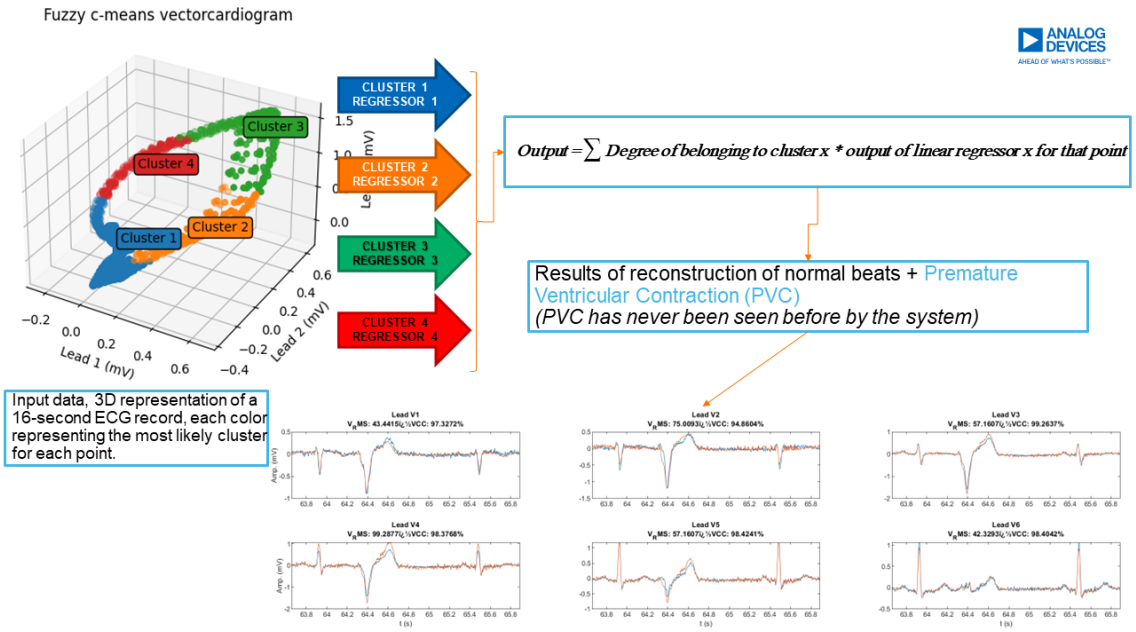

Fig. 3.16 Description of the FCM-based reconstruction algorithm, in which the points are clustered into subgroups using the FCM algorithm. The points with the highest degree of membership of each subgroup train their respective linear regressor. To calculate the model output, each regressor output given a potential is weighted according to its degree of membership in each of the generated subgroups. The result of the reconstruction of a PVC, which the model has not seen during the training phase, is also shown below.

trained, the fuzzy c-means and linear regression models, the output of the reconstruction algorithm is computed as follows. The use of fuzzy clusters instead of classic clusters allows a smoother transition, assigning percentages of membership instead of static labels. Thus, each point is assigned a degree of membership to each of the clusters, which determines the weight of the regressor assigned to that cluster in determining the output at that time, as explained in Figure 3.16.

This model's number of hyperparameters is quite high, and their adjustment is not trivial. To carry out the optimization of all these parameters, we could follow different strategies. For example, a grid optimization, although the high number of these combinations, as shown in Table 3.1, made us opt for an approach based on random search [86]. Although it does not explore the whole spectrum of possibilities, this gives us an overview of the model and allows us to choose one of the best configurations, if not the best. In Table 3.1, we can see the different possible hyperparameter configurations and the decisions made for each category.

For the clustering algorithm, we have defined 4 hyperparameters and one more for the regressor to study:

- The first and most obvious hyperparameter is the number of clusters to be formed. Of all, $c = 4$ has been chosen since, in addition to presenting the best results, it encompasses a certain sense with the number of events occurring in the heartbeat, namely the atrial and ventricular depolarizations and repolarizations.

- The distance from the points to the centroids can be calculated by the classical Euclidean distance or by other metrics, such as the Manhattan distance. Although this parameter has remained classical, there is no obvious motivation or improvement to use the latter.

- The parameter that determines the diffusivity of the FCM is regulated by the parameter m, and the standard value of $m = 2$ has been maintained because there have been no notable improvements in the choice of other values.

- The initialization of the centroids can be performed randomly, as the classical FCM algorithm determines. However, there is a variant of initialization described in the k-means++ algorithm [87], in which the goal is to spread around the initial centroid by assigning the first centroid randomly and then selecting the rest of the centroids based on the maximum squared distance. The idea is to push the centroids as far as possible from one another. This initialization algorithm was selected because it shortened the computation time and reduced the number of calculations until convergence occurred.

- The type of regressor used could be linear or logistic. However, in order to maintain the maximum possible linearity of the model, the former was chosen. Additionally, the logistic regressor provided artifacts due to its non-linear nature. This regressor is trained by means of the least squares algorithm, which has been extensively studied and analyzed previously.

Clustering				**Regressor**
Nº of clusters	**Distance metric**	**m**	**Centroid initialization**	**Method**
2	**Euclidian**	1.5	**K++**	**Linear**
3	Manhattan	**2**	None	Logistic
4		3		

Table 3.1 Hyperparameter grid for each sub-model, both FCM clustering model and regression model. In bold, the chosen hyperparameter based on prior studies and our own research.

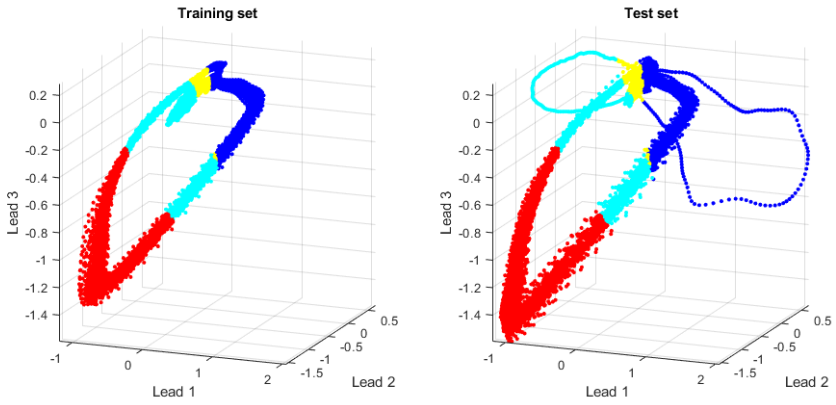

Fig. 3.17 Vectorcardiogram representation of the ECG recording, split as train and test, respectively. Each color determines the most likely degree of belonging in a certain cluster for each point. It can be appreciated that a different loop in the test group corresponds with a PVC.

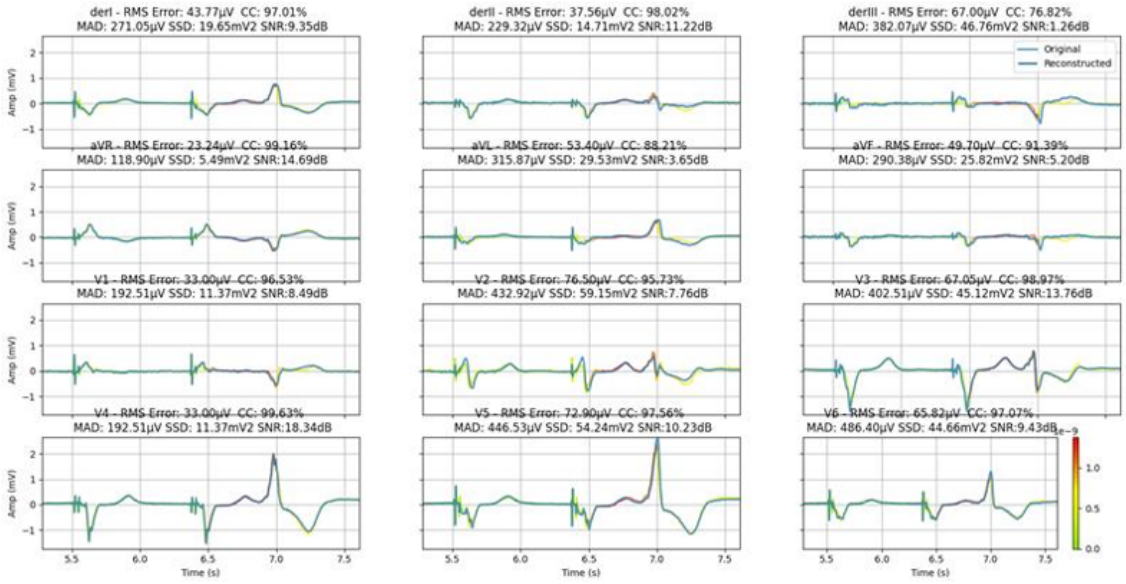

Fig. 3.18 Reconstruction of a recording from a patient with an Implantable Automatic Defibrillator also showing a PVC using the FCM model to perform the reconstruction, which has not seen this ectopic event during the training phase. The original signal is in blue, and the reconstruction is in a gradient from green to red as a reconstruction auxiliary visualization based on a robustness value extracted from the relation between the frontal leads, similar to that explained in the previous subsection about Frontal Leads Regularization (3.2). In addition, each lead's FOMs of the reconstruction performance are shown in the title.

Results

Here we show some of the preliminary results of this proposed new architecture for the reconstruction model. As already stated, one of the major concerns is the reconstruction of

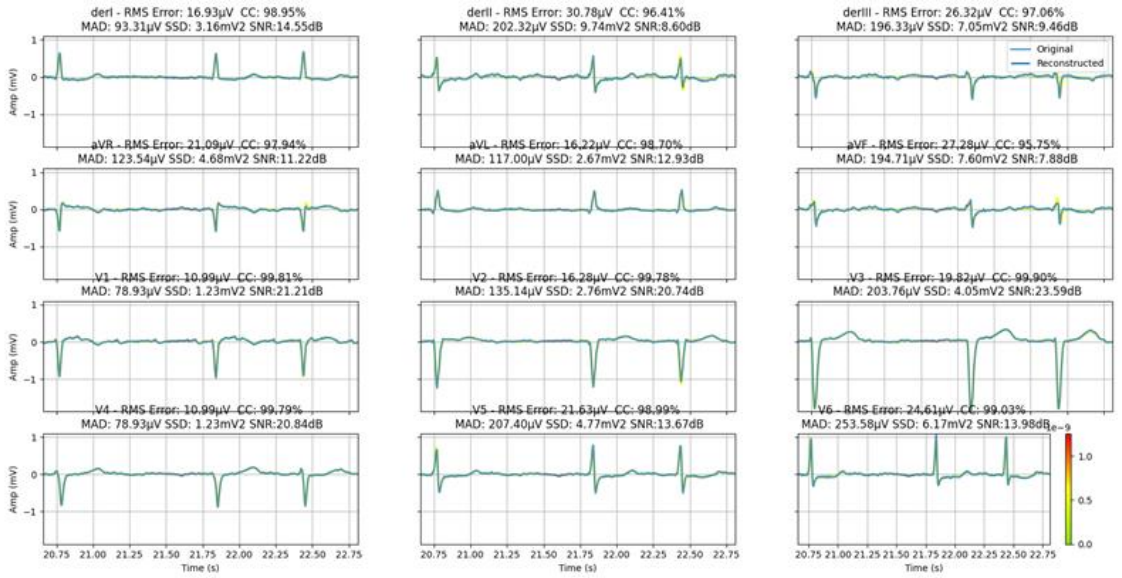

Fig. 3.19 Reconstruction of a recording from a patient with Atrial Flutter presenting an Atrial Fibrillation episode using the FCM model to perform the reconstruction. The original signal is in blue, and the reconstruction is in a gradient from green to red, as the figure above explains. In addition, each lead's FOMs of the reconstruction performance are shown in the title.

ectopic events, especially when the system has not seen them during training, as shown in Figure 3.17. For this purpose, this type of recording is extremely useful in characterizing our models since the other aspects of the reconstruction (morphology resolution, rhythm preservation, etc.) are usually fulfilled satisfactorily.

This model was tested in real patients with some pathologies of clinical interest. The reconstruction of an ectopic event, like the aforementioned PVC, is shown in Figure 3.18. It was also tested in pathologies that affect both cardiac rhythm and ECG wave morphology, such as atrial fibrillation, which can cause the disappearance of P waves, as shown in Figure 3.19. However, the complete characterization of this algorithm will be carried out in the first large clinical trial at the Hospital Clinico Universitario de Valencia, which will involve about 100 patients in which this algorithm will be tested against the largest possible number of pathologies and will be reviewed by experts who will validate its accuracy. This will determine if this approach fulfills all the requirements to be implemented in our final system.

Next Steps

This model has been preliminary validated with the previously shown results, which were quite promising. The computational speed of the training algorithm is up to ten times faster

than that of neural networks, and the results are either the same or better in some cases. Therefore, pending final validation in clinical trials, it was decided to protect this content with a patent with international extension [68].

A future improvement to be considered is to connect both parts of the model, clustering, and regressor, so that the output of the algorithm and the error with respect to the original signal can compute a kind of cost function that this first clustering takes into account, thus leaving both parts connected to provide of greater accuracy.

3.4 "A Sledgehammer to Crack a Nut": Deep Learning Approaches

Healthcare is one of the fields benefiting the most from the continuous research in Artificial Intelligence (AI). New algorithms are constantly being created and improved, allowing their application in a vast number of fields, including healthcare. In this section, we will analyze whether there is a real need or benefit to implementing this kind of algorithm in our particular case or, on the contrary, these approaches might not always be optimal, and we would be "cracking nuts with a sledgehammer"[1]. This section is adapted from the internal conference presented at Analog Devices GTC 2023 entitled “A sledgehammer to crack a nut: Do we really need Deep Learning algorithms?”.

Background

As a sample of this strong collaboration of AI in the field of health, we show the best algorithms designed for the Physionet Challenge 2021 [88, 89] on pathology detection by ECG analysis. They were all based on deep learning approaches, as shown in Table 3.2.

Machine learning and deep learning are subsets of AI that involve algorithms and models that learn from data and make predictions or decisions. Machine learning encompasses a broad range of techniques where algorithms are trained on data to recognize patterns and make predictions without being explicitly programmed. These techniques include linear regression, decision trees, and support vector machines. On the other hand, deep learning is a specific type of machine learning involving artificial neural networks with many layers, hence "deep", that can automatically learn hierarchical representations of data. Deep learning has gained significant attention and popularity due to its remarkable performance in various tasks such as image and speech recognition, natural language processing, and reinforcement learning. The key difference lies in the complexity and depth of the neural

[1] English translation of the Spanish saying "Matar moscas a cañonazos".

networks used, with deep learning models capable of learning intricate features from raw data, while traditional machine learning techniques often require manual feature engineering [90], as represented in Figure 3.20.

Ranking	Team Name	Algorithm Architecture Type
1	ISIBrno-AIMT	Residual CNN + Transformer
2	DASIL-SNU	CNN
3	NIMA	CNN
4	cardiochallenger	Transformer
5	CeZIS	CNN

Table 3.2 Top 5 best results in the Physionet Challenge 2021, focused on the identification of cardiac abnormalities from ECGs and assessed the diagnostic potential of reduced-lead ECGs relative to the standard but less accessible twelve-lead ECG.

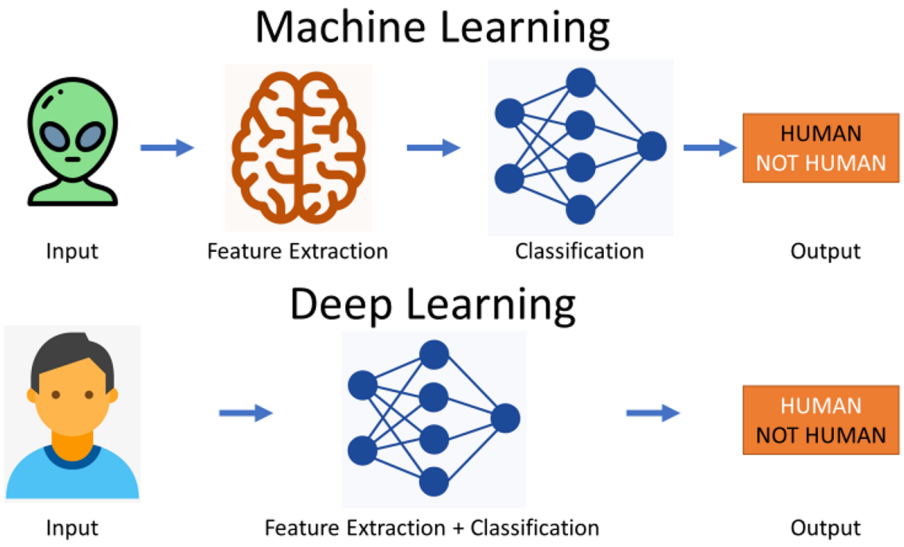

Fig. 3.20 Machine learning and deep learning flows, showing their different methodologies.

In this project, while trying to find the optimal method to perform our task, the reconstruction of electrocardiographic leads from a reduced set of them, the idea of using a deep learning algorithm arises. It may bring some advantages, such as being able to carry out the reconstruction more efficiently, as it is a more complex model. Mainly because these models can approximate much more complex functions. Understanding the organs and tissues of the body as some kind of dielectrics that the electrical currents cross, these algorithms can model the functions of the heart current propagation through the body's dielectrics. However, the

restrictions that these models show made us question whether these models really provide such an overwhelming advantage when it comes to training these networks for each patient in a personalized way. Moreover, there are already studies suggesting that, in certain specific cases, such massive models may not be the optimal solution [91, 92]. Some consideration has been given to generating a more complex generalized model rather than a personalized one for each patient, although this study is pending for future steps.

Machine Learning	**Deep Learning**
More suitable for small data	Suitable for high complexity problems
Easier explainability	Overall better accuracy
Faster and easier to implement	Better support for big data
Relies on good feature extraction	Complex features can be learned
Require feature engineering	Lack of explainability
Difficult to learn complex functions	High computational cost

Table 3.3 Pros and cons for both machine learning and deep learning approaches

ECG Lead Reconstruction Case

As mentioned, our main objective is the reconstruction of the 12-lead standard system (10 electrodes) by means of 3 independent leads formed by 4 electrodes located on the torso using a reconstruction algorithm. Another approach to this work may be described as an approximation to the forward and inverse problems in cardiology [93]. The idea is that potential distributions measured on the human torso surface are caused by the electrophysiological activity of the heart, so, given a computer model of the body's anatomical structures and their physiological properties, it is possible to obtain the corresponding body surface potential maps (BSPM). This described the so-called forward problem of electrocardiography. On the contrary, the aim of solving the inverse problem of electrocardiography is to reconstruct the heart activity from a given set of BSPMs, as shown in Figure 3.21.

Our goal can be stated as solving both problems at the same time. The inverse problem, which involves collecting the information from the heart at an external point on the surface of the torso (where we place the electrodes) and obtaining the activity of the heart, and the direct problem afterward, in which we take that activity from the heart and represent how it will be collected at a different point (the standard 12-lead system) of the surface. This process can be modeled by means of a machine learning algorithm that adapts specifically to each patient's conditions, modeling different dielectric arrangements from organs, blood, tissues, etc.

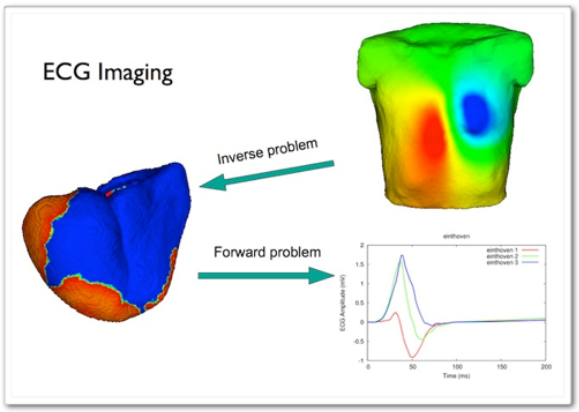

Fig. 3.21 Forward and Inverse problems in cardiology. Extracted from [93].

Some constraints are intrinsically related to our problem, even more so when we envision this as part of a system to be used for clinical purposes, not just as a theoretical approach or pure research.

- Explainability: The more complex a model is, the more difficult it will be to interpret the internal process followed to arrive at that solution, which is known as the black box problem. A CNN already has some tools to visualize the internal process, but more complex ones like the Transformers do not, or they are too complex for experts in other fields to interpret and understand: how to explain to a clinician why we have reached a certain conclusion?

- Regulation: Algorithms must comply with FDA regulations for software as a medical device (SaMD) [83], so the algorithm must meet the applicable requirements. At the moment, deep learning or models that are too complex, especially non-linear ones, make it hard to obtain FDA approval to implement them as part of a medical device, for example.

- Data availability: We have very few samples extracted from each individual patient, as we are training a specific model for each individual, orienting our approach to the increasing trend of personalized medicine [94]. When training deep learning models, they are trained with huge datasets with thousands of records and patients, despite the existence of transfer learning techniques to reduce the size of the individual training data.

- Computational Cost: Our models need to be running in a real-time framework, so the high speed of training and execution is crucial. While models such as the FCM

approach are quite fast, taking just a few seconds, training bigger models, as mentioned here, could take several minutes, which increases the cost and reduces the attractiveness of the solution.

As mentioned in previous chapters, other works already analyze these more sophisticated approaches to the reconstruction problem [95, 63]. But to validate or at least accurately characterize how these models perform in our particular problem, we decided to implement a convolutional neural network following the architecture proposed in [96] to compare with the proposed FCM-based model we developed previously.

Our hypothesis is that these complex models, such as CNNs or LSTMs, in addition to not needing so many parameters to characterize the ECG output, have a certain memory, storing intervals rather than points at each instant. We need to explore what happens when the model has been trained only with normal beats and their corresponding dynamics but is then exposed to an ectopic event that breaks these dynamics, propagating the beat, for example, from ventricular auto triggering, as in the case of PVC. It is to be expected that the model has internalized these healthy dynamics, and when an abnormal event occurs, the model is unable to reconstruct them correctly. In contrast, both approaches, whether ANN or FCM, have always been based on single instants of time since we understand the reconstruction problem as the projection of the potential in the body. This defines the process as an instantaneous event in which the beat propagates through the dielectrics of the body, not as a model that must reconstruct the beat or the ECG signal as a trend or process because, although these dynamics can be correctly interpreted if we only see healthy beats, they can be greatly affected in certain pathologies. This, once again, is clearly seen in the performance of these reconstruction models when exposed to a PVC that the system has not seen in the training phase.

Results

We trained both models, the one proposed by us using FCM and the one based on CNN proposed by [96], with a recording that only presented normal beats in the training phase. Subsequently, we analyzed the reconstruction of the PVC presented by the recording at later times. Both models satisfactorily reconstruct normal beats, as can be seen in Figures 3.22 and 3.23. However, Figure 3.22 shows that the reconstruction of the PVC using the FCM-based algorithm is much more faithful to the original than the reconstruction of the CNN model in Figure 3.23. When cardiologists have analyzed the reconstruction of this type of event, they clarified that it is not so important to maintain the wave amplitude as it is to maintain the correct reconstruction of the wave phases, that is, to maintain the wave orientation and, if

this is positive, that the reconstruction is also positive, and vice versa. And this is guaranteed by the FCM model, not by the CNN one.

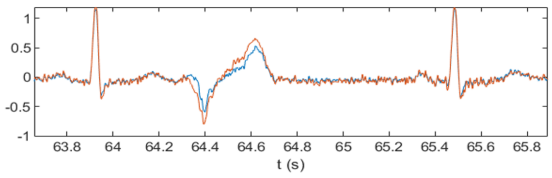

Fig. 3.22 FCM reconstruction of a couple of normal heartbeats and a PVC for a record where the ectopic event was not present during the training phase. The original signal is in blue and the reconstructed one is in orange.

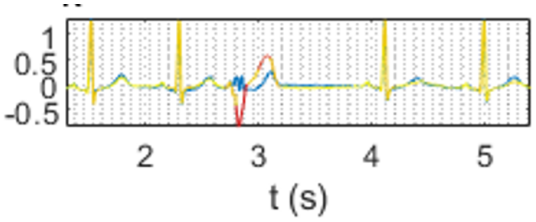

Fig. 3.23 CNN reconstruction of a couple of normal heartbeats and a PVC for a record where the ectopic event was not present during the training phase. The original signal is in blue and the reconstructed one is in a gradient from green to red, where the reconstruction most fails.

With these results, the FCM-based alternative is still the ideal candidate to develop the rest of the study since the CNN did not offer notable improvements, and this type of reconstruction based on models with a certain memory may have negative consequences in some cases, as hypothesized.

Conclusions

We should use the abundant heuristics that experts have built over a century of ECG study. When picking which method to use, it's not just how powerful it is. We also need to think about considering aspects such as regulations and the role of this method within the whole system.

Deep learning is a powerful technique, but it's only as good as how we use it and if it fits the job correctly. Keeping things simple is smart, finding solutions that are easy to understand and use instead of making them overly complicated and, sometimes, inaccurate.

So, to be successful in performing the ECG Lead reconstruction, we need to rely on the experts and keep it simple.

3.5 Conclusions

In this chapter we have explored new alternatives to improve or to perform autonomously the 12-lead reconstruction.

We have initially proposed simple and obvious improvements to our previous ANN-based proposal, such as modifying the cost function or using expert committees, and then moved to more refined proposals, such as performing a nonlinear transformation of the input data, to improve the convergence time of the results and, perhaps, their efficiency.

New architectures have also been proposed for our model, based on simple but more sophisticated alternatives such as automatic segmentation by an FCM algorithm or more complex models such as those based on memory cells or deep networks.

To validate all this, and as an illustrative method, we have used the particular case of the reconstruction of ectopic events in the ECG by the model when it had not been trained with it, thus analyzing the response of the model to unknown but relevant and quite common events.

It has been shown that the quality of the reconstruction, although very positive in all cases, shows a better trade-off between efficacy and efficiency in the model based on FCM and linear regressors. This is why this will be our proposed model to be validated in clinical trials, with a view to be implemented in a potential final system.

Chapter 4

Clinical Trial Validation

4.1 Introduction

Once the reconstruction algorithm has been designed and refined, its clinical effectiveness must be validated. A clinical study was designed to be carried out at the Hospital Clínico Universitario de València with the aim of evaluating and validating the reconstruction algorithm based on fuzzy c-means models, as well as the effectiveness of the different electrode positions and configurations from which to perform the reconstruction. This chapter contains the summary of the study and the clinical report submitted to the responsible entity, in this case, the Foundation for Research of the Hospital Clínico de la Comunidad Valenciana INCLIVA [97], which manages biomedical research at the Hospital Clínico Universitario de Valencia and its Health Department, as well as certain groups of scientific excellence of the Faculty of Medicine of the University of Valencia and the Carlos Simón Foundation. This clinical report and all of its content have been created by the Thesis's author, and it's allowed to display its entire content. It will be included in its original form after this introduction, in Section 4.2.

4.1.1 Hypothesis

The aim of this study is to evaluate the possibility of reconstructing the standard 12-lead system using different algorithms as well as to identify the most suitable location of the electrodes for a proper reconstruction. Our hypothesis is that it is possible to reconstruct the standard 12-lead with information gathered from three leads that might be positioned in a reduced system. For these goals to be accomplished, it has been defined three different objectives: (1) To evaluate the reconstruction of the standard 12-leads ECG, (2) to identify

the optimal location for each patient, and (3) to evaluate if there exists a pattern among patients with the same pathology and/or the same phenotype.

4.1.2 Material and Methods

The study will be conducted in 100 patients, 30 patients with a normal electrocardiogram, and 70 patients with suspected pathological electrocardiogram. Patients with a normal electrocardiogram will be patients who are going to have a preoperative test, whose protocol consists of performing a series of diagnostic tests that include an electrocardiogram. Patients with potential pathological electrocardiograms will be patients who are going to have an electrocardiogram since there is suspicion that they have some type of heart disease, either at the hospital or on an outpatient basis (Holter). At the end of the study, 108 patients had to be enrolled in the efficacy analysis, from which eight had to be discarded due to abundant noise artifacts or missing channels, as will be discussed in detail in the clinical report.

The efficacy of the reconstruction shall be assessed using two different methodologies. A subjective method was initially considered to compare reports written by two cardiologists analyzing measured and reconstructed ECG (blind test). Both reports must be coincident to consider the reconstruction to be accurate. This proposed methodology was not possible to accomplish due to the pandemic (this study was started in 2020), which provoked the trial to resume very slowly due to the delays in surgeries and follow-up appointments. Consequently, this limited the number of cardiologists involved in reviewing the reconstruction results from a clinical perspective. To overcome this latter limitation, the results were presented exclusively to the Principal Investigator (PI) of the study at the end of it. Finally, objective methods were proposed, which include calculating several FOMs between the measured and reconstructed ECG signals to assess the reconstruction performance, which are the CC, RMS, MAD, SSD, and SNR.

4.1.3 Results

The results prove that the limits for all FoMs determined are achieved by a wide set of configurations with which to perform the reconstruction for the set of all patients. Regarding the subjective method, various complications led to the modification of the methodology of this part. To accomplish this, the results of the reconstruction were shown visually so that the original signal and the reconstruction were superimposed and labeled so the clinicians can verify whether the reconstruction has indeed been successful. In this regard, the cardiologist responsible for verifying these results, the Principal Investigator of the project, has extensive experience in reading and interpreting ECGs. He verified that all the

events seen in the original signal were perfectly visible in the reconstructed signal. Events such as depolarizations, repolarizations, or ectopic beats were perfectly reproduced in the reconstructed signals for all the leads from the 12-lead cart.

A difference can be observed among the different electrode configurations selected to carry out the reconstruction between different patients. There is a single optimal position for all, but it is different for each patient, and the results are fairly close among the top positions, with no clear winners. No significant differences have been found in any of the subgroups of patients. The small amount of data from some of these subgroups prevents us from drawing any conclusion in this sense since they are such small groups that the origin of their variation may not necessarily be due to belonging or not in that subgroup. However, records with implantable devices and pacemakers show several deviations when performing reconstruction. They have been considered of vital importance, given the sensitivity that the correct treatment of these data poses in these patients, and this matter will be discussed and analyzed in further detail.

4.1.4 Conclusions

These clinical trial results confirm the initial hypothesis that reconstruction using a reduced set of leads is possible with a high level of accuracy, as we check how these values obtained for the FoMs correspond visually with a perfect reconstruction of the target leads without visible errors. Therefore, we can say that our results are satisfactory, and the reconstruction quality is good enough to consider our algorithms robust enough to test it under ambulatory conditions.

However, the challenges that implantable devices represent when performing reconstruction have been considered of vital importance, given the sensitivity that the correct treatment of these data poses in these patients. So a further study has been designed, presented at an International Conference, investigating the best way to deal with it. The proposed system involves identifying these pulses and eliminating them during the training process of the reconstruction model since they are pulses already distorted by the nature of the signal and the recorder itself. This will be discussed in depth in the Section 4.3, after the clinical trial report.

4.2 Clinical Trial Report

4.3 Challenges in ECG Lead Reconstruction in Patients with Pacemakers and Implantable Defibrillators

4.3.1 Introduction

Pacemakers and implantable cardioverter-defibrillators (ICD) are devices that stimulate the heart tissue when its natural electrical activity is absent. Oftentimes, implanted pacemaker activity is hardly perceptible on a normal ECG trace because the very fast pulses are filtered by the recording devices but, in other cases, they may affect the waveform and, unless properly identified, may potentially affect the performance of modules that perform automatic analysis or classification of heartbeats. Although many modern analog front ends monitor the ECG signals at a very high sampling frequency to correctly detect pacemaker pulses regardless of single, dual, or three-chamber pacing [98], it was not part of our ECG system in the clinical trial shown in previous Section 4.2. This induced misleading conclusions regarding these ECG reconstructions on this specific subgroup, so a new experiment was proposed to assess the importance of these pulses in the ECG reconstruction and how it can be managed to avoid this weakness.

The aim of this study is to assess the robustness of an algorithm based on ANN to reconstruct the standard 12-lead system of a clinical ECG from a reduced number of leads acquired with a portable monitoring device, as proposed in our previous work [67], in the presence of pacemaker and ICD pulses. We will study the effect on training the network with ECG records which includes frequent pacemaker activity. The reconstruction performed with the original record will be compared with the masked pulses for training the system using a detection algorithm integrated into some analog front ends, which in this study will be replaced by a software algorithm applied in our dataset. The hypothesis is that the algorithm will perform a better reconstruction if it does not encounter these artifacts in training. This section is an adaptation of the Conference Paper [69].

4.3.2 Materials and Methods

ECG Records

Actual data were acquired in the Hospital Clínico Universitario de Valencia from the previous clinical trial. Electrocardiogram records lasting between 60 and 120 seconds were recorded with a sampling rate of 1 kHz from 13 patients with a pacemaker or an implantable cardiac

defibrillator, 10 records from men and three from women. In addition, and as a control, 87 records were added to the study, both from healthy patients and those with other pathologies, none of which showed pulses of this type. The ECG records were preprocessed to mitigate noise. Two 4th-order Butterworth IIR bi-directional filters were applied. A low-pass filter with a 150 Hz cut-off frequency mitigates myoelectric noise and high-frequency interference, and a high-pass filter with a 0.67 Hz cut-off frequency reduces baseline wandering and offset.

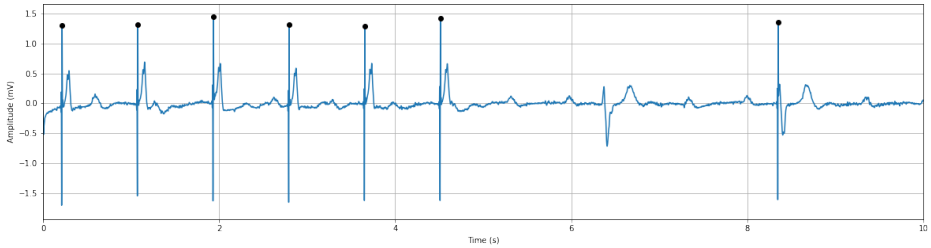

Fig. 4.1 Example of a segment of one of the ECG records. The pacemaker pulses have been marked by the developed pulse detection algorithm. A series of ventricular contractions triggered by the device appear after the pulse, as well as an independent contraction of the patient's heart.

Reconstruction Model

The reconstruction is based on an ANN using a MLP. To synthesize each of the 12 leads from the three acquired leads, a one-hidden layer feed-forward ANN system is trained with the Levenberg-Marquardt algorithm. Therefore, each ANN has a single neuron in the output layer. The non-linear transfer function applied in the hidden layer is the hyperbolic tangent sigmoid function. The number of neurons in the single hidden layer was empirically established based on a sweep of different layer sizes, choosing a trade-off between the optimal result and an acceptable computational expense. This was obtained empirically based on the results of the stability and accuracy of the model [67].

Pacemaker/ICD Masking

This network was trained in areas with no artifacts caused by the activity of implantable devices. Therefore, data that have these pulses annotated should be used, or, failing that, a pacemaker and ICD pulse detection algorithm should be applied to mask these sections so that they are not part of the training of the reconstruction algorithm. Ideally, this pulse detection algorithm should be implemented at a hardware level in the device where signals can be sampled at a higher frequency (e.g., 2 kHz) since, if sampled at the normal much lower

rates, the pulse will be severely distorted and will not be easy to detect. Fortunately, some modern ECG analog front ends, such as the ADAS1000 from Analog Devices, Inc., include this feature of pulse detection [99]. In this study, having already taken the records before, it was not possible to activate this algorithm by hardware, so a software detection algorithm in the digital record was designed to mark the pulses that may appear in these records. The pulse detection algorithm is an update of the one proposed in [100] with certain parameters modified to achieve higher accuracy. Figure 4.1 shows how the detection algorithm correctly identifies these pulses and creates 20 ms windows to mask the whole impulse and the possible time warping that the response of the digital filters might cause.

4.3.3 Results

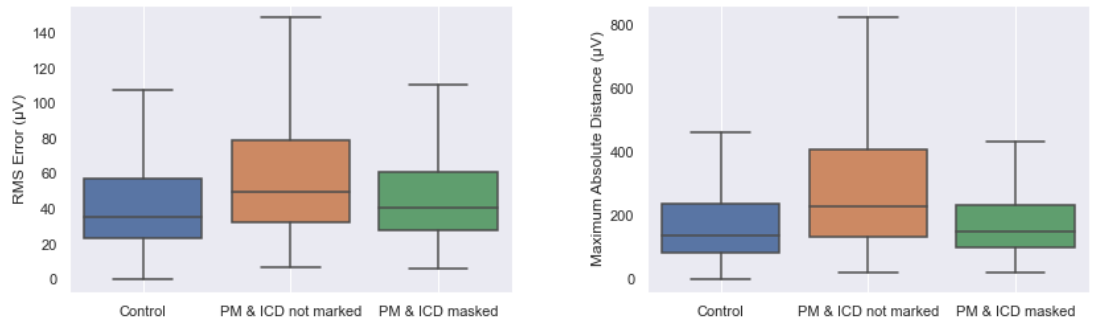

Fig. 4.2 Boxplots of the RMS Error and MAD, respectively, obtained for each of the groups studied, the control (absence of pulses) ECG records, the records with pacemaker and ICD pulses without taking into account, and the last one is the records with the pulses masked.

The models are individually trained for every patient to achieve the best possible reconstruction. The size of the training set was empirically set to 16 seconds (16,000 samples at a sampling frequency of 1 kHz). The remaining of the record, 104 seconds (104,000 samples), is used for test. All results shown have been obtained from the test part of the records. In the case of the records with external excitation activity (marked pulses), these parts have been removed from the training set, and more samples have been included in the training set to obtain 16,000 training samples. In these cases, the test sets are a bit shorter. The results have been expressed in terms of median and interquartile ranges represented in the form of boxplots in Figure 4.2.

The control results are within the expected range, in agreement with those obtained in the clinical trial referred in previous Section 4.2. In the groups of interest, the one with the ECG records with pacemaker and ICD pulses and the one in which they were identified, marked,

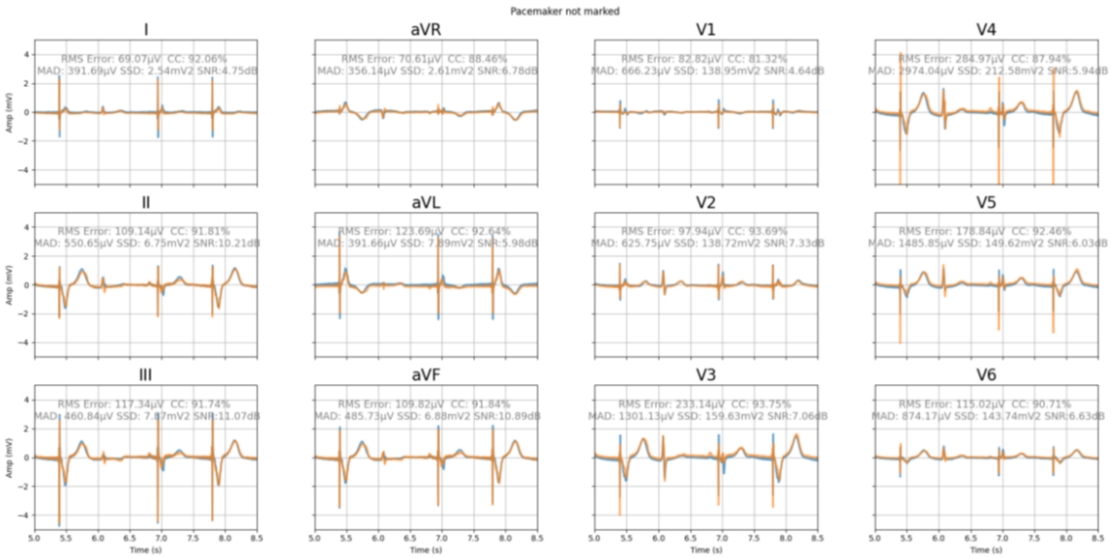

Fig. 4.3 ECG reconstruction without the pacemaker annotation. In blue, the original signal and, superimposed in orange, the reconstructed signal.

and avoided, several differences were observed. The group with the annotations mostly replicated what was seen in the control group, both in this study and in the clinical trial. In addition, there was an improvement in several FOMs with respect to the group containing the unannotated records. To illustrate these differences, the reconstruction of one of the records is reproduced. In it, four beats are shown, the second one being the only one that has been provoked autonomously by the heart, and the remaining three presenting a stimulus.

In Figure 4.3, the reconstruction and training have been performed considering the entire signal, i.e., including the areas showing pulses from an implantable device. Although the reconstruction is quite acceptable, it does not faithfully reproduce certain aspects of the signal, such as the baseline of lead aVL or the depolarization in lead II. In contrast, in Figure 4.4, these excitation pulses were excluded from training and reconstruction, and a better reconstruction is achieved, not only for the pacemaker pulses (not considered to obtain the FoMs), but the entire signal.

4.3.4 Conclusions

This work has demonstrated the feasibility of refining an ambulatory ECG system that can reconstruct the signals expected from a standard 12-lead system, even in the presence of implantable cardiac devices such as pacemakers or ICDs. Identifying the pulses produced by these devices allows the reconstruction system to disregard them when obtaining its parameters during the training phase, thus allowing the system to adjust more faithfully to the

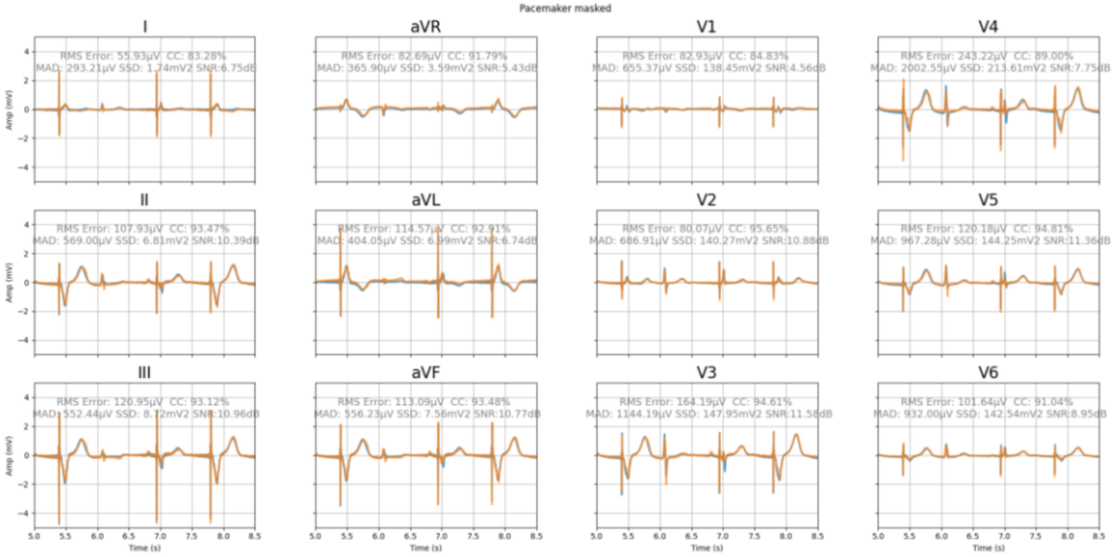

Fig. 4.4 ECG reconstruction with the pacemaker pulses hidden to the training segment. In blue, the original signal and, superimposed in orange, the reconstructed signal.

heart's natural activity, avoiding pulse distortion in the collected ECG signal. To obtain this improvement, these stimuli must be identified, either by early detection on the analog front ends or, as in this study, by software detection algorithms. In the future lines of this Thesis, it will be proposed that further studies shall be carried out with data from pathological records to assess the technique's robustness, generalization, and diagnostic effectiveness.

Chapter 5

Ambulatory Trial Validation

5.1 Introduction

Once the reconstruction algorithm has been validated in the clinical environment. A clinical study was designed at the Consorcio Hospital General Universitario de València (CHGUV) with the aim of evaluating and validating the reconstruction algorithm in ambulatory use, which is the final use case of this system. This chapter contains the summary of the study and the clinical report submitted to the responsible entity, in this case, the Asociación Española del Medicamento AEMPS [101], the State agency responsible for guaranteeing to society, from a public service perspective, the quality, safety and efficacy, and correct information on medicines and medical devices, from their research to their use. This clinical report and all of its content have been created by the Thesis's author, and he is allowed to display its entire content. It will be included in its original Spanish form after this summary.

5.1.1 Hypothesis

The hypothesis focuses on corroborating that the reconstruction algorithm, under development, is capable of providing a reliable reconstruction similar to the 12-lead ECG, with only 3 leads, regardless of whether the signals were recorded in the office or in ambulatory conditions. The main objective is to evaluate the impact of signal quality on the performance of the ECG reconstruction algorithm. As secondary objectives, it will be studied whether the use of fewer measurement points negatively affects the performance of the algorithm, whether there are differences according to cardiac phenotypes, as well as which positions offer better reconstruction.

5.1.2 Material and Methods

The study was designed to include 30 patients who will be attending the Holter Nurse Consultation for 24-hour Holter monitoring, requested for any indication by the responsible physician. 41 patients with suspected heart disease have been included in the study, but 11 patients had to be discarded as a consequence of not having the minimal number of required recordings. Final data included records from 13 men and 17 women who presented the following pathologies: Ventricular Hypertrophy (2 patients), Arrhythmias (12), Myocardial Infarction (2), Extrasystole (1), Heart Failure (1), Tachycardia (3) and Other types of pathologies (9).

Data were recorded both in the clinic and in an ambulatory scenario while the patient developed his/her normal activity. Both records were taken with different devices specially adapted to both situations. To validate both recordings, two recordings were taken at the same time at the same electrode position to ensure that the signal collected was the same in both devices.

Two different methodologies shall assess the efficacy of the reconstruction. A subjective method, which includes several interviews, will be organized to discuss with the cardiologists to analyze this information. And objective methods, which include several figures of merit such as the CC, RMS, MAD, SSD, and SNR, were calculated between the measured and reconstructed ECG signals to determine the quality of the ECG acquired by the aECG device under ambulatory conditions. For very noisy records, with artifacts, or when it was not possible to obtain simultaneous recordings from both devices, the reconstruction was compared by grouping the beats in templates, to which the figures of merit mentioned above were applied, as shown in Figure 5.1.

5.1.3 Results

	RMS (μV)	**CC** (%)	**MAD** (μV)	**SSD** (mV^2)	**SNR** (dB)
Mean	117.46	52.76	535.04	12.42	1.21
Std dev	84.41	30.98	396.84	19.64	4.42
25%	58.41	29.71	250.26	1.96	-1.36
50%	88.9	52.06	445.8	4.61	0.35
75%	165.24	79.02	710.92	14.81	4.5

Table 5.1 Results obtained for the five FOMs for patients with both the clinical record as the control record and the ambulatory record as the ones used to perform the reconstruction. Mean, standard deviation, and quartile distributions are shown.

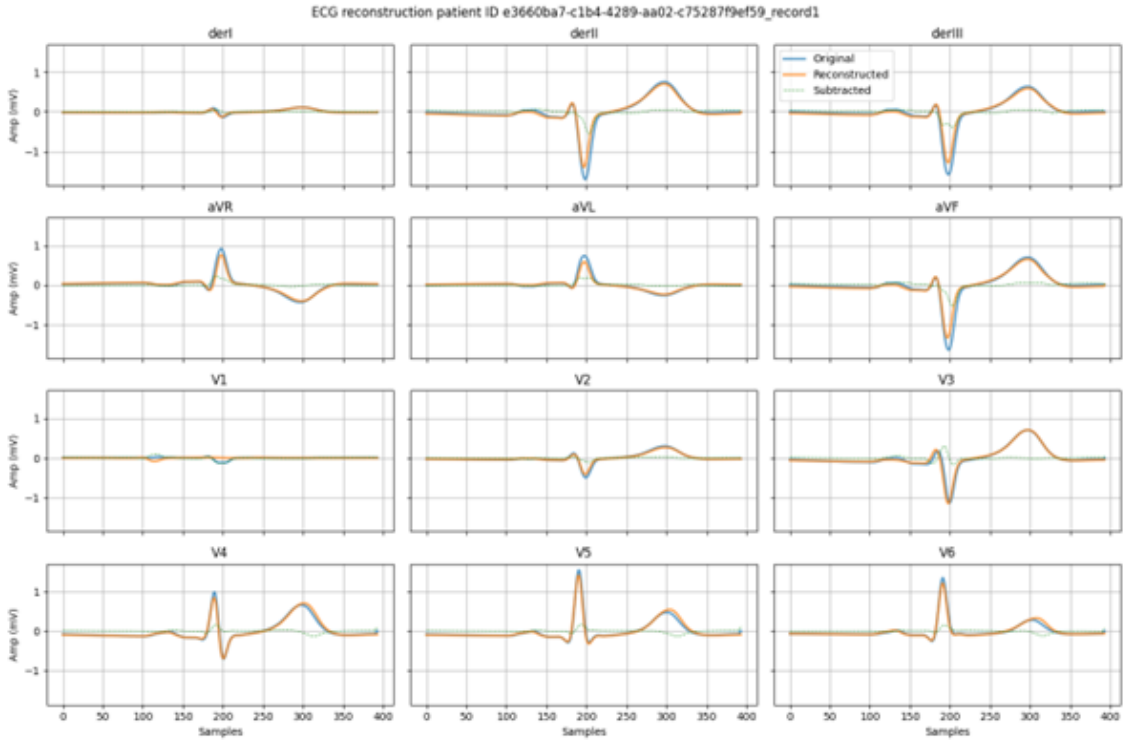

Fig. 5.1 Reconstruction of the ECG of a patient in which the simultaneous recording of the standard system and the ambulatory recording could not be used. In blue, the original signal and, superimposed, its reconstruction in orange. In addition, an extra line, dashed in green, showing the error between the two signals, has been added as an aid.

The results presented in this report confirm our hypotheses. The results show a very good performance of the reconstruction algorithm responsible for generating the standard 12-lead system using 3 independent leads.

The objective analysis of five figures of merit was done compared with the subjective analysis with cardiologists who are experts in reading and interpreting ECGs. We can say that both tests have been successfully passed. The figures of merit shown in Table 5.1 show that the defined thresholds of success have been passed for all patients, which gives us great confidence that the model is sufficiently robust for various adverse conditions. The subjective analysis has been quite positive, with the ability to reliably reconstruct spurious events such as repolarizations or ectopic beats being endorsed by the clinician, even though the system had not seen these events during training. Some of the comments the clinician registered about the results were:

- "*The algorithm is able to reconstruct spurious or punctual events not seen by the model during the training phase. The case of repolarization is very interesting.*"

- "*A tool like this is clinically useful as it provides a lot of information in a less obtrusive way compared to other solutions.*".

5.1.4 Conclusions

The results are satisfactory, and the quality of the reconstruction has allowed experts to make diagnoses and identify pathological events in the same way as they would in the clinical setting, but using ambulatory records. This demonstrates that our algorithms are robust enough to be used in their final intended use, the ambulatory monitoring. This confirms the performance and robustness of the reconstruction strategy, which may allow its use as part of operational clinical devices.

5.2 Clinical Trial Report

Chapter 6

Conclusions

When the work related to this PhD Thesis was launched, the number of articles related to the reconstruction of electrocardiographic leads was high but, surprisingly, relatively old. The bulk of this field referred to work from the last century, with little activity in the early years of the millennium. This was surprising because, although there were well-established systems, it is not commonly seen in clinical practice. That all changed shortly after we started working on this when it became clear that there was a resurgence in the number of publications. With the advancement in the field of artificial intelligence with the great expansion in machine learning and deep learning in recent years, as well as its rapid adoption by the world of healthcare, researchers have put their forces to apply all these advances in the reconstruction of the ECG.

6.1 Summary and Conclusions

This Thesis has presented a system for the reconstruction of electrocardiographic leads using a reduced system of independent leads supported by the use of machine learning models. In addition, its development has been considered with a view to its implementation as part of a final ambulatory monitoring system, with the challenges that this entails.

ECG Lead reconstruction methods have been stable for a long time, using mainly linear combination-based approaches, either automatically learned or empirically determined. In the first step of the Thesis, the effectiveness of these new ANN-based algorithms was studied against the more classical implementations of linear regression or linear regression applied specifically to the different waves of the ECG segment. In addition, special emphasis was placed on two key aspects that have not always been taken into account: the evaluation method and the position of the electrodes to perform the reconstruction. A study was conducted on which were the best figures of merit that could best describe the effectiveness of the

reconstruction and which were the best positions to carry out this task. Preliminary results showed that this new approach offered superior results to the more classical methods, with a noticeable difference. However, new techniques could be explored, especially considering that the model's explainability was an important part and should not be disregarded.

- To improve these results, several alternatives were explored. An attempt was made to improve the ANN architecture by implementing a committee of experts that provided greater stability to the model output and, therefore, greater accuracy. The data input layer was also modified to shorten the convergence time and improve the results. These changes were an advantage over the vanilla model of the network but added to the complexity of the model. Faced with this, a solution was sought that was somewhere between simple and ingenious. The automatic segmentation of the ECG and its subsequent segregation into different regressors are all united by means of a fuzzy model that gives it a much greater smoothness than other models that might have resembled it in the past.

- The results were promising, reaching very similar or even higher values than all the proposed models but also being much faster both when training and executing them. This is why it was postulated as the definitive proposal for our reconstruction model, although it remained to validate its effectiveness against the most modern models of the state of the art, those based on deep learning.

- These models based on Deep Learning, of increasing importance in all fields, including the biomedical, were considered as possible candidates, although the absence of really strong performance, together with their other shortcomings such as models too similar to black boxes and the difficulties that these models pose when facing regulatory entities and non-experts in the field made us discard them.

- Once the reconstruction algorithm is developed and refined, it needs clinical validation. A clinical study was planned at the Hospital Clínico Universitario de València to assess this algorithm's effectiveness, alongside testing different electrode positions and configurations for the reconstruction process. The clinical trial results confirm the initial hypothesis that reconstruction using a reduced set of leads is highly accurate, evidenced by the close correspondence of FOMs with a visually error-free reconstruction of the leads supported by the cardiologists. This suggests satisfactory results and robust algorithms suitable for testing under ambulatory conditions in the following clinical trial.

- Acknowledging the challenges posed by implantable devices in reconstruction, a subsequent study proposes a system to identify and eliminate distorted pulses during the reconstruction model's training process, enhancing the fidelity of ambulatory ECG systems even in the presence of devices like pacemakers or ICDs. By disregarding these pulses, the system can better adapt to the heart's natural activity, improving signal quality. Future research aims to assess the technique's robustness and diagnostic effectiveness with pathological records, suggesting promising avenues for refinement and application.

- Following the validation of the reconstruction algorithm in a clinical setting, a study was conducted at the Consorcio Hospital General Universitario de València (CHGUV) to assess its performance in ambulatory use, representing the final intended application of the system. The study summary and clinical report, submitted to the responsible entity, the Asociación Española del Medicamento AEMPS, underscore the satisfactory results, indicating that the reconstructed signals facilitated accurate diagnoses and identification of pathological events similar to those made in clinical settings. This affirms the robustness of the algorithms for ambulatory monitoring, confirming their suitability for operational clinical devices.

In conclusion, this Thesis has presented a novel algorithm for ECG lead reconstruction, guided by the goal of integrating it into a final ambulatory monitoring system, recognizing the complexities inherent in such an implementation. The algorithm's effectiveness was demonstrated through rigorous experimentation, surpassing classical methods and exhibiting promising results in accuracy and efficiency. Various enhancements were explored, including the implementation of expert committees and fuzzy models, resulting in improved performance and speed. The subsequent clinical validation affirmed the algorithm's effectiveness in real-world settings, highlighting its potential for ambulatory monitoring applications. Moreover, the proposed system showed adaptability to challenges posed by implantable devices, further enhancing its utility and robustness. Future research aims to continue refining the algorithm and exploring its diagnostic effectiveness in diverse clinical scenarios, paving the way for its widespread adoption in operational clinical devices.

6.2 Future Lines

Future research will focus on refining the system, the algorithm's architecture, and training methods to improve its performance and versatility in different clinical contexts.

- The use of a generalized model when the system fails will be explored, providing the clinician with a backup model that may be implemented using more complex models.
- Efforts will be made to optimize the integration of the algorithm into ambulatory monitoring systems to ensure seamless operation and compatibility with existing healthcare infrastructure.
- Studies of the algorithm's diagnostic efficacy with pathology data will continue to validate its reliability and accuracy in detecting and characterizing cardiac abnormalities.
- Collaborative initiatives with regulatory agencies and healthcare professionals will be pursued to streamline the algorithm's approval process and facilitate its adoption in clinical practice.

Overall, future lines of research aim to consolidate the algorithm's position as a cornerstone technology in the field of electrocardiographic monitoring, providing clinicians with valuable insights into patients' cardiac health and paving the way for improved patient care and outcomes.

References

[1] A. C. Guyton, *Human physiology and mechanisms of disease*. Saunders, 1992.

[2] *Heart information center: Heart anatomy*, en, Online; accessed 7 March 2019, 2019. [Online]. Available: https://www.texasheart.org/heart-health/heart-information-center/topics/heart-anatomy/.

[3] S. Mendis, P. Puska, B. e. Norrving, W. H. Organization, *et al.*, *Global atlas on cardiovascular disease prevention and control*. World Health Organization, 2011.

[4] *Cardiovascular diseases*, en, Online; accessed 3 March 2019, 2019. [Online]. Available: https://www.who.int/en/news-room/fact-sheets/detail/cardiovascular-diseases-(cvds).

[5] *The global economic burden of non-communicable diseases*, en, Online; accessed 14 March 2019, 2019. [Online]. Available: http://www.championadvocates.org/en/champion-advocates-programme/the-costs-of-cvd.

[6] K. Ng, S. R. Steinhubl, C. DeFilippi, S. Dey, and W. F. Stewart, "Early detection of heart failure using electronic health records: Practical implications for time before diagnosis, data diversity, data quantity, and data density," *Circulation: Cardiovascular Quality and Outcomes*, vol. 9, no. 6, pp. 649–658, 2016.

[7] C. Tobón, C. A. Ruiz-Villa, E. Heidenreich, L. Romero, F. Hornero, and J. Saiz, "A three-dimensional human atrial model with fiber orientation. electrograms and arrhythmic activation patterns relationship," *PloS one*, vol. 8, no. 2, e50883, 2013.

[8] L. Sörnmo and P. Laguna, *Bioelectrical signal processing in cardiac and neurological applications*. Academic Press, 2005, vol. 8.

[9] A. Bayès de Luna, "Bases de la electrocardiografía," *Semiología Electrocardiográfica I: Génesis del ECG y patrones de normalidad. Barcelona: Prous Science*, 2006.

[10] J. M. Nerbonne, "Molecular basis of functional voltage-gated k+ channel diversity in the mammalian myocardium," *The Journal of Physiology*, vol. 525, no. 2, pp. 285–298, 2000.

[11] J. Malmivuo and R. Plonsey, *Bioelectromagnetism: principles and applications of bioelectric and biomagnetic fields*. Oxford University Press, USA, 1995.

[12] R. Paine, *Generation and Interpretation of the Electrocardiogram*. Lea & Febiger, 1988.

[13] J. M. F. Corral, J. M. Ferrero, J. S. Rodríguez, A. A. Vives, *et al.*, *Bioelectrónica. Señales Bioeléctricas*. Ed. Univ. Politéc. Valencia, 1994.

[14] H. Kennedy, "Ambulatory (holter) electrocardiography recordings," *Cardiac electrophysiology. From cell to bedside (2nd ed.)*, pp. 1–024, 1995.

[15] F. M. Fesmire and E. E. Smith, "Continuous 12-lead electrocardiograph monitoring in the emergency department," *The American Journal of Emergency Medicine*, vol. 11, no. 1, pp. 54–60, 1993.

[16] D. Jabaudon, J. Sztajzel, K. Sievert, T. Landis, and R. Sztajzel, "Usefulness of ambulatory 7-day ecg monitoring for the detection of atrial fibrillation and flutter after acute stroke and transient ischemic attack," *Stroke*, vol. 35, no. 7, pp. 1647–1651, 2004.

[17] B. Surawicz and T. Knilans, *Chou's electrocardiography in clinical practice: adult and pediatric*. Elsevier Health Sciences, 2008.

[18] P. Kaewfoongrungsi and D. Hormdee, "Support vector regression-based synthesis of 12-lead ecg system from the standard 5 electrode system using lead v1," *Engineering and Applied Science Research*, vol. 43, pp. 494–498, 2016.

[19] S. Mittal, C. Movsowitz, and J. S. Steinberg, "Ambulatory external electrocardiographic monitoring: Focus on atrial fibrillation," *Journal of the American College of Cardiology*, vol. 58, no. 17, pp. 1741–1749, 2011.

[20] A. Pantelopoulos and N. G. Bourbakis, "A survey on wearable sensor-based systems for health monitoring and prognosis," *IEEE Transactions on Systems, Man, and Cybernetics, Part C (Applications and Reviews)*, vol. 40, no. 1, pp. 1–12, 2009.

[21] C. Steinberg *et al.*, "A novel wearable device for continuous ambulatory ecg recording: Proof of concept and assessment of signal quality," *Biosensors*, vol. 9, no. 1, p. 17, 2019.

[22] *Zio xt*, en, Online; accessed 24 March 2019, 2019. [Online]. Available: https://www.irhythmtech.com/products-services/zio-xt.

[23] M. Masoumian Hosseini, S. T. Masoumian Hosseini, K. Qayumi, S. Hosseinzadeh, and S. S. Sajadi Tabar, "Smartwatches in healthcare medicine: Assistance and monitoring; a scoping review," *BMC Medical Informatics and Decision Making*, vol. 23, no. 1, p. 248, 2023.

[24] W. Einthoven, "The different forms of the human electrocardiogram and their signification.," *The Lancet*, vol. 179, no. 4622, pp. 853–861, 1912.

[25] F. N. Wilson, F. D. Johnston, A. G. Macleod, and P. S. Barker, "Electrocardiograms that represent the potential variations of a single electrode," *American Heart Journal*, vol. 9, no. 4, pp. 447–458, 1934.

[26] L. Pourafkari, S. Joudi, S. Ghaffari, A. Tajlil, B. Kazemi, and D NADER, "St-segment elevation in the right precordial leads in patients with acute anterior myocardial infarction," *Balkan Medical Journal*, vol. 33, no. 1, pp. 58–63, 2016.

[27] S. H. Braat, P. Brugada, C. de Zwaan, J. M. Coenegracht, and H. Wellens, "Value of electrocardiogram in diagnosing right ventricular involvement in patients with an acute inferior wall myocardial infarction.," *Heart*, vol. 49, no. 4, pp. 368–372, 1983.

[28] E. Van Gorselen, F. Verheugt, B. Meursing, and A. O. Ophuis, "Posterior myocardial infarction: The dark side of the moon," *Netherlands Heart Journal*, vol. 15, no. 1, p. 16, 2007.

[29] A. Welinder *et al.*, "Comparison of signal quality between easi and mason-likar 12-lead electrocardiograms during physical activity," *American Journal of Critical Care*, vol. 13, no. 3, pp. 228–234, 2004.

[30] J. Francis, "Ecg monitoring leads and special leads," *Indian Pacing and Electrophysiology Journal*, vol. 16, no. 3, pp. 92–95, 2016.

[31] G Fontaine, "Stimulation studies and epicardial mapping in ventricular tachycardia: Study of mechanisms and selection for surgery.," *Reentrant Arrhythmias*, vol. 334, 1977.

[32] M. Elmaghawry, M. Alhashemi, A. Zorzi, and M. H. Yacoub, "A global perspective of arrhythmogenic right ventricular cardiomyopathy," *Global Cardiology Science and Practice*, vol. 2012, no. 2, p. 26, 2014.

[33] E. Frank, "An accurate, clinically practical system for spatial vectorcardiography," *Circulation*, vol. 13, no. 5, pp. 737–749, 1956.

[34] J. Hyttinen, "Development of regional aimed ecg leads especially for myocardial ischemia diagnosis," Ph.D. dissertation, Tampere University of Technology, 1994.

[35] G. E. Dower, A. Yakush, S. B. Nazzal, R. V. Jutzy, and C. E. Ruiz, "Deriving the 12-lead electrocardiogram from four (easi) electrodes," *Journal of Electrocardiology*, vol. 21, S182–S187, 1988.

[36] *12-lead ecg monitoring with easi lead system*, en, Online; accessed 3 April 2019, 2019. [Online]. Available: https://www.theonlinelearningcenter.com/scorm/module7566_5/story_content/external_files/easi.pdf.

[37] G. Wehr *et al.*, "A vector-based, 5-electrode, 12-lead monitoring ecg (easi) is equivalent to conventional 12-lead ecg for diagnosis of acute coronary syndromes," *Journal of Electrocardiology*, vol. 39, no. 1, pp. 22–28, 2006.

[38] B. L. Nørgaard, B. M. Rasmussen, M. Dellborg, and K. Thygesen, "Positional changes of spatial qrs-and st-segment variables in normal subjects: Implications for continuous vectorcardiography monitoring during myocardial ischemia," *Journal of Electrocardiology*, vol. 33, no. 1, pp. 23–30, 2000.

[39] S. Nelwan, "Evaluation of 12-lead ecg reconstruction methods for patient monitoring," Ph.D. dissertation, Erasmus Universiteit Rotterdam (EUR), 2005.

[40] S. P. Nelwan, J. A. Kors, S. H. Meij, J. H. van Bemmel, and M. L. Simoons, "Reconstruction of the 12-lead electrocardiogram from reduced lead sets," *Journal of Electrocardiology*, vol. 37, no. 1, pp. 11–18, 2004.

[41] J. Kors, G Van Herpen, A. Sittig, and J. Van Bemmel, "Reconstruction of the frank vectorcardiogram from standard electrocardiographic leads: Diagnostic comparison of different methods," *European Heart Journal*, vol. 11, no. 12, pp. 1083–1092, 1990.

[42] D. D. Finlay, C. D. Nugent, J. G. Kellett, M. P. Donnelly, P. J. McCullagh, and N. D. Black, "Synthesising the 12-lead electrocardiogram: Trends and challenges," *European Journal of Internal Medicine*, vol. 18, no. 8, pp. 566–570, 2007.

[43] S. Maheshwari, P. Rajalakshmi, A. Acharyya, P. E. Puddu, and M. Schiariti, "Accurate and reliable 3-lead to 12-lead ecg reconstruction methodology for remote health monitoring applications," en, in *IEEE 15th International Conference on e-Health Networking, Applications and Services*, 2013.

[44] A. Mitra, P. Kundu, and R. Gupta, "Segment specific modeling of electrocardiogram for improved reconstruction error," in *2020 IEEE Applied Signal Processing Conference (ASPCON)*, IEEE, 2020, pp. 16–20.

[45] D. Q. Feild, C. L. Feldman, B. M. Hor, *et al.*, "Improved easi coefficients: Their derivation, values, and performance," *Journal of Electrocardiology*, vol. 35, no. 4, pp. 23–33, 2002.

[46] J. P. Martínez, P. Laguna, S. Olmos, O. Pahlm, J. Pettersson, and L. Sörnmo, "Assessment of qt-measurement accuracy using the 12-lead electrocardiogram derived from easi leads," *Journal of Electrocardiology*, vol. 40, no. 2, pp. 172–179, 2007.

[47] L. Lancia, M. Pisegna Cerone, P. Vittorini, S. Romano, and M. Penco, "A comparison between easi system 12-lead ecgs and standard 12-lead ecgs for improved clinical nursing practice," *Journal of Clinical Nursing*, vol. 17, no. 3, pp. 370–377, 2008.

[48] R. Trobec and I. Tomašić, "Synthesis of the 12-lead electrocardiogram from differential leads," *IEEE Transactions on Information Technology in Biomedicine*, vol. 15, no. 4, pp. 615–621, 2011.

[49] J Millet-Roig, M. Guillem, J Igual, R Llinares, and R Ruiz, "Contributions for the optimal lead placement for the study of atrial fibrillation applying independent component analysis to 64 body surface potential mapping recordings," in *2006 Computers in Cardiology*, IEEE, 2006, pp. 389–392.

[50] M. de la Salud Guillem, A. Bollmann, A. M. Climent, D. Husser, J. Millet-Roig, and F. Castells, "How many leads are necessary for a reliable reconstruction of surface potentials during atrial fibrillation?" *IEEE Transactions on Information Technology in Biomedicine*, vol. 13, no. 3, pp. 330–340, 2009.

[51] M Puurtinen, J Hyttinen, and J Malmivuo, "Optimizing bipolar electrode location for wireless ecg measurement–analysis of ecg signal strength and deviation between individuals," *International Journal of Bioelectromagnetism*, vol. 7, no. 1, pp. 236–239, 2005.

[52] S. Nedios, I. Romero, J.-H. Gerds-Li, E. Fleck, and C. Kriatselis, "Precordial electrode placement for optimal ecg monitoring: Implications for ambulatory monitor devices and event recorders," *Journal of Electrocardiology*, vol. 47, no. 5, pp. 669–676, 2014.

[53] T. He, G. Clifford, and L. Tarassenko, "Application of independent component analysis in removing artefacts from the electrocardiogram," *Neural Computing & Applications*, vol. 15, pp. 105–116, 2006.

[54] M. H. Ostertag and G. R. Tsouri, "Reconstructing ecg precordial leads from a reduced lead set using independent component analysis," in *2011 Annual International Conference of the IEEE Engineering in Medicine and Biology Society*, IEEE, 2011, pp. 4414–4417.

[55] G. R. Tsouri and M. H. Ostertag, "Patient-specific 12-lead ecg reconstruction from sparse electrodes using independent component analysis," *IEEE Journal of Biomedical and Health Informatics*, vol. 18, no. 2, pp. 476–482, 2013.

[56] Gerven, Marcel, and S. Bohte, *Artificial neural networks as models of neural information processing*, en. Frontiers Media SA, 2018.

[57] R. P. Duin, "Learned from neural networks.," in *Lommel, België*, ASCI, 2000, pp. 9–13.

[58] H. Atoui, J. Fayn, and P. Rubel, "A novel neural-network model for deriving standard 12-lead ecgs from serial three-lead ecgs: Application to self-care," *IEEE Transactions on Information Technology in Biomedicine*, vol. 14, no. 3, pp. 883–890, 2010.

[59] H. Atoui, J. Fayn, and P. Rubel, "A neural network approach for patient-specific 12-lead ecg synthesis in patient monitoring environments," in *Computers in Cardiology, 2004*, IEEE, 2004, pp. 161–164.

[60] H. Zhu, Y. Pan, K.-T. Cheng, and R. Huan, "A lightweight piecewise linear synthesis method for standard 12-lead ecg signals based on adaptive region segmentation," *PloS one*, vol. 13, no. 10, e0206170, 2018.

[61] H. J. Lee, D. S. Lee, H. B. Kwon, D. Y. Kim, and K. S. Park, "Reconstruction of 12-lead ecg using a single-patch device," *Methods of Information in Medicine*, vol. 56, no. 04, pp. 319–327, 2017.

[62] F. Chen, Y. Pan, K. Li, K.-T. Cheng, and R. Huan, "Standard 12-lead ecg synthesis using a ga optimized bp neural network," in *2015 Seventh International Conference on Advanced Computational Intelligence (ICACI)*, IEEE, 2015, pp. 289–293.

[63] J. Sohn, S. Yang, J. Lee, Y. Ku, and H. C. Kim, "Reconstruction of 12-lead electrocardiogram from a three-lead patch-type device using a lstm network," *Sensors*, vol. 20, no. 11, p. 3278, 2020.

[64] M. Matyschik, H. Mauranen, P. Bonizzi, and J. Karel, "Feasibility of ecg reconstruction from minimal lead sets using convolutional neural networks," in *2020 Computing in Cardiology*, IEEE, 2020, pp. 1–4.

[65] I. Tomasic, R. Trobec, and M. Lindén, "Can the regression trees be used to model relation between ecg leads?" In *Internet of Things. IoT Infrastructures: Second International Summit, IoT 360° 2015, Rome, Italy, October 27–29, 2015, Revised Selected Papers, Part I*, Springer, 2016, pp. 467–472.

[66] P. Kenedi, I Préda, J Thuer, Á Székely, M Skribek, and D Triebl, "Effect of body position on a mobile, vector-derived, 12-lead electrocardiogram," *EC Cardiology*, vol. 5, pp. 589–595, 2018.

[67] A. Grande-Fidalgo, J. Calpe, M. Redón, C. Millán-Navarro, and E. Soria-Olivas, "Lead reconstruction using artificial neural networks for ambulatory ecg acquisition," *Sensors*, vol. 21, no. 16, p. 5542, 2021.

[68] A. Grande-Fidalgo, J. Calpe Maravilla, M. Redon Segrera, V. Gopinathan, and T. Akl, *Electrocardiogram lead reconstruction using machine learning*, Patent WO2022043196, Mar. 2022. [Online]. Available: https://patentscope.wipo.int/search/en/detail.jsf?docId=WO2022043196&_cid=P11-LW7M44-01830-1.

[69] A. Grande-Fidalgo, J. Calpe, and E. Soria-Olivas, "Challenges in ecg lead reconstruction in patients with pacemakers and implantable defibrillators," in *Proceedings of the 2023 10th International Conference on Bioinformatics Research and Applications*, 2023, pp. 101–106.

[70] B. M. Horacek, J. W. Warren, D. Q. Feild, and C. L. Feldman, "Statistical and deterministic approaches to designing transformations of electrocardiographic leads," *Journal of Electrocardiology*, vol. 35, pp. 41–52, 2002.

[71] U. Satija, B. Ramkumar, and M. S. Manikandan, "An automated ecg signal quality assessment method for unsupervised diagnostic systems," *Biocybernetics and Biomedical Engineering*, vol. 38, no. 1, pp. 54–70, 2018.

[72] F. Perdigon Romero, L. Vázquez Romaguera, C. Román Vázquez-Seisdedos, C. Ferreira Fernandes Costa Filho, M. Guimarães Fernandes Costa, and J. E. Neto, "Baseline wander removal methods for ecg signals: A comparative study," *arXiv e-prints*, arXiv–1807, 2018.

[73] J. Pan and W. J. Tompkins, "A real-time qrs detection algorithm," *IEEE Transactions on Biomedical Engineering*, vol. BME-32, no. 3, pp. 230–236, 1985.

[74] M. Hagan and M. Menhaj, "Training feedforward networks with the marquardt algorithm," en, *IEEE Transactions on Neural Networks*, vol. 5, no. 6, 989–993, 1994.

[75] A. Němcová, R. Smíšek, L. Maršánová, L. Smital, and M. Vítek, "A comparative analysis of methods for evaluation of ecg signal quality after compression," *BioMed Research International*, vol. 2018, 2018.

[76] B. Horáček, J. W. Warren, D. Q. Feild, and C. L. Feldman, "Statistical and deterministic approaches to designing transformations of electrocardiographic leads," en, *Journal of Electrocardiology*, vol. 35, 41–52, 2002.

[77] P. Romero, L. V. R. Francisco, C. R. Vázquez-Seisdedos, C. F. F. C. Filho, M. G. F. Costa, and J. E. Neto, *Baseline wander removal methods for ecg signals: A comparative study*, en, arXiv preprint arXiv:1807.) (11359)., 2018.

[78] T. P. Hettmansperger and J. W. McKean, *Robust nonparametric statistical methods*, en. CRC Press, 2010.

[79] J. Yu, X. Wang, X. Chen, and J. Guo, "Automatic premature ventricular contraction detection using deep metric learning and knn," *Biosensors*, vol. 11, no. 3, p. 69, 2021.

[80] A. J. C. Sharkey, "On combining artificial neural nets," *Connection Science*, vol. 8, no. 3-4, pp. 299–314, 1996.

[81] A. N. Bhagoji, D. Cullina, C. Sitawarin, and P. Mittal, "Enhancing robustness of machine learning systems via data transformations," in *2018 52nd Annual Conference on Information Sciences and Systems (CISS)*, IEEE, 2018, pp. 1–5.

[82] T. J. Wagner, P. Auclair, B. T. Langhals, *et al.*, "Effect of trigonometric transformations on the machine learning prediction and quality control of air temperature," *Faculty Publications*, 2022.

[83] T. J. Hwang, A. S. Kesselheim, and K. N. Vokinger, "Lifecycle regulation of artificial intelligence–and machine learning–based software devices in medicine," *Jama*, vol. 322, no. 23, pp. 2285–2286, 2019.

[84] *Fuzzy c-means clustering (fcm) algorithm*, en, Online; accessed 14 May 2024, 2021. [Online]. Available: https://medium.com/geekculture/fuzzy-c-means-clustering-fcm-algorithm-in-machine-learning-c2e51e586fff.

[85] J. C. Bezdek, R. Ehrlich, and W. Full, "Fcm: The fuzzy c-means clustering algorithm," *Computers & Geosciences*, vol. 10, no. 2-3, pp. 191–203, 1984.

[86] J. Bergstra, R. Bardenet, Y. Bengio, and B. Kégl, "Algorithms for hyper-parameter optimization," in *Advances in Neural Information Processing Systems*, J. Shawe-Taylor, R. Zemel, P. Bartlett, F. Pereira, and K. Weinberger, Eds., vol. 24, Curran Associates, Inc., 2011. [Online]. Available: https://proceedings.neurips.cc/paper_files/paper/2011/file/86e8f7ab32cfd12577bc2619bc635690-Paper.pdf.

[87] D. Arthur, S. Vassilvitskii, *et al.*, "K-means++: The advantages of careful seeding," in *Soda*, vol. 7, 2007, pp. 1027–1035.

[88] M. A. Reyna *et al.*, "Will two do? varying dimensions in electrocardiography: The physionet/computing in cardiology challenge 2021," in *2021 Computing in Cardiology (CinC)*, IEEE, vol. 48, 2021, pp. 1–4.

[89] M. A. Reyna *et al.*, "Issues in the automated classification of multilead ecgs using heterogeneous labels and populations," *Physiological Measurement*, vol. 43, no. 8, p. 084 001, 2022.

[90] I. Goodfellow, Y. Bengio, and A. Courville, *Deep learning*. MIT press, 2016.

[91] L. O. Hall, A. M. Bensaid, L. P. Clarke, R. P. Velthuizen, M. S. Silbiger, and J. C. Bezdek, "A comparison of neural network and fuzzy clustering techniques in segmenting magnetic resonance images of the brain," *IEEE Transactions on Neural Networks*, vol. 3, no. 5, pp. 672–682, 1992.

[92] R. Shwartz-Ziv and A. Armon, "Tabular data: Deep learning is not all you need," *Information Fusion*, vol. 81, pp. 84–90, 2022.

[93] D. Farina, "Forward and inverse problem of electrocardiography," Ph.D. dissertation, IBT, Universität Karlsruhe (TH), 2008.

[94] J. Hoggatt, "Personalized medicine—trends in molecular diagnosticsy: Exponential growth expected in the next ten years," *Molecular Diagnosis & Therapy*, vol. 15, pp. 53–55, 2011.

[95] M. Matyschik, H. Mauranen, P. Bonizzi, and J. Karel, "Feasibility of ecg reconstruction from minimal lead sets using convolutional neural networks," en, in *Computing in Cardiology*, IEEE, 2020, 1–4.

[96] L.-d. Wang, W. Zhou, Y. Xing, N. Liu, M. Movahedipour, and X.-g. Zhou, "A novel method based on convolutional neural networks for deriving standard 12-lead ecg from serial 3-lead ecg," *Frontiers of Information Technology & Electronic Engineering*, vol. 20, no. 3, pp. 405–413, 2019.

[97] *Fundación para la investigación del hospital clínico de la comunidad valenciana homepage*, es, Online; accessed 2 April 2024, 2023. [Online]. Available: https://www.incliva.es/.

[98] J. Kruse and C. Redmond, "Detecting and distinguishing cardiac pacing artifacts," *Analog Dialogue*, vol. 46, no. 11, pp. 1–6, 2012.

[99] *Adas1000 low power, 5-electrode electrocardiogram analog front end with respiration measurement and pace detection*, en, Online; accessed 2 May 2019, 2018. [Online]. Available: https://www.analog.com/en/products/adas1000.html..

[100] E. D. Helfenbein, J. M. Lindauer, S. H. Zhou, R. E. Gregg, and E. C. Herleikson, "A software-based pacemaker pulse detection and paced rhythm classification algorithm," *Journal of Electrocardiology*, vol. 35, p. 95, 2002.

[101] *Agencia española de medicamentos y productos sanitarios homepage*, es, Online; accessed 2 April 2024, 2023. [Online]. Available: https://www.aemps.gob.es/.